J. Print Media Technol. Res.
Vol. I No. 3 (135-200)
September 2012

ISSN 2223-8905
CODEN JPMTBI
UDC 655

3-2012

Journal of Print and Media Technology Research

Thematic issue: Printed electronics

Guest Editor Timothy C. Claypole

Scientific contents

Editor-in-Chief Nils Enlund (Helsinki)
Executive editor Mladen Lovreček (Zagreb)
Published by iarigai The International Association of Research Organizations for the Information, Media and Graphic Arts Industries
www.iarigai.org

9 772223 890003

J. Print Media Technol. Res.
1(2012)3, 135-200
September 2012

No. 3-2012

ISSN 2223-8905
CODEN: JPMTBI

Journal of Print and Media Technology Research

A peer-reviewed quarterly

PUBLISHED BY

The International Association of Research Organizations
for the Information, Media and Graphic Arts Industries

Washingtonplatz 1, D-64287 Darmstadt, Germany
http://www.iarigai.org E-mail: journal@iarigai.org

A mission statement

To meet the need for a high quality scientific publishing platform in its field, the International Association of Research Organizations for the Information, Media and Graphic Arts Industries, iarigai, publishes this quarterly peer-reviewed research journal.

The journal will foster multidisciplinary research and scholarly discussion on scientific and technical issues in the field of graphic arts and media communication, thereby advancing scientific research, knowledge creation, and industry development. Its aim is to be the leading international scientific journal in the field, offering publishing opportunities and serving as a forum for knowledge exchange between all those interested in contributing to or learning from research in this field.

By regularly publishing peer-reviewed, high quality research articles, position papers, surveys, and case studies as well as, in a special section, review articles, topical communications, opinions, and reflections, the journal promotes original research, international collaboration, and the exchange of ideas and know-how. It also provides a multidisciplinary discussion on research issues within the field and on the effects of new scientific and technical developments on society, industry, and the individual. Thus, it serves the entire research community, as well as the global graphic arts and media industry.

The journal covers fundamental and applied aspects of at least, but not limited to, the following topics:

Printing technology and related processes

- Conventional and special printing
- Packaging
- Printed functionality (including polymer electronics, sensors, and biomaterials)
- Printed decorations
- Printing materials
- Process control

Premedia technology and processes

- Color reproduction and color management
- Image and reproduction quality
- Image carriers (physical and virtual)
- Workflow and management
- Content management

Emerging media and future trends

- Media industry developments
- Developing media communications value systems
- Online and mobile media development
- Cross-media publishing

Social impact

- Media in a sustainable society
- Consumer perception and media use

The Journal of Print and Media Technology Research is published both in print and electronically.

Further details and guidelines for authors can be found on the inside back cover, as well as downloaded from http:// www.iarigai.org/publications/journal

Subscriptions

http:// www.iarigai.org/publications/journal/order or send a request to office@iarigai.org

✉ Contact e-mail: journal@iarigai.org

Journal of Print and Media Technology Research

3-2012

September 2012

Thematic issue

Printed electronics

Guest Editor

Timothy C. Claypole

J. Print Media Technol. Res. 1(2012)3, 135-200

Printed in Croatia by Narodne Novine d.d. Zagreb

Contents

A word from the Guest Editor

Timothy C. Claypole
University of Wales, Swansea, UK

E-mail: T.C.Claypole@swansea.ac.uk

Graphic printing is a precision manufacturing process that enables the creation of microstructures, i.e. printing dots and lines in register to create an image. Micro manufacture by printing is the application of layers of grey "active" material in a pattern that produces a product on a flexible substrate. Thus, printing offers the most likely route of practically realising nano and micro technology. Thus, there is the opportunity to apply existing printing skills/equipment to new products or for enhancement of existing products.

The theme of this edition is focused on printing for the manufacture of flexible electronics. The range of papers represents a cross section of the current work in this exciting field. What all these papers illustrate is that manufacture by printing of flexible electronics is a disruptive technology that will revolutionize the manufacture of existing products and enable new products. It is on the cusp of being good enough to realize many new applications for printing technology.

However, there is still a need to consistently achieve small feature sizes with quality control appropriate to the electronics industry. This will require the development of processes and materials, the key to which is a scientific understanding of the process physics. The interest in this area can be seen in the increasing number of papers being submitted to journals and conferences on printing as an advanced manufacturing process for additive manufacture of functional materials.

JPMTR 009 | 1207
UDC 655:621.38

Original scientific paper
Received: 2012-04-10
Accepted: 2012-07-23

Adapted gravure printing process for the production of carbon based electrodes

Frank Siegel[1], *Albert Kohl*[3], *Eugen Enns*[3], *Wolfgang Deger*[3], *Holger Dziallas*[3], *Andreas Willert*[2], *Reinhard R. Baumann*[1,2]

[1] Chemnitz University of Technology, Germany
[2] Fraunhofer ENAS, Chemnitz, Germany
[3] SolviCore GmbH & Co. KG, Hanau, Germany

E-mails: name.surname@mb.tu-chemnitz.de
E-mail: andreas.willert@enas.fraunhofer.de

Abstract

The industrial production of fuel cell components such as catalyst electrodes based on carbon is a promising field of research in respect to printing processes, ink development and optimization of the printed functionalities. This paper presents an adapted gravure printing process to deposit a thick layer of material on a flexible substrate within one impression. Due to a developed gravure screen with maximized dipping volumes it is possible to quintuple the deposited material within one impression unlike utilizing conventional gravure or flexography printing processes. Additionally, the ink characteristics and the process speed are influencing the layer quality in respect to the amount and sizes of defects.

Keywords: gravure printing, screening, line screen, dipping volume, electrodes, PEM fuel cell, rheology, defect analysis

1. Introduction

A major environmentally friendly alternative to traditional fossil fuels based power sources are Proton Exchange Membrane Fuel Cells (PEMFCs) converting hydrogen and oxygen into water by generating an electric current. The electrochemically active component of these fuel cells, the Membrane Electrode Assembly (MEA), is manufactured following mainly batch process workflows or slow film creation technologies. The industrial production of fuel cell electrodes is a promising field of research regarding coating processes, ink development and optimization of functional layers. Various methods for MEA manufacturing have been published in journals or are protected by patents: rolling powder (Bevers et al., 1998), dispersion spraying (Ralph et al., 1997), screen printing (Starz et al., 1999) of thick films on Gas Diffusion Layers (GDL), carrier substrates or directly onto the Proton Exchange Membrane and sputtering (Litster and McLean, 2004). Recently inkjet printing routes have been described to deposit the catalyst layer onto different substrates (Edwards et al., 2007; Taylor et al., 2007; Towne et al, 2007; Mercier et al., 2010). However, the productivity of flat-bed printing and inkjet techniques is low compared to industrial printing technologies like flexography or gravure printing. But both printing technologies are applying too little material onto the substrate within one impression, hence there is a need of a certain number of subsequent printing steps to achieve the right amount of material (Bois et al., 2011). Furthermore, common industrial coating processes are applied to coat the substrates with limited patterning opportunities like blade coating (Park et al., 2010) and slot die coating (Choudhury et al., 2010; Steenberg et al., 2012) which are resulting in low-yield processes caused by subsequent punching steps to get the desired structure causing material losses.

To increase the availability of fuel cells for a broad variety of applications industrial production of MEAs has to be established. The employment of continuous production techniques based on web-fed machinery can definitely contribute to a strong reduction of the manufacturing costs of MEAs (Tsuchiya and Kobayashi, 2004) and therefore support the widespread utilization of these promising, alternative energy sources.

Gravure printing is a highly productive and efficient web based production technique commonly used for printing of high quality magazines and packaging on different substrates with run lengths beyond 300 000 prints. Nevertheless, gravure printing has an enormous potential to fulfill the demands of functional printing. This technology is widely used in coating applications by modifications of the gravure process itself. This paper presents recent results of combining the benefits of gravure printing and gravure coating to achieve thick material layers for the fabrication of catalytic electrodes based on carbon for the MEAs of Proton-Exchange-Membrane Fuel Cells (PEMFCs).

2. Research strategy

There are different workflow approaches to manufacture catalyst layers for fuel cells. Basically, two different modes are known: applying the catalyst layer onto the so called Gas Diffusion Layer (GDL) or onto the Polymer Electrolyte Membrane (PEM) (Mehta and Cooper, 2003). The PEM is in respect to printing processes a very complicated substrate which deforms heavily under mechanical or thermal stress and after deposition of liquids. For this reason, a so called decal method is utilized to transfer the deposited catalyst electrode from a carrier substrate with low surface energy (ETFE or PTFE) to the PEM substrate.

The basis of the research strategy is a highly efficient and productive roll-to-roll gravure printing process. To identify tasks of the work, certain production requirements have been defined. The electrodes should have a thickness of 5 to 10 µm and it should be possible to print onto substrates with low surface energies enabling detaching the electrode in an adjacent workflow step (decal method).

The key aspects of the production process parameters are:

- high throughput (i.e. $m^2\ h^{-1}$)
- no individualization but layout flexibility (i.e. electrode designs)
- high reliability (i.e. functional layers)
- high robustness (i.e. a reliable process parameter regime)

The quality requirement for the printed layers is in particular:

- electrode quality (i.e. number of defects, geometric size of defects, roughness of layer surface, edge sharpness of printed areas)

Solving these tasks requires a research strategy which is depicted in Figure 1. To prevent the loss of noble metal catalyst material (Pt, Ru) the presented experiments were carried out with model-inks with the basic content of carbon, binder and solvent but without the catalyst. To evaluate the applied screens, the influence of ink rheology and process parameters these model-inks were printed on PET films.

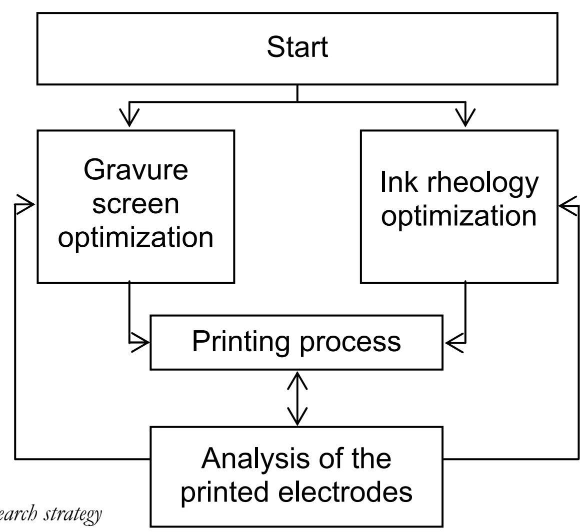

Figure 1: Scheme of the research strategy

3. Ink properties

The rheology of the applied ink has a significant effect on the printing process itself and its process window. Further it determines the results regarding the layer quality, defects, thickness and layer roughness and waviness. The main parameters for determining the ink properties are the flow curve and the yield point of the inks. If the yield point is too high the printed layer will show a big waviness and a large amount of defects caused by bad leveling characteristics. In this investigation several different model-ink formulations were used for pretests to get closer to an ideal rheology. Two different model-inks with a solid content of 9 wt% and 13 wt% and their influence onto the printed layer quality will be discussed further.

To characterize both model-inks the Linear-Viscoelastic range (LVE range) and the flow curves were measured. The LVE range gives an indication of the ideal viscous (loss modulus G") and ideal elastic parts (storage modulus G`) of dispersions. Fig. 2 shows the diagrams of the LVE range and the flow curves. Model-ink I has both a high storage modulus as well as a loss modulus of nearly the same value but the storage modulus prevails. For this reason a yield point of around 20 000 Pa can be identified. So model-ink I will have a slower leveling characteristic than the adjusted model-inkII. This model-inkII has no significant yield point in the LVE range due to a higher loss modulus than the storage modulus and the elastic part is breaking down under shear stress.

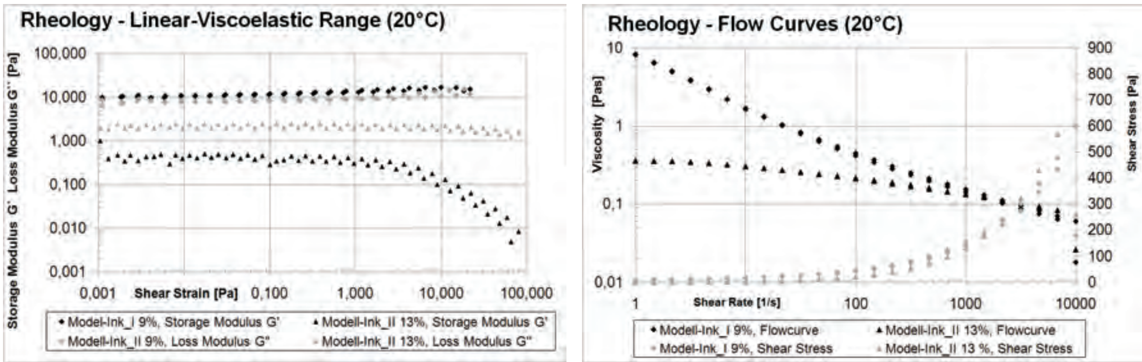

Figure 2: Rheological characteristics of two different model-inks with a solid content of 9 wt% and 13 wt%, Linear-Viscoelastic range and flow curves

Furthermore, the flow curve of model-ink I is typical shear-thinning. It has an initial viscosity of around 10 000 mPas (at 1 1/s and 20 °C) and under shear-stress 140 mPas (at 1 000 1/s and 20 °C). Model-ink II has less shear-thinning characteristics with a viscosity of around 130 mPas (at 1 000 1/s and 20 °C). Under stress both model-inks are almost comparable but after shearing the leveling quality for model-ink I will be insufficient caused by the distinct elastic part (storage modulus).

The rheology of inks is determining the whole printing process, from inking the cylinder to the printing step and the grade of leveling on the substrate afterwards.

4. Gravure screen design

Conventional graphic arts screens for the gravure printing process are designed and built for the reproduction of defined dots for grey level simulation and therefore color impression. It is indeed possible and popular to use conventional electro-mechanically engraved screens for functional printing. For the basic experiments graphic arts driven electro-mechanically engraved screens were applied to deposit the lower viscous model-ink II. This approach is intellectual property of Polyfuel Inc. (Cox et al., 2001). Carrying out these experiments we tried to push the limits of achievable layer thickness but could not even get to 1 μm. Table 1 shows an overview of the employed electro-mechanically engraved screens and their typical dimensions and dipping volumes. Our conclusion is that for manufacturing thick electrodes with the presented purpose graphic arts screens with dipping volumes of up to 16 ml m $^{-2}$ at 48 L cm $^{-1}$ are not sufficient.

Table 1: Graphic arts screens electro-mechanically engraved and their dimensions

	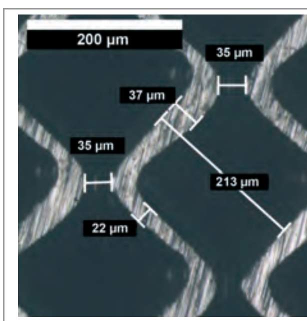	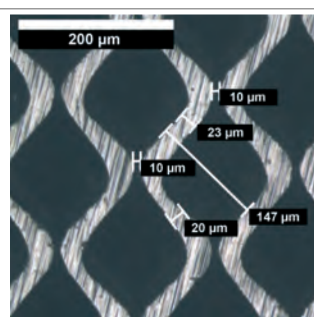	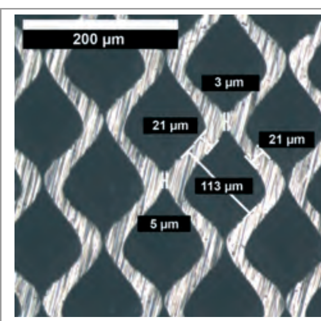
Screen ruling	48 L cm $^{-1}$	70 L cm $^{-1}$	90 L cm $^{-1}$
Dipping volume	~ 16 ml m $^{-2}$	~ 9 ml m $^{-2}$	~ 6 ml m $^{-2}$
Layer thickness model-ink II	0.8 μm	0.6 μm	0.4 μm

Based on these results we focused our further research on new gravure screens and filed them in a patent (Baumann et al., 2010). In order to maximize the dipping volume, line screens with continuous walls (closed screens) and walls with intermittent structures (open screens) have been designed with dipping volumes varying from 95-140 ml m $^{-2}$ and experimentally evaluated. The forms were manufactured by etching.

In Figure 3 a micrograph of an open line screen is shown with a screen ruling of 7L cm $^{-1}$, wall widths of around 100 μm and interruptions of more than 1 000 μm.

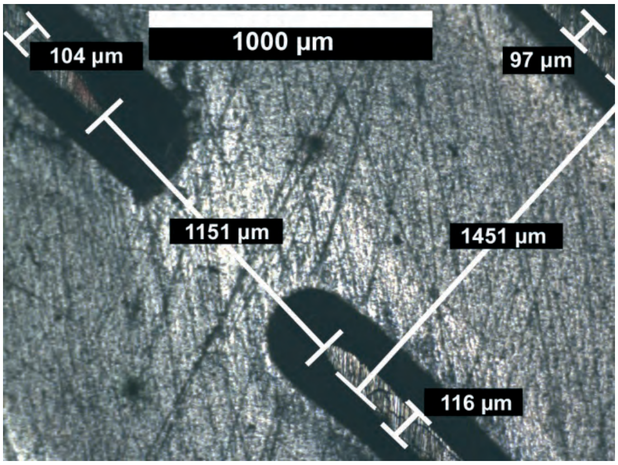

Figure 3: Micrograph of an open line screen with a screen ruling of 7 L cm^{-1}

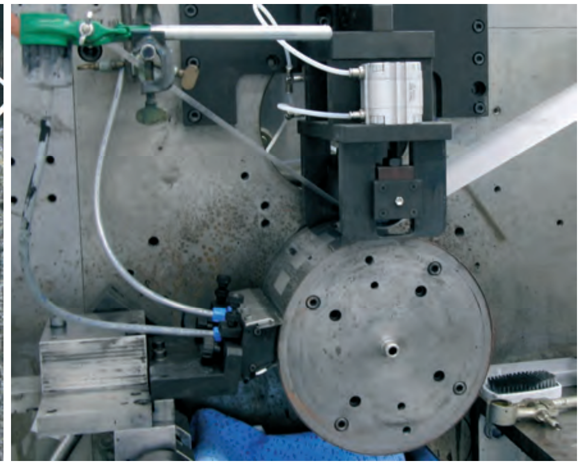

Figure 4: Gravure printing unit with chamber blading system (left side of the cylinder)

5. Experimental setup

For the printing experiments a roll-to-roll narrow web gravure printing machine was employed which is based on the LaborMAN concept of manroland Druckmaschinen AG (Siegel et al., 2010). To reduce solvent evaporation and the required initial amount of ink in the chamber a small volume closed chamber blading system was developed. In Figure 4 the printing unit is shown.

The chamber blading system was set at 270 °, the printing nip is at 0 ° with an impression roller of 80 ° shore.

The first set of experiments was performed to evaluate the designed open and closed line screens with different screen parameters like screen ruling and interruptions. Therefore, a printing form with small electrodes sizes of 20 x 20 mm² with different types of line screens was developed and employed for printing model-ink I and model-inkII to estimate their usability for the proposed application. A selection of four screens are further discussed in chapter 6 "Results and discussion" describing the influence of screen ruling, the difference between closed and open line screens and the ink characteristics. Based on these results the second set of experiments was carried out to assess the productivity of the process itself. Another printing form with larger electrodes sizes of 75 x 75 mm² and employed closed and open line screens was developed.

This form was used to print model-ink II and increase process speed up to 60 m min^{-1}.

The printed electrodes were characterized by a visual inspection system with a connected software analysis (ImageJ) regarding amount and sizes of defects.

For the small sized electrodes (20 x 20 mm²) the resolution of the digitalization is about 20 µm/pixel. Due to the large size of the other electrodes (75 x 75 mm²) and the aim to digitize the whole electrode the resolution is limited for these experiments to 98 µm/pixel. The thickness of the electrodes was measured using a Dektak 150 profiler from Veeco.

6. Results and discussion

6.1 Screens and interdependence with the model-inks

Both model-inks were printed with four different line screens (closed and open, different screen rulings) at a speed of 0.6 m min^{-1} on PET film. Table 2 gives an overview of the applied screens and the printing results. The size of a square is 20 x 20 mm². There is a significant difference of the resulting layer quality between model-ink I (high viscous, high yield point) and model-ink II (medium viscous, very low yield point). Regarding model-ink I it was shown that the ink has insufficient leveling characteristics, the grooves were printed but there is no flooding of the wall areas. The edge sharpness is low caused by shifting the ink during the doctoring process and the low resolution of the screen. Applying the open line screen seems to be an approach to partly overcome the leveling problems.

However, in contrast to the described results model-ink II is showing a very good layer quality. It should be noted that the screen ruling influences the waviness of the edges of the electrodes, like the known saw-tooth effect.

Table 2: Printing results and the applied line screens (printed squares with a size of 20 x 20 mm²)

Type of screen	Screen dimensions	Model-ink I	Model-ink II
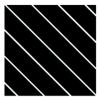	closed 3 L cm^{-1} ~140 ml m^{-2}		
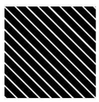	closed 7 L cm^{-1} ~115 ml m^{-2}	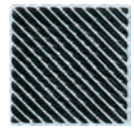	
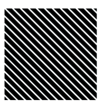	closed 10 L cm^{-1} ~95 ml m^{-2}	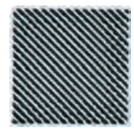	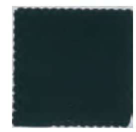
	open 7 L cm^{-1} ~125 ml m^{-2}		

Quantitatively, after digitizing the samples optically, defects were counted and surveyed by image analysis and histograms were created. For an easy readability the generated histograms are visualized within a bubble diagram shown in Figure 5. The larger the extent of a bubble the larger the amount of defects classified to the size of the defect in mm². Additionally, the total defect area in percentage is given and the used screen parameters.

Figure 5 shows that most of the defects are very small over the varied screen rulings applying model-ink I or model-ink II with a small size class of <0.01mm². Moreover, the electrodes printed with model-ink I have a lot large sized defects up to 10 mm² and above. In particular, the effect of utilizing an open line screen is significant for model-ink I caused by a better allocation of the ink in comparison to a closed screen. However, in comparison the optimized model-ink II has a very good performance from 7 L cm^{-1} up to 10 L cm^{-1}, closed and open line screens at a low process speed of 0.6 m min^{-1}. For the screen at 3 L cm^{-1} large effects with sizes between 0.1 and 10 mm² can be noted. For both model-inks the defect minimum is at 7 L cm^{-1}. On these results screen rulings around 3 L cm^{-1} are not expedient for further experiments.

Finally, the layer thickness was measured for the best results, model-ink II and open as well as closed 7 L cm^{-1} line screens. The goal of achieving layer thicknesses of around 10 µm was not reached but at least it was possible to manufacture electrodes with a mean thickness of 5 µm by means of a one impression gravure printing technique (see Figure 7).

This is more than five times higher than when applying a 48 L cm^{-1} graphic arts screen with the same model-inkII.

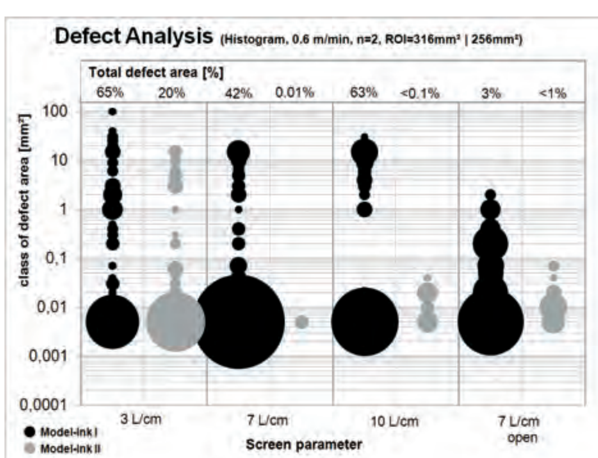

Figure 5: Defect analysis: Bubble-histogram and mean total defect area in percentage, printing speed 0.6 m min^{-1}, ROI = 316 mm² and 256 mm²

6.2 Screen and process speed

To assess the productivity of the process, printing experiments have been carried out with electrodes of 75 x 75 mm² employing both types of line screens at 7 L cm $^{-1}$, model-ink II on PET. Table 3 is showing the printing results printed at speeds of 18, 36 and 60 m min $^{-1}$, respectively. The appearance of the printed layers is changing significantly at higher speeds.

Table 3: Printed layer quality at three different printing speeds, closed and open screens

Type of screen	Printing results 18 m min $^{-1}$	Printing results 36 m min $^{-1}$	Printing results 60 m min $^{-1}$
Closed line screen 7 L cm $^{-1}$	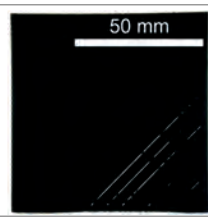	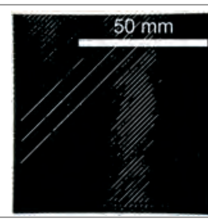	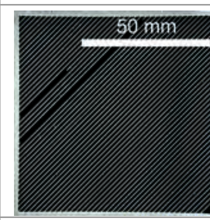
Open line screen 7 L cm $^{-1}$	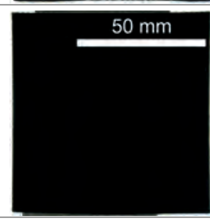	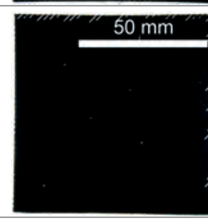	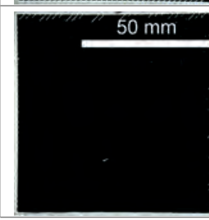

For printing speeds above 18 m min $^{-1}$ the different visual appearances between open and closed screens is getting much more obvious. The results of the image analysis are shown in Figure 6.

It is clearly shown, that closed screens (black) are inducing more and larger defects than open ones (gray). In particular for the closed screens the amount of large defects caused by non-flooding of the wall areas is very obvious in Table 3 and Figure 6. With increasing printing speed open line screens are much more favourable than the closed ones.

A reason for this is the ink filling of the grooves with high dipping volume characteristics. At a given ink rheology the time available for filling is reduced when increasing the printing speed. Two simultaneous processes occur during the ink filling: a viscosity dependent ink flow and a flow resistance due to squeezing out the air from the grooves. Furthermore, the emptying of the grooves is also time-dependent. The open wall structure is supporting the ink flow especially with inappropriate ink characteristics resulting in a more homogenous printed layer.

The mentioned time-dependence of filling and emptying of the gravure grooves is affecting also the layer thickness. Figure 7 shows the mean layer thicknesses for the different printing speeds.

In comparison the investigated closed and open line screens are producing similar layer thicknesses whereby the open screens are producing fewer defects. The loss of layer thickness with increasing speed is significant for both screen types and is lead back to the limited filling and emptying process of the grooves.

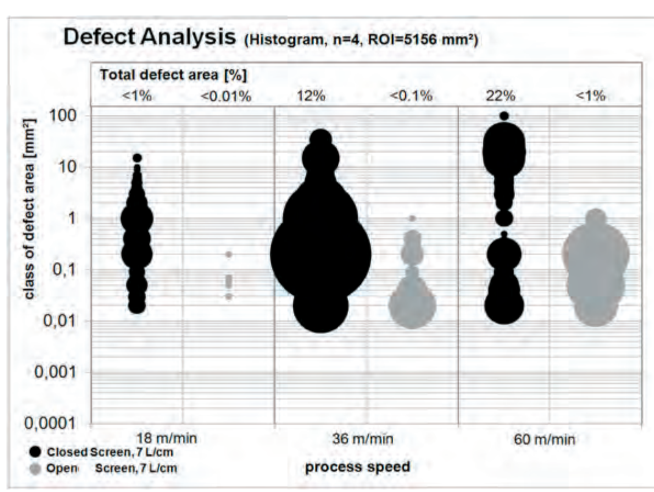

Figure 6: Defect analysis - bubble-histogram and mean total defect area in percentage

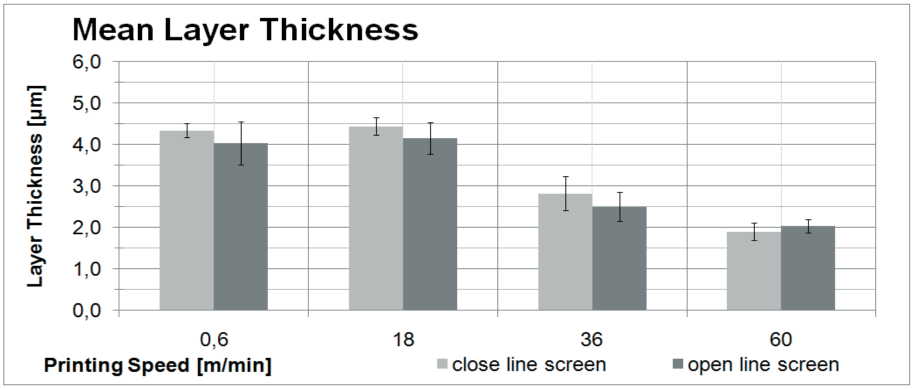

Figure 7: Mean layer thicknesses of 12 measurements allocated over two samples for different printing speeds

7. Conclusions

Starting from graphic arts screens, improved line screens were developed with appropriate high dipping volumes to print carbon based electrodes. Compared to the employed electro-mechanically engraved screens, this approach makes it possible to quintuple the amount of material which is deposited within one impression onto the substrate. Furthermore, it was shown that the printing process has a significant influence on layer quailty (amount and size of defects) and layer thickness. At speeds up to 18 m min^{-1} homogeneous layers with negligible defects have been printed.

But the investigated screens are also a general benefit for other applications where there is a need of structured thick material layer deposition on flexible substrates, mainly for active materials like functional layers for electrochemical devices or sensors. Gravure printing is capable to complement rotary screen printing in the lower film thickness range utilizing a lower viscosity range like it is common for rotary screen printing. But applying novel gravure screens with maximized dipping volumes requires an adaption of the whole printing process, combining ideas of gravure coating and printing.

References

Baumann, R. R., Willert, A., Siegel, F. and Kohl, A., 2010. Solvicore GmbH & Co. KG. *Method for producing catalyst layers for fuel cells.* Patent Publication WO 2010136204

Bevers, D., Wagner, N. and von Bradke, M., 1998. Innovative production procedure for low cost electrodes and electrode/membrane structures. *International Journal of Hydrogen Energy,* Vol. 23, No. 1, pp. 57-63

Bois, C., Blayo, A., Chaussy, D., Vincent, R. and Nayoze, C., 2011. Characterisation of catalyst layers for fuel cell printed by flexography. *Advances in Printing and Media Technology,* Vol. 38, pp. 237-245.

Choudhury, B. and Tannenbaum, H.P., 2010. E. I. Du Pont de Nemours and Company. *Improved catalyst coated membranes having composite, thin membranes and thin cathodes for use in Direct Methanol Fuel Cells.* Patent Publication WO 2011028998.

Cox, P., Diez, D., Servaites, J. and Olmeijer, D., 2001. Polyfuel Inc. *Printing of catalyst on the membrane of fuel cells.* Patent Publication WO 03054991.

Edwards, C., Vanheusden, K., Kowalski, M. And Caruso, J., 2007. Cabot Corporation. *Roll-to-roll Manufacturing of Electronic and Optical Materials. Patent Publication* WO 2007106699.

Litster, S. and McLean, G., 2004. PEM fuel cell electrodes. *Journal of Power Sources,* No. 130, pp. 61-76.

Mehta, V. and Cooper, J.S., 2003. Review and analysis of PEM fuel cell design and manufacturing, *Journal of Power Sources*, Vol. 114, No. 1, pp. 32-53.

Mercier, A-G., Vincent, R., Nayoze, C., Blayo, A. and Soucemarianadin, A., 2010. Inkjet printing of catalyst layers used in fuel cells membrane electrode assemblies. *Advances in Printing and Media Technology,* Vol. 37, pp. 319-325.

Park, I.-S., Li, W. and Manthiram, A., 2010. Fabrication of catalyst-coated membrane-electrode assemblies by doctor blade method and their performance in fuel cells. *Journal of Power Sources*, Vol. 195, No. 20, pp. 7078-7082.

Ralph, T. R., Hards, G. A., Keating, J. E. Campbell, S. A., Wilkinson, D. P., Davis, M., St-Pierre, J. and Johnson, M. E., 1997. Low Cost Electrodes for Proton Exchange Membrane Fuel Cells. *Journal of Electrochemical Society,* Vol. 144, No. 11, pp. 3845-3857.

Siegel, F., Hösel, M., Willert, A., Akowanou, C., Heinz, S., Knittel, D. and Baumann, R.R., 2010. Concept for a hybrid R2R laboratory printing press. In: *Proceedings of the International Conference on Flexible and Printed Electronics*, Hsinchu, Taiwan, October 2010.

Starz, K.-A., Zuber, R., Goettenauer, W., Fehl, K. and Diehl, M., 1999. Umicore AG & Co. *Method of applying electrode layers on a tape-like polymer electrolyte membrane for fuel cells*. EPO Patent Publication EP 1037295.

Steenberg, T., Hjuler, H.A., Terkelsen, C., Sanchez, M., Cleemann, L.N. and Krebs, F.C., 2012. Roll-to-roll coated PBI membranes for high temperature PEM fuel cells. *Energy Environmental Science*, Vol. 5, pp. 6076-6080

Taylor, A.D., Kim, E.Y., Humes, V.P., Kizuka, J. and Thompson, L.T., 2007. Inkjet printing of carbon supported platinum 3-D catalyst layers for use in fuel cells, *Journal of Power Sources*, Vol. 171, No. 1, pp.101-106.

Towne, S., Viswanathan, V., Holbery, J. and Rieke, P., 2007. Fabrication of polymer electrolyte membrane fuel cell MEAs utilizing inkjet print technology. *Journal of Power Sources,* Vol. 171, No. 2, pp. 575-584.

Tsuchiya, H. and Kobayashi, O., 2004. Mass production cost of PEM fuel cell by learning curve. *International Journal of Hydrogen Energy,* Vol. 29, No. 10, pp. 985-990.

JPMTR 010 | 1208
UDC 655:621.38

Research paper
Received: 2012-05-03
Accepted: 2012-07-09

Characterisation of catalyst layers for fuel cells printed by flexography

Chloé Bois[1], *Anne Blayo*[1], *Lionel Chagas*[1], *Rémi Vincent*[2], *Christine Nayoze*[2], *Didier Chaussy*[1]

[1] Laboratory of Pulp and Paper Science and Graphic Arts, Grenoble Institute of Technology, St. Martin d'Hères, France

E-mail: anne.blayo@pagora.grenoble-inp.fr

[2] CEA, LITEN, Grenoble, France

Abstract

Fuel cells are a promising solution for electrical power production in a context of fossil fuel shortage and environmental concern. They allow the conversion of chemical energy into electrical energy. They use hydrogen as an energy carrier, oxygen as a second reactive gas and only produce water. In the fuel cell core, two layers are called catalyst layers. They are composed of carbon nanoparticles, which insure the electrical conductivity, of an ionomer called Nafion® that allows the water diffusion and of platinum nanoparticles that catalyse the electrochemical reactions.

Inks have been formulated with these three elements and have been deposited using a flexography process following a multilayer protocol. The catalyst layers have been electrochemically tested with success. However, these electrochemical characterisations are currently long and destructive. Consequently, the implementation of continuous process in the fuel cell manufacturing requires an adaptation of the characterisation techniques.

Colour characterisation used in the printing field, optical density and reflectance spectra measurements are fast, non destructive and can be implanted in line. This paper postulates that they could be used as a complementary tool for characterise catalyst layers.

As the platinum is a crucial element in the fuel cell, the relevance of these techniques is evaluated on their ability to measure different platinum amounts. In order to increase the platinum quantity, variations of the quantity of ink deposited are performed: either the volume (cm^3 m^{-2}) of anilox cylinders is modified, or the number of superimposed layers of ink varies. (ii) For changing the platinum nanoparticles amount in the catalyst layer, a reference ink, with no platinum, was formulated. The catalyst layers with similar ink loadings but not the same platinum amounts were then manufactured.

The influence of the ink type is visible on the optical density values; however, the ink loadings are not discriminated by this technique. The reflectance spectra measurement shows better discriminations: (i) it is able to discriminated catalyst layers made with the two anilox cylinders; (ii) the influence of the number of ink layers superimposed is also clearly measurable and, (iii) the spectra of each type of ink have different shapes and values. Consequently, the influence of the ink loading and of the platinum amount is measurable by this technique. Besides, printing defects have also an influence of the reflectance spectra.

This promising technique requires further studies: (i) on the quantification of platinum nanoparticles amounts, (ii) on the influence of variations of other components (Nafion®) quantity and amount, and (iii) on the possibility of evaluation of printing defects by this technique.

Keywords: fuel cell, functional inks, catalyst layer, flexography, reflectance, ink load control

1. Introduction

1.1 The context of the reseach

In 19th century, fuel cells were discovered and are now the core of numerous research programs. At the end of the 20th century, the interest grew in Proton Exchange Membrane Fuel Cells (PEMFCs) especially for portative and transport applications. These fuel cells are composed of a stack of a Membrane Electrode Assemblies (MEA's). MEA's are multilayered materials where two electrodes are separated by an electrolytic membrane. The electrodes are composed of a Gas Diffusion Layer (GDL) and a Catalyst Layer (CL). The catalyst layer contains functional elements (platinum catalyst, proton and electron conductors). MEA's are fed with reactive gases (oxygen and hydrogen) and electrochemical reactions take place into the catalyst layers following the equations [1] in anode and [2] in cathode.

$$2H_2 \rightarrow 4H^+ + 4e^- \qquad [1]$$

$$O_2 + 4H^+ + 4e^- \rightarrow 2H_2O \qquad [2]$$

$$2H_2 + O_2 \overset{4e^-}{\longleftrightarrow} 2H_2O + energy \qquad [3]$$

The products of these reactions are water and heat as described in equation [3].

1.2 Fuel cell manufacturing

The catalyst layers of the fuel cells are commonly manufactured by blade coating (Schonert et al., 2004; Mustafa et al., 2004; Park et al. 2010; Hwang et al., 2011) or spray techniques (Chaparro et al., 2010; Martin et al., 2010; Hwang et al., 2011). One major concern of fuel cell making is the cost of platinum catalyst. It tends to limit the growth of fuel cell use. Printing processes can be considered as alternative techniques of catalyst layer production. The printing techniques tested are ink jet (Taylor et al., 2007; Mercier et al., 2010; Bois et al., 2012b) and screen printing (Andrade et al., 2009; Bois et al., 2012b). They allow larger surface of production, and less waste of expensive components during the manufacturing. This study used the flexography printing process, which allows transferring functional inks that contains platinum onto a GDL, considered as a printing substrate.

1.3 The objectives of the research

The catalyst layer characterisation is commonly performed by either single cell performance tests or half-cell tests. These characterisations need specific equipment and take some hours (Bultel et al., 2002; Pozio et al., 2002; Franco et al., 2007; Yuan et al., 2011). It is therefore crucial to characterise the print quality of the catalyst layers at each step of the flexography manufacturing.

As the print quality is commonly quantified by colour measurements, the relevance of two techniques is investigated: optical density and reflectance spectrum measurements. Moreover, these techniques have the major advantages to be fast, in-line and non destructive. If they are pertinent, they could become a complementary characterisation to the electrochemical techniques.

2. Materials and methods

2.1 Flexography proofing

Printing was performed with a Flexiproof, a sheet-fed laboratory proofing device for flexography (Testing Machines Inc. TMI, New Castle, USA). This device recreates the ink transfer of a flexography system. The ink transfer is controlled by the gap between the form cylinder and the anilox, and the gap between the form cylinder and the printing cylinder. The cliché pattern is a solid of 5×5 cm^2. Catalyst inks are deposited at constant speed of 25 m min^{-1}.

The control of the quantity of ink deposited onto the substrate is made by (i) using anilox cylinders with different volumes (cm^3 m^{-2}), corresponding to the volume of the cells of one meter square of anilox. In this study, two anilox cylinders with 4 and 13 cm^3 m^{-2} volume values were used. (ii), transferring a variable number of ink layers by a multilayer protocol (Bois et al., 2012a). The required number of ink layers (from one to six in this study) was transferred wet on wet. The samples were named by considering the number of ink layers they were composed of, for example, 2L corresponds to a catalyst layers made by the superimposition of two layers of ink. The printed sample was then dried at room conditions (23 °C and 50 RH %) for at least 24 h. The system was washed before each trial to eliminate the risk of mixing an ink with the residue of the previous trial.

2.2 Inks

Two water-based inks for catalyst layers were formulated to fulfilled process and fuel cell requirements. Water, already used in running MEA, was chosen as the vehicle of the catalyst ink solvent. It limits the potential pollutants that should damage electrochemical properties of the membrane electrode assembly. Furthermore, it is compatible with flexography process and reduces the use of volatile organic components. Some functional elements were added to the ink formulation:

(i) Nafion® polymer dispersion (22 w/w % Nafion) in aliphatic alcohols and deionised water (DuPont TM, Wilmington, USA), the ionomers form polymeric channels in the catalyst layer that diffuse the proton from the catalyse sites to the electrolyte (Xie et al., 2010; Jeon et al., 2010; Sasikumar et al., 2004).

(ii) Carbon powders at various ratio to the platinum nanoparticles:

Either carbon-supported platinum catalysts (Tanaka Kikinzoku, Tokyo, Japan) that allows the electron conduction due to carbon nanoparticles percolation and catalyses the electrochemical reactions [1] and [2] due to the platinum (45.4 w/w % platinum as regards to the carbon-supported platinum) (Fraga et al., 2002; Calvillo et al., 2011).

This component was used to formulate the ink I_{33} which is used for manufacturing catalyst layers.

A carbon powder (Cabot Corporation, Alpharetta, USA) was used as a replacement for the carbon supported platinum, in order to control the amount of platinum in the dry content if required. This carbon powder enters in the formulation of the ink I_0. This ink is a model ink which has similar properties than the ink I_{33}, except the presence of catalyser.

Both inks have the same dry content in volume (26 ± 2 w/w %).

2.3 Substrates

Gas Diffusion Layers are nonwoven substrates made of carbon fibres network and polytetrafluoroethylene (PTFE). The carbon network assures the electron conductivity, the PTFE the water management, and a specific porous structure leads to water, and reactive gas diffusion.

The GDL used in this study is a SGL 24 BC (SGL Group, Wiesbaden, Germany). It has been characterised as a classical printing substrate. The GDL has a thickness of 247.6 ± 1.3 µm, a specific weight of 101.7 ± 2.0 g m^{-2}, and a density of 410.7 ± 12.5 kg m^{-3}. It is composed of two layers.

A carbon fibres network with polytetrafluoroethylene polymer named a macroporous layer (Fig. 1b), and (ii) a microporous layer composed of carbon nano-particles and polytetra-fluoroethylene polymer (Fig. 1a and 2). The presence of PTFE confers to the microporous layer surface a highly hydrophobic character, which is known to limit the affinity with water-based inks.

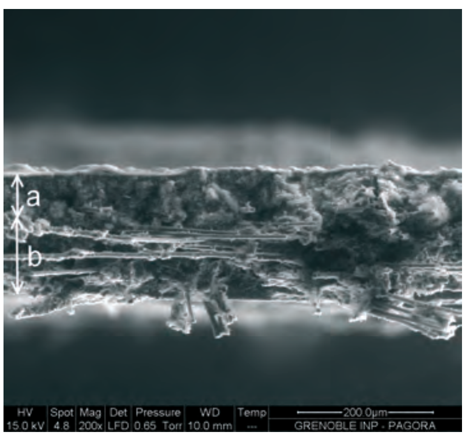

Figure 1: SEM cross view of SGL 24 BC: a) microporous layer and b) macroporous layer

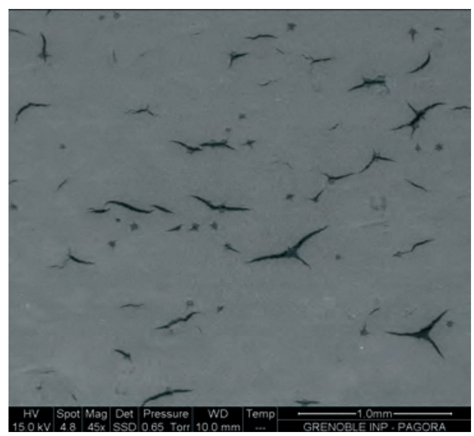

Figure 2: SEM surface view of SGL 24 BC (microporous layer surface)

2.4 Catalyst layers conventional characterisation

Catalyst layer specimens printed with the Flexiproof are firstly characterised by their dry ink loading (mg cm^{-2}), called in this study ink loading. It represents the weight of dry ink transferred onto the substrate per unit of surface. It is determined by the measure of the mass of the substrate sample before and after printing when the catalyst layer is completely dried. Then, considering the area of the solid on the cliché plate, the ink loading (mg_{ink} cm^{-2}) is calculated. This parameter is commonly used in fuel cell field to calculate the amount of functional particles (platinum for example) in a catalyst layer (Sasikumar et al., 2004). Finally, with regard to the ink characteristics, the platinum (mg_{Pt} cm^{-2}) and Nafion® (mg_{nafion} cm^{-2}) loading were calculated. The catalyst layer thickness was calculated by difference between the GDL thickness and the Gas Diffusion Electrode (a GDL with a catalyst layer) thickness. Ten thickness measurements are performed on each GDL and GDE before calculating the value of the catalyst layer thickness.

2.5 SEM observations of catalyst layers

An Environmental Scanning Electron Microscopy (ESEM) on a Quanta 200 FEI device (Everhart-Thornley Detector) (FEI, Hillsboro, USA) was used to characterise the morphology of the catalyst layer (Denneulin et al., 2009). Pictures were acquired using Back Scattered Electrons detection (BSE). It consists of high energy electron beam that is reflected out of the sample detection volume. The particularity is that the heavy elements backscatter the incident electrons more strongly than the light elements. So, elements with a high atomic number (Z) appear brighter on the image. The platinum element has an atomic number equal to 78, while the other elements existing in the inks, catalyst and gas diffusion layers have a lower atomic number, namely: carbon (Z = 6), oxygen (Z = 8), fluorine (Z = 9) and sulphur (Z = 16). Hence, it allows a contrast of the platinum atoms of the nanoparticles that enters in the composition of the ink I_{33} (Hirano et al., 1997). Consequently, the more the BSE detects carbon supported catalyst nanoparticles in a zone, the more this zone appears bright in the picture. For example, because of the presence of catalyst, the catalyst layer at the surface of the sample presented in Figure 3 is brighter than the substrate on which it is deposited.

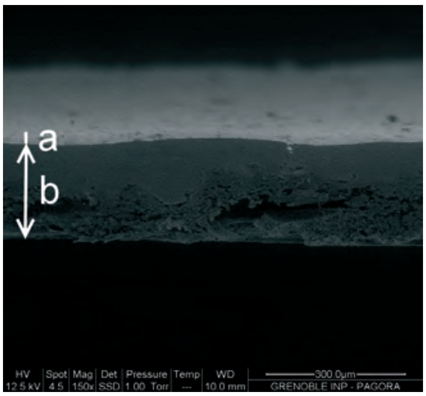

Figure 3: SEM (BSE) cross view of a catalyst layer (a) printed on a GDL (b) by the superimposition of five layers of ink I_{33} with the anilox of 4 cm³ m⁻²

2.6 Colour characterisation

2.6.1 Optical density values

The optical density was measured using a GretagMacBeth, C 19 densitometer (X-rite, Grand Rapids, USA). The principle of an optical density measurement is explained in the following. When an incident light with an intensity equal to I_0 illuminates the surface of a material, the light can be either reflected in the specular direction or be absorbed, transmitted or reflected back (retrodiffused) after multiple scattering phenomena (multiple reflection and/or refraction phenomena due to the interaction of light with the material). The retrodiffused part (intensity I_R) is used to define the optical density OD, given as follows at a given wavelength λ [4].

$$OD(\lambda) = -\log\left(\frac{I_R(\lambda)}{I_0(\lambda)}\right) \qquad [4]$$

The lower the retrodiffused part of the incident light intensity, the higher the optical density and the darker the surface is visually experienced.

To define a density value fully, it is necessary to specify the geometric and spectral conditions of the measuring system. Geometric conditions of the C 19 densitometer are described in ISO 5-4 (45/0 or 0/45) and the spectral conditions in ISO 5-3. For reflexion density, incandescent tungsten illumination (standard illuminant A) and status E are used respectively to illuminate the material and select the spectral response. In this study, as deposited inks contain carbon powder particles that are opaque, an increase in optical density will indicate an increase in thickness of the deposited ink layer. The device is calibrated using the GDL.

2.6.2 Reflectance spectrum

The reflectance spectra of catalyst layers were measured in this work with an i1 Pro spectrophotometer (X-Rite, Grand Rapids, USA). The reflectance values were measured from 380 to 730 nm, with a 10 nm step, with 45 °/0 ° ring illumination optics.

The measurements were performed on a circular surface of 6.0 mm. Before each test, this device was calibrated with a ceramic tile based on barium sulphate according to DIN 5033 and then each catalyst layer was characterised ten times.

For each transfer number, five samples are printed. The results presented in this paper are the average of five measurements performed on each of the five samples with constant printing parameters.

2.6.3 Ink intrinsic reflectance and optical density

The intrinsic reflectance and the intrinsic optical density values of the inks (called R_∞ and OD_∞) were evaluated on a sample made by depositing a substantial quantity of ink onto a substrate. In this study, the inks were coated onto a GDL by scraping the ink at 0.5, 1, 1.5 and 2 mm from the substrate. The reflectance spectrum, the optical density and the thickness were then measured on the dry deposit. The measures were performed until there was no significant variation of the reflectance and optical density with regard to the deposit thickness. These values of reflectance and optical density are considered as the intrinsic values, noted R_∞ and OD_∞.

3. Results and discussion

3.1 Multilayer protocol

The multilayer protocol allows the deposition of water-based inks onto the hydrophobic surface of the GDL. Indeed, as the affinity between the ink and the substrate is poor, the first ink layer acts as an adhesion promoter. Subsequently, it insures the good transferability of the upper ink layers. The multilayer protocol produces continuous catalyst layers, as the one depicted in Figure 3, which reached similar electrochemical properties than catalyst layers made by conventional processes (Bois et al., 2012a). Catalyst layer manufacturing by flexography aims to transfer a precise quantity of functionnal ink onto a specific substrate. The ink quantity is a significant parameter since the catalyst layers are defined by their quantity of platinum by unit of surface (mg cm⁻²) referred to as loading. For each anilox cylinder, the number of ink layers superimposed varies. The ink loading of each sample was measured as shown in Figure 4.

For each anilox cylinder, the ink loadings increases, with the number of ink layers transferred. The amount of ink deposited at each transfer is 0.04 ± 0.01 and 0.17 ± 0.03 mg cm^{-2} for anilox cylinders of 4 and 13 cm^3 m^{-2} respectively. At each transfer, the 13 cm^3 anilox leads to the deposition of more than four times more ink loading onto the substrate. The manufactured catalyst layers have platinum loadings that range from 03 ± 0.01 to 0.20 ± 0.01 mg cm^{-2} by superimposing one to five layers of ink with the anilox cylinders of 4 cm^3 m^{-2}. The catalyst layers made with the anilox of 13 cm^3 m^{-2} have an ink loading that varies from 0.20 ± 0.01 to 0.96 ± 0.01 mg cm^{-2} by superimposing from one to six ink layers. This figure also highlights that catalyst layers made by the superimposition of five ink layers with the 4 cm^3 m^{-2} anilox reaches a similar ink loading (0.2 mg cm^{-2}) as a catalyst layer made by the deposition of one ink layer with the anilox cylinder of 13 cm^3 m^{-2}.

The catalyst layer thickness values are presented in Figure 5. The protocol of thickness measurement is unable to give relevant thickness values for the catalyst layers made with the anilox of 4 cm^3 m^{-2}. Indeed, the thickness of these catalyst layers were too low to be discriminated from the substrate thickness variations (the standard deviation of the GDL thickness has been estimated at 1.3 µm in part 2.3). Consequently, Figure 5 only details the thickness values measured on catalyst layers made with the anilox of 13 cm^3 m^{-2}.

The thickness values increase from 3.0 ± 1.7 µm to 11.9 ± 2.2 µm when the number of ink layers superimposed on the substrate increase from one to five. When six layers of ink are superimposed, even if the ink loading remains consistent with the expected trend described in Figure 4, the thickness decreases to 7.5 ± 1.3 µm. Two hypotheses have been proposed to explain this unexpected value. The first one was a possible substrate compression during the multi-print. The thickness of a GDL was measured before and after six printing with the same printing parameters than the catalyst layer protocol except that no ink was used. After six nip passages the value of the GDL's thickness increases of 0.2 µm. Compared to the standard deviation of the thickness measurement, which is higher than 1.5 µm, 0.2 µm is not a significant thickness difference. Consequently, the substrate compression is probably not the cause of the catalyst layer thickness decreasing. A second hypothesis is the possibility of the ink strike through the substrate. SEM observations might highlight this phenomenon. However, it would be difficult to distinguish if the ink has entered into the substrate because of the deposition technique or because of the preparation of SEM samples.

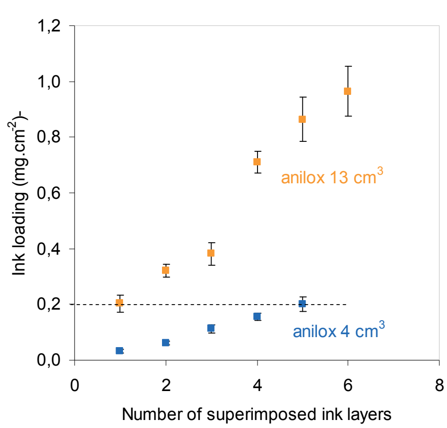

Figure 4: Ink loading as a function of the number of superimposed ink layers onto GD

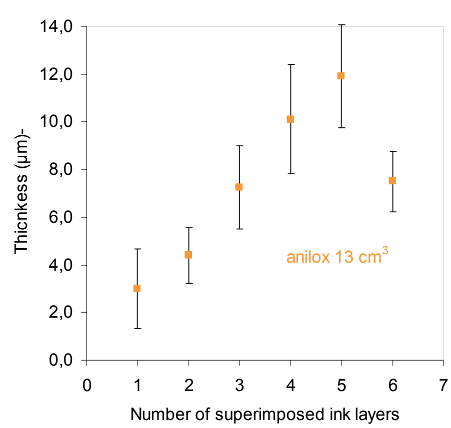

Figure 5: Thickness as a function of the number of superimposed ink layers onto GD

3.2 Relevance of optical density measurements for catalyst layer

Optical density was tested as a characterisation technique on specimens of catalyst layer previously described. The investigations focused on (i) the influence of the platinum amount in the ink on the optical density and (ii) the influence of the number of ink layers superimposed. The results of optical density values in black are shown in Figure 6.

Considering the specimens manufactured with the anilox cylinder that has a volume equal to 4 cm^3, and for each number of superimposed layers, the optical densities discriminates the inks I_0 and I_{33}. The optical densities of the layers made with the ink I_{33} present noticeable differences as a function of the anilox volume. Considering the ink I_{33}, the optical densities of the specimens made with the anilox with a volume equal to 13 cm^3 m^{-2} are higher than the one obtained with the 4 cm^3 m^{-2}. With this ink, the optical densities as a function of the ink loading increase then tend to reach an asymptote. The value of this asymptote could be equal to the intrinsic optical density (OD_∞) of the Ink I_{33}.

Consequently, at higher platinum loading, it appears that the optical densities of specimens made with the ink I_{33} show poor variations.

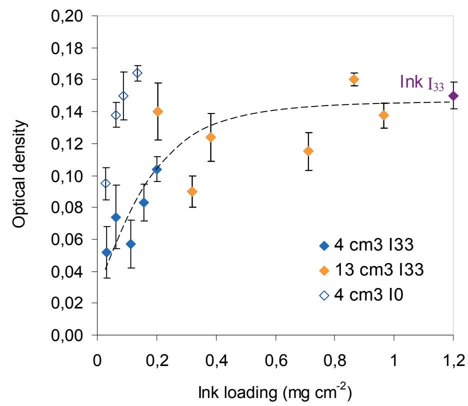

Figure 6: Optical densities in black of specimens of GDLs made by multilayer protocol and of the ink I_{33} (the ink is arbitrarily placed at and ink loading equal to 1.2 mg cm^{-2}, the dotted line have been draw only to facilitate the understanding of the figure)

The optical density allows discriminating (i) the both types of ink tested: with or without platinum, at the same ink loading, and (ii) variations of ink loadings, such as the difference of loadings, induce by the use of 13 or 4 cm^3 m^{-2} anilox, with the same ink type. However, it appears difficult to significantly measure the ink loading influence on the optical density at ink loading higher than 0.2 mg cm^{-2}. Moreover, parameters, such as the presence of platinum in the ink, the anilox volume use, or the number of ink layer cannot be determined with such a technique.

3.3 Relevance of characterisation of catalyst layers by reflectance spectrum measurement

Similarly to the optical density tests, the characterisation of catalyst layer by reflectance spectra measurements is performed on (i) specimens with the same platinum amount in the ink, but different ink loading values (3.3.1), (ii) specimens that have the similar ink loading values, but different platinum amount in their dry content (3.3.2).

3.3.1 Influence of the ink loading on the reflectance spectrum

In this section, all catalyst layers were manufactured using the ink I_{33} that contains platinum. The reflectance spectra measured on catalyst layers made with the anilox cylinders 4 and 13 cm^3 m^{-2} are shown in Figures 7 and 8 respectively. The reflectance spectra of the substrate and the intrinsic reflectance of the ink are also shown on these figures.

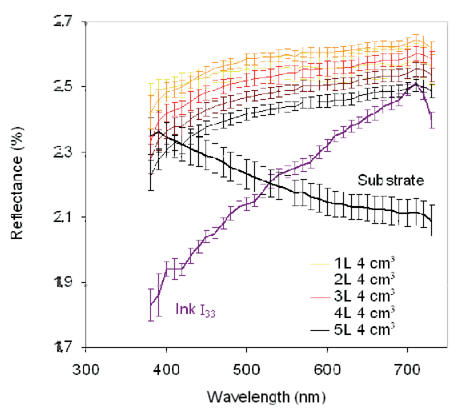

Figure 7: Reflectance spectra of specimens made with the ink I_{33} deposited with an anilox of 4 cm^3 m^{-2}

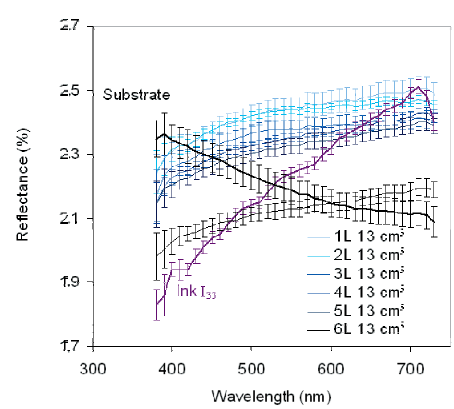

Figure 8: Reflectance spectra of specimens made with the ink I_{33} deposited with an anilox of 13 cm^3 m^{-2}

Whatever the wavelength value, the major trend is that the increase of the catalyst layer ink loading leads to reduce the reflectance value. The reflectance values show that the substrate influence diminishes with increasing the number of superimposed ink layers. The reflectance values tend toward the intrinsic values of the ink as expected by the Kubelka-Munk model (Hébert and Hersch, 2006). Thereby, the catalyst layers made with the 4 cm^3 m^{-2} anilox have lower reflectance values than those obtained on the catalyst layers made with the 13 cm^3 m^{-2} anilox cylinder. However, the specimens made by the deposition of one layer with the 4 and 13 cm^3 m^{-2} anilox cylinders have lower reflectance values than their counterpart made by the superimposition of two layers. An earlier study (Bois et al., 2011) described printing defect appearing when the first layer of ink is transferred onto the SGL 24 BC.

In Fig. 9, a picture represents the deposition of one layer of I_{33} ink with anilox cylinders of 4 and 13 cm^3 volumes.

A patterning occurs with a marbling appearance. This defect is a typical printing problem, well known as indicating a lack of affinity between the ink and the surface. It was expected during the deposition of a water-based ink onto a substrate with such a high hydrophobic behaviour. Thus, the ink film splitting in the nip is not favourable to ink transfer and the ink is only partially transferred. This leads to an inhomogeneous ink layer. Consequently, the reflectance spectra of speci-

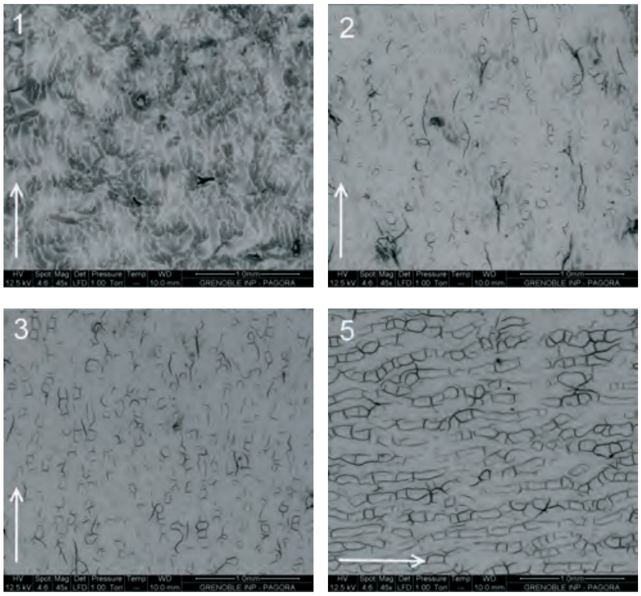

Figure 9:
SEM (BSE) observations of the surface of catalyst layers made by the superimposition of one, two, three and five ink layer(s).

The printing direction is indicated by the white arrows

mens made by one layer are impacted by the substrate surface. This hypothesis is supported by (i) the surface fractions of substrate that is not covered by the ink when one ink layer is transferred onto the substrate. The values are estimated to reach 60 ± 10 % and 30 ± 5 % with the anilox cylinders 4 and 13 cm^3 m^{-2} respectively. (ii), the reflectance spectrum of the substrate. Its reflectance spectrum ranges from 2.35 ± 0.06 % at 380 nm to 2.09 ± 0.05 % at 730 nm when the intrinsic reflectance spectrum of the ink I_{33} varies from 1.85 ± 0.07 % at 380 nm to 2.44 ± 0.05 % at 730 nm. If 60 to 30 % of the substrate are not covered by the ink, the substrate impact on the reflectance of the catalyst layer may be significant, as it is when considering half tone reproduction (Yang, 2003). In this study, it will tend to increase the reflectance value of the catalyst layer at low wavelength and reduce the reflectance values of the samples at higher wavelength values compared to the intrinsic reflectance of the ink.

Manufacturing catalyst layers by superimposing several ink layers leads to improved print quality. Consequently, when more ink layers are superimposed, the fraction of substrate not covered by the ink decreases. The reflectance values of the catalyst layer decrease, becoming darker and darker as expected. At the higher ink loading tested in this study (0.96 ± 0.01 mg cm^{-2}) the reflectance values do not reach the values of the intrinsic reflectance of the ink, showing an impact of the substrate on the reflectance measure.

The values of reflectance for wavelength equals to 390, 550 and 650 nm were extracted from the reflectance spectra and are given as a function of the ink loading in Figure 10.

The general trend described before, when reflectance spectra were compared as regards to the number of ink layers superimposed, remains visible. The reflectance values decrease with the increase of the ink loading. The particularity observed when only one ink layer is deposited onto the substrate is clearly visible for the catalyst layer made with the anilox of 4 cm^3 m^{-2}.

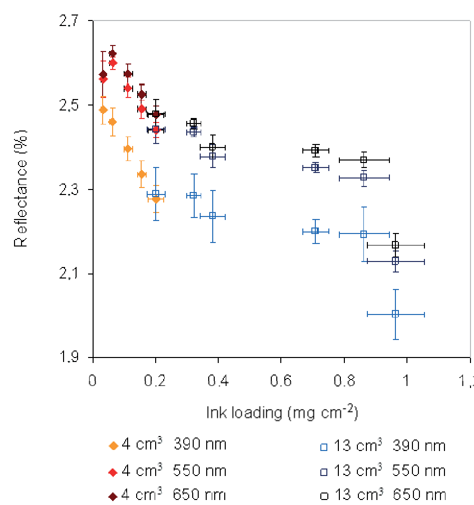

Figure 10: Reflectance values as a function of the specimens' ink loadings

However, the catalyst layer made with one ink layer with the anilox of 13 cm^3 m^{-2} shows expected results. In addition, this catalyst layer has an ink loading equal to 0.20 ± 0.01 mg cm^{-2} and reaches a reflectance value of 2.44 ± 0.03 %. This catalyst layer has a similar ink loading than one made by the superimposition of five layers with a 4 cm^3 m^{-2} anilox (0.20 ± 0.01 mg cm^{-2}), which has a reflectance value equal to 2.48 ± 0.03 %.

Hence, it confirms the correlation between ink loading and reflectance value, whatever the protocol of ink deposition is.

3.3.2 Influence of the platinum amount on the reflectance spectrum

The influence of the platinum amount on the reflectance of catalyst layers was evaluated using two inks I_{33} (with 33 w/w% platinum in the ink dry content) and I_0 (free of platinum). In order to obtain samples with similar platinum loadings, catalyst layers are manufactured with these two inks by superimposing one, two and three ink layers with the anilox of 4 $cm^3\ m^{-2}$. The reflectance spectra are measured on the catalyst layers and compared with the reflectance spectrum of the substrate in Figure 11.

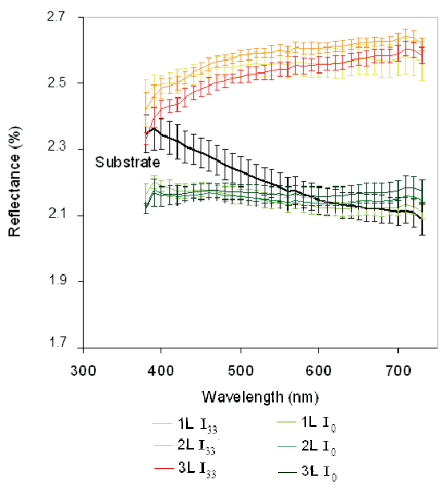

Figure 11: Reflectance spectra of specimens made with the I_{33} and I_0 deposited with an anilox of 4 $cm^3\ m^{-}$

The reflectance spectra of the samples made with the ink I_0 have values that range from 2.1 ± 0.02 to 2.2 ± 0.02 %. These values are significantly lower than the reflectance values of catalyst layers made with the ink I_{33} that varies from 2.64 ± 0.05 % to 2.33 ± 0.02 %. Therefore, the catalyst without platinum appears darker than the one containing platinum. Moreover, the shapes of the curves differ depending of the platinum presence. It also may indicate the type of ink transferred onto the SGL substrate. It is additional information that can be taken from reflectance spectrum measurement.

3.4 Use of reflectance spectra to characterise the superimposition of layers with different platinum amount

Reflectance spectra measurement allows accurate discrimination of the two inks studied in this paper. Subsequently, this technique was applied to visualise the consequences of the multilayer protocol on the structure of the catalyst layer manufacture by flexography. Tests were performed to observe where the components of an ink layer were located, after the superimposition wet on wet of several ink layers.

Layers of ink I_{33} are transferred onto SGL 24 BS samples. Then, without any drying, layers of ink I_0 are superimposed. Then, reflectance spectra are measured as described in Figure 12.

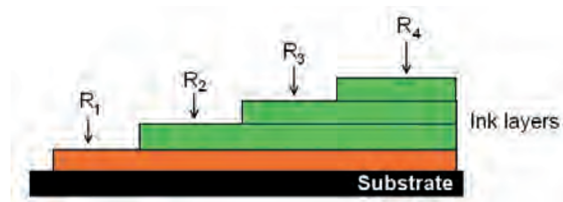

Figure 12: Scheme of the reflectance measures performed on the multilayer made by the superimposition of the inks I_{33} and I_0

SEM observations and reflectance measurements aim to follow the evolution of location of the platinum nanoparticles in the catalyst layer (Figure 15) and the recovering of catalyst layers with platinum by layers without platinum nanoparticles (Figure 13).

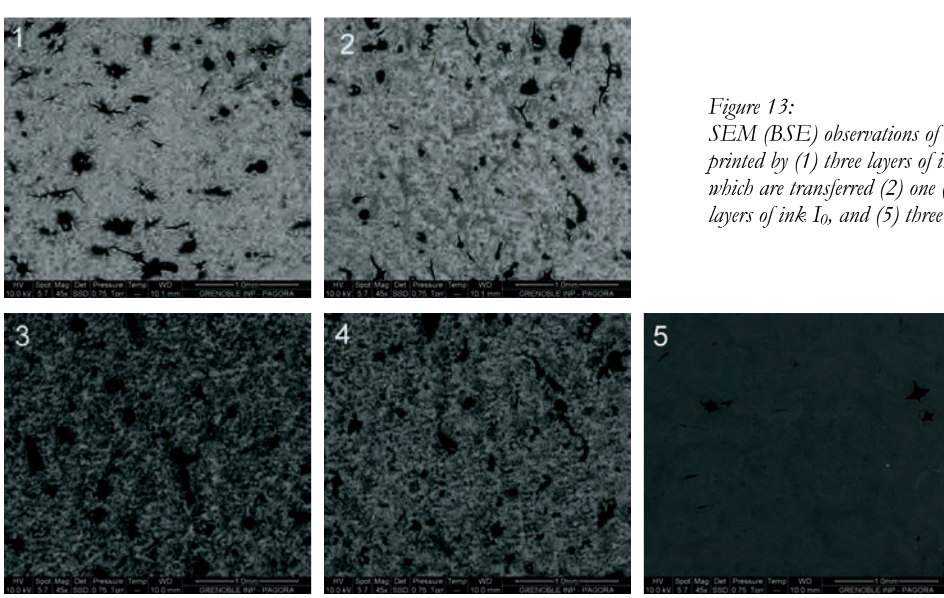

Figure 13: SEM (BSE) observations of the surface of specimens printed by (1) three layers of ink with platinum I_{33}, on which are transferred (2) one (3) two and (4) three layers of ink I_0, and (5) three layers of ink I_0

Figure 13 shows SEM surface view taken with the BSE device on different samples: (1) the sample printed by three layers of ink I_{33}, this is used the reference of brightness of surface view of layers containing platinum, (2-4) the previous sample (1) of ink I_{33} is then covered by one, two and three layer(s) of ink I_0, (5) finally, another reference is made by printing three layers of ink I_0, this sample is a reference of brightness of surface view of layers without platinum.

These observations are completed with the reflectance values of these samples at 390 nm shown in Figure 14.

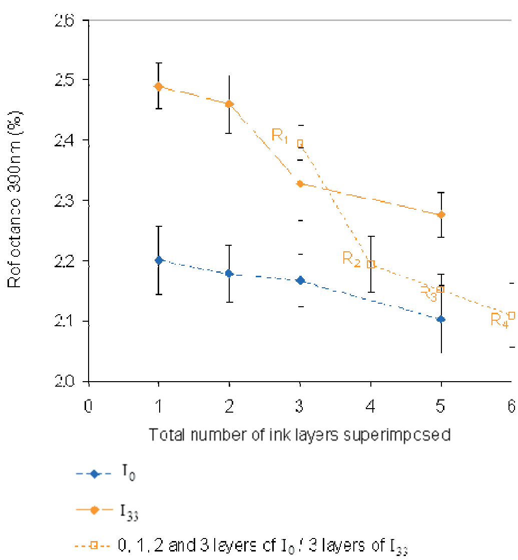

Figure 14: Reflectance of catalyst layer samples at 390 nm deposited on GDL as a function of the number of total ink layers transferred onto the substrate

The reflectance values at 390 nm of the samples previously described are compared with the reflectance values of samples made by one, two and three ink layers of the inks I_{33} or I_0 that were discussed in the previous sections. The reflectance values at 390 nm and the surface views of the samples present the same trends:

(i) the reflectance value R_1 of the sample composed three layers of ink I_{33} (Figure 13/1) is similar to the expected reflectance value, (ii) the more layers of ink I_0 are superimposed onto the three layers of ink I_{33} (Figure 13 samples 2, 3 and 4), the more the brightness of the SEM pictures diminishes, and the more the reflectance values at 390 nm tend from the reflectance values of layers only made by the ink I_{33} toward the reflectance of those only made by layer of ink I_0.

However, the multilayer (Figure 13/4) appears brighter than the reference made by three layers of ink I_0 (Figure 13/5). As an additional characterisation, the cross view of the sample of Figure 13/4 is presented in Figure 15.

This cross view is similar to those of the conventional catalyst layer of Figure 3. Figure 15 shows the microporous layer (Figure 15/a) of the GDL on which the printed catalyst layer is composed of two distinct parts. As compared to Figure 3, here, the catalyst layer shows a double layer: close to the GDL, the three ink layers with platinum nanoparticles appear brighter (Figure 15/b), and above them, the three layer of ink I_0 (Figure 15/c) are as dark as the microporous layer. This observation tends to confirm the reflectance values of Figure 14: no mixing between the layers with different compositions is visible.

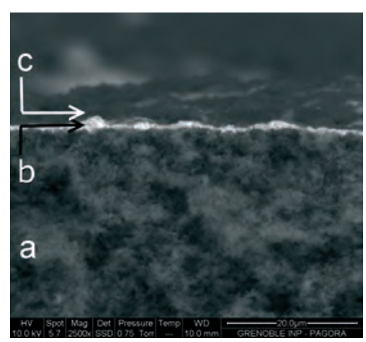

Figure 15: Cross view of GDL (a) printed with three layers of ink with platinum nanoparticles (b) covered by three layers platinum free ink (c)

4. Conclusion

In order to evaluate the platinum loading deposited onto a GDL for manufacturing fuel cell components by a multilayer protocol, two characterisation techniques have been tested on catalyst layers:

(i) Optical density in black offers a possible discrimination between catalyst layers with strong difference of ink loadings and catalyst layers with different amount of platinum nanoparticles. However, neither the ink loading variations nor the ink amount can be quantified using this technique.

(ii) Reflectance spectra were measured. This characterisation technique discriminates catalyst layer with same ink loading and different platinum amounts as well as catalyst layer with different ink loading whatever the two types of anilox used.

The reflectance is then applied to evaluate the potential migration of platinum nanoparticles when several ink layers are superimposed. Ink layers with platinum nanoparticles are printed on a GDL, and then they are recovered by layers free of platinum elements. The reflectance values of this multilayer are completed by SEM cross and surfaces view and tend to confirm that no mixing is measurable or visible between the different ink layers.

The measure of the reflectance is technically relevant for catalyst layer characterisation. Moreover, it is a fast, continuous and in-line technique and then economically pertinent compared to the conventional characterisation techniques.

As a complementary characterisation, this technique will be a great opportunity that will help to develop the use of continuous printing processes for fuel cell manufacturing. Further studies will look into the possibility of reflectance spectrum measurements to discriminate platinum quantity, not only by the superimposition of ink layers made with the same amount of platinum, but also to define the amount of platinum in layers made by ink formulated with different amounts of platinum.

References

Andrade, A. B., Mora Bejarano, M., Cunha, E. F., Robalinho, E. and Linardi, M., 2009. Fabrication of High Precision PEMFC Membrane Electrode Assemblies by Sieve Printing Method. *Journal of Fuel Cell Science and Technology* 6 2 021305

Bois, C., Blayo, A., Chaussy, D., Vincent, R., Mercier, A.-G. and Nayoze, C., 2012a. Catalyst Layers for PEMFC Manufactured by Flexography Printing Process: Performances and Structure. *Fuel Cells* 12 2

Bois, C., Blayo, A., Vincent, R., Nayoze, C. and Chaussy, D., 2011. Characterisation of catalyst layers for fuel cell printed by Flexography. *Advances in Printing and Media Technology* 38 237-245

Bois, C., Blayo, A., Vincent, R., Nayoze, C. and Chaussy, D., 2012. The Relevance of Printing Processes in Proton Exchange Membrane Fuel Cell Manufacturing. *TAGA Proceedings*, 18-21 March, Jacksonville, Florida, USA

Bultel, Y., Genies, L., Antoine, O., Ozil, P. and Durand, R., 2002. Modeling impedance diagrams of active layers in gas diffusion electrodes: diffusion, ohmic drop effects and multistep reactions. *Journal of Electroanalytical Chemistry* 527 143

Calvillo, L., Gangeri, M., Perathoner, S., Centi, G., Moliner, R. and Lázaro, M. J., 2011. Synthesis and performance of platinum supported on ordered mesoporous carbons as catalyst for PEM fuel cells: Effect of the surface chemistry of the support. *International Journal of Hydrogen Energy* 9805-9814

Chaparro, A.M., Folgado, M. A. , Ferreira-Aparicio, P., Martín, A. J., Alonso-Álvarez, I. and Daza, L., 2010. Properties of Catalyst Layers for PEMFC Electrodes Prepared by Electrospray Deposition. *Journal of The Electrochemical Society* 157 7 993-999

Denneulin, A., Bras, J., Blayo, A., Khelifi, B., Roussel-Dherbey, F. and Neuman, C., 2009. Substrate pre-treatment of flexible material for printed electronics with carbon nanotube based ink. *Nanotechnology* 20 385701

Fraga, M. A., Jordão, E., Mendes, M. J., Freitas, M. M. A., Faria, J.L. and Figueiredo, J. L., 2002. Properties of Carbon-Supported Platinum Catalysts: Role of Carbon Surface Sites. *Journal of Catalysis* 355–364

Franco, A., Schott, P., Jallut, C. and Maschke, B., 2007. A multi-scale dynamic mechanistic model for the transient analysis of PEFCs. *Fuel Cells* 7 99

Hébert, M. and Hersch, R. D., 2006. Reflectance and transmittance model for recto-verso halftone prints. *Journal of the Optical Society of America A* 23 10

Hirano, S., Kim, J. and Srinivasan, S., 1997. High performance proton exchange membrane fuel cells with sputter-deposited Pt layer electrodes. *Electrochim. Acta* 1997 42 1587

Hwang Doo Sung, Park Chi Hoon, Yi Sung Chul and Lee Young Moo, 2011, Optimal catalyst layer structure of polymer electrolyte membrane fuel cell. *International Journal of Hydrogen Energy* 36 9876-9885

Jeon Sunyeol, Lee Jisun, Rios Gema, M., Kim Hyoung-Juhn, Lee Sang-Yeop, Cho Eun Ae, Lim Tae-Hoon and Jang Jong Hyun, 2010. Effect of ionomer content and relative humidity on polymer electrolyte membrane fuel cell (PEMFC) performance of membrane-electrode assemblies (MEAs) prepared by decal transfer method. *International Journal of Hydrogen Energy* (2010) 9678-9686

Kettler, P.B., 2003. Platinum Group Metals in Catalysis: Fabrication of Catalysts and Catalyst Precursors. *Organic Process Research & Development* 7 342-354

Martin, S., Garcia-Ybarra, P. L. and Castillo, J.L., 2010. Electrospray deposition of catalyst layers with ultra-low Pt loadings for PEM fuel cells cathodes. *Journal of Power Sources* 195 2443-2449

Mercier, A.-G., Vincent, R., Nayoze, C., Blayo, A. and Soucemarianadin A., 2010. Inkjet Printing of Catalyst Layers Used in Fuel Cells Membrane Electrode Assemblies. *Advances in Printing and Media Technology* 37 319-325

Mustafa, U. H., Shige, I., Suzuki, H., Kobayashi, T., Miyazaki, Y., Ioroi, T., Yasuda, K., 2004, Dispersion control of nanoparticles and the effect of the coating condition on the performance of proton-exchange membrane fuel cells (PEMFCs). *Journal of Chemical Engineering of Japan* 37 1 31-39

Park In-Su, Li Wen and Manthiram, A., 2010. Fabrication of catalyst-coated membrane-electrode assemblies by doctor blade method and their performance in fuel cells. *Journal of Power Sources* 195 7078-7082

Pozio, A., De Francesco, M., Cemmi, A., Cardellini, F. and Giorgi, L., 2002. Comparison of high surface Pt/C catalysts by cyclic voltammetry. *Journal of Power Sources* 105 13

Sasikumar, G., Ihm, J.W. and Ryu, H., 2004. Dependence of optimum Nafion content in catalyst layer on platinum loading. *Journal of Power Sources* 132 11-17

Schonert, M., Jakoby, K., Schlumbohm, C., Mergel, J. and Stolten, D., 2004. Manufacture of Robust Catalyst Layers for the DMFC. *Fuel Cells* 4 3 175-179

Taylor, A .D., Kim, E.Y., Humes ,V. P., Kizuka, J. and Thompson, L. T., 2007. Inkjet printing of carbon supported platinum 3-D catalyst layers for use in fuel cells. *Journal of Power Sources* 171 101-106

Xie Jian, Xu Fan, Wood David L., More, K. L., Zawodzinski, T. A. and Smith, W. H. 2010. Influence of ionomer content on the structure and performance of PEFC membrane electrode assemblies. *Electrochimica Acta* (2010) 7404-7412

Yang Li, 2003. Characterization of inks and ink application for ink-jet printing: model and simulation. *Optical Society of America* 20 7

Yuan Xiao-Zi, Li Hui, Zhang Shengsheng, Martin, J. and Wang Haijiang, 2011. A review of polymer electrolyte membrane fuel cell durability test protocols. *Journal of Power Sources* 196 9107-9116

JPMTR 011 | 1211
UDC 655:621.38

Original scientific paper
Received: 2012-06-16
Accepted: 2012-07-17

Printing carbon nanotube based supercapacitors

Alexandra Hartman[1,2], *Liam O'Hara*[2], *Charles Tonkin*[2], *Duncan Darby*[2], *John Gustafson*[1], *William Ray*[1,2], *Vera Lockett*[1]

[1] Nth Degree Technologies Worldwide, Tempe, AZ, USA
E-mails: ahartman@NthDegreeTech.com
jgustafson@NthDegreeTech.com
wjr@NthDegreeTech.com
vlockett@NthDegreeTech.com

[2] Clemson University, Clemson, SC, USA
E-mails: lohara@clemson.edu
tonkin@clemson.edu
ddarby@clemson.edu

Abstract

Living in a world of portable electronics, there is great need for energy storage devices. Currently, these devices are mainly batteries which have such limitations as power inefficiencies and a relatively short cycle life. Double layer supercapacitors are promising alternatives to batteries at least in some applications which have lower energy densities but much higher power densities and a very long life span. As electronic devices are getting smaller in size, the bulkiness of modern energy storage devices is another concern. For these reasons, the research into the production of printable supercapacitors was carried out.

In this work, the supercapacitor electrodes were made from a combination of multi-walled carbon nanotubes and an ionic liquid. The materials were ground into a gel and then formulated into a printable functional ink. The supercapacitor electrodes were then printed onto a conducting carbon foam substrate and sandwiched on top of a membrane. Supercapacitors inks were formulated with two ionic liquids: 1-ethyl-3-methylimidazolium ethylsulfate and 1-ethyl-3-methylimidazolium bis(trifluoromethylsulfonylimide). The best formulation of inks was 40 w % of mixture of IL and carbon nanotubes in 1:9 proportion and 60 w % 1-methyl-2-pyrrolidinone.

The charge/discharge curves were used to calculate the current density and specific capacitance. Supercapacitors made of printed electrodes with 1-ethyl-3-methylimidazolium ethylsulfate were found to perform the best at lower and higher current densities (0.97 F cm^{-2} at 0.008 A cm^{-2} and 0.48 F cm^{-2} at 0.07 A cm^{-2}). Supercapacitors with 1-ethyl-3-methyl-imidazolium bis(trifluoromethylsulfonylimide) showed 0.61 F cm^{-2} at 0.008 A cm^{-2} and 0.39 F cm^{-2} at 0.07 A cm^{-2}. 1-ethyl-3-methylimidazolium bis(trifluoromethylsulfonylimide) based supercapacitors kept 86 % and 1-ethyl-3-methylimidazolium ethylsulfate based supercapacitors established at 78 % of initial performance after 100-150 cycles indicating relatively long life of the devices.

Keywords: multiwall carbon nanotubes, ionic liquid, printed supercapacitors

1. Introduction

With the world constantly developing new technologies in smaller sizes the need for thin film flexible energy storage devices is growing. Thin film batteries already exist on the market for powering devices such as wireless imbedded sensors, radio frequency identification tags, implantable medical devices, and non-volatile memory backup (Innovative Research and Products Inc., 2007). However, thin film batteries still have shortcomings like slow charge /discharge rates and a relatively short cycle life time. Supercapacitors store less energy than batteries but have the advantage that they can be charged and discharged in seconds and can withstand over a million charge/discharge cycles (Conway, 1999). In such applications as power tools, flash lights or uninterruptible power supply, supercapacitors are superior to batteries and manufacturing of thin film flexible supercapacitors is important.

A supercapacitor is an energy storage device that accumulates electric charges at the interface between an electronic conductor and an ionic conductor. A characteristic parameter for a supercapacitor is specific capacitance, F g^{-1}, which depends on many factors, including surface area of electrodes, double layer capacitance at the electrode / electrolyte interface, electrostability and conductivity of the electrolyte (Conway, 1999). The electrodes for double layer supercapacitors available on the market are usually made from activated charcoals. There is research in carbide derived carbon, graphene and carbon nanotube based supercapacitors which show higher potential for these materials in terms of increased energy density (Ji et al., 2011). Aqueous and non-aqueous electrolyte solutions are common ionic conductors used in supercapacitors. Recently, novel research in the application of ionic liquids (ILs) as an electrolyte for supercapacitors appeared to be promising (Katakabe et al., 2005). An ionic liquid is a special class of molten salts that is liquid at room temperature (Ohno, 2005). Their general traits include: high ionic conductivity, high thermal stability, nonvolatility, nonflammability, and high electrostability. A high operating voltage in supercapacitors has been realized by employing ionic liquids to values beyond three volts (Katakabe et al., 2005). Since a typical aqueous electrolytically based supercapacitor performs around 1.2 volts, an operating voltage of three volts or higher is a dramatic difference.

In this work, carbon nanotubes, ionic liquids, and conventional printing as a means of the electrode fabrication were used.

CNT-based supercapacitors and techniques of their assembly have been investigated by several research groups. For example, a research group from the University of California used an air gun that mimics the head of an ink-jet printer to deposit an entangled layer of CNTs suspended in water on a plastic substrate (Bourzac, 2009). The plastic substrate was then used to sandwich a gel electrolyte material. They were able to achieve a device with high power density of 70 kilowatts per kilogram. However, the energy density was insufficient to operate devices such as a cell phone. Boyea et. al. (2007) used a similar method called electrostatic spray deposition of binder free multiwalled CNTs onto a porous substrate. The CNT manufacturing method influenced the specific capacitance of each configuration: 10 F g^{-1} was achieved using CNTs grown by chemical vapor deposition, whereas 79 F g^{-1} was achieved using fluidized bed multiwall CNTs. Although the results were promising, this technique is both expensive and not a conventional printing process. Researchers from Stanford University created thin film CNT supercapacitors on commercial paper using a Meyer rod for coating and even ink-jet printing (Hu et al., 2010). A specific capacitance of 33 F g^{-1} and a device with a specific power of 250 kilowatts per kilogram hour were achieved in an organic electrolyte. Electrodes in supercapacitors based upon single walled CNTs on cloth fabric were deposited utilizing ink-jet printing (Chen et al., 2010). The yield from this research was a specific capacitance of 138 F g^{-1}, and a device with power density of 96 kilowatts per kilogram, and energy density of 18.8 watt hours per kilogram. None of the above supercapacitors assembly techniques follow true conventional printing processes and, therefore, are unable to create high throughput and economical devices that can be readily scaled up. This indicates that there is a need to further develop this approach.

Only a few works where carbon nanotubes were screen printed can be found in literature. The fabrication of CNT derived electrochemical sensors that exhibit high electrochemical reactivity and are mechanically stable has been achieved with screen printing (Wang and Musameh, 2004). Carbon nanotube based field emitter arrays for application in liquid crystal displays as the back lighting unit were also screen printed (Park, 2005). We have found no literature on CNT screen printing for energy storage devices.

Conventional printing, such as screen printing, affords the opportunity to print large quantities of supercapacitors at a lower applied cost in comparison with other methodologies currently being employed (spin coating, ink-jet printing, electrostatic spray deposition, etc.). Thus, printing carbon nanotubes is a desirable means to manufacture supercapacitors.

The purpose of this work was to develop printable and well performing supercapacitors. The use of carbon nanotubes allows for a substantial increase in power and energy density, while the ionic liquids provide a higher operating voltage. Using screen printing as the deposition technique means an affordable way to manufacture large quantities of supercapacitors. Not only are the produced supercapacitors environmentally friendly, due to material choice, they are also flexible and light weight.

2. Methods

2.1 Materials

Multi-wall carbon nanotubes (MWCNT) with surface area of 800 m^2 g^{-1} were provided by SouthWest Nano Technologies (SWeNT). The ionic liquids (ILs) were purchased from Iolitec at 99 % purity. The structure of the ions comprising the ionic liquids used, 1-ethyl-3-methylimidazolium bis(trifluoromethylsulfonylimide) (C_2mim TFSI) and 1-ethyl-3-methylimidazolium ethylsulfate (C_2 mimES), is shown in Figure 1. Their conductivity and viscosity are presented in Table 1.

The solvents used in preparation of MWCNT inks (1-methyl-2-pyrrolidinone (anhydrous, 99.5 %), propylene carbonate (99.7 %), 2-etho-xyethanol (99 %), di(propylene glycol) methyl ether mixture of isomers (99 %), and dipropylene glycol (99 %) were purchased from Sigma-Aldrich (Table 2). Celgard3501 membrane material was used for assembling the supercapacitors. The meshes for printing the MWCNT inks were purchased from Sefar and were PET 1500 43/110-80 and Sefar PET 1000 24/60-120. The inks were printed on Carbon Paper Grade 1 carbon foam (400 m^2 g^{-1}) which was acquired from Marketech International, Inc.

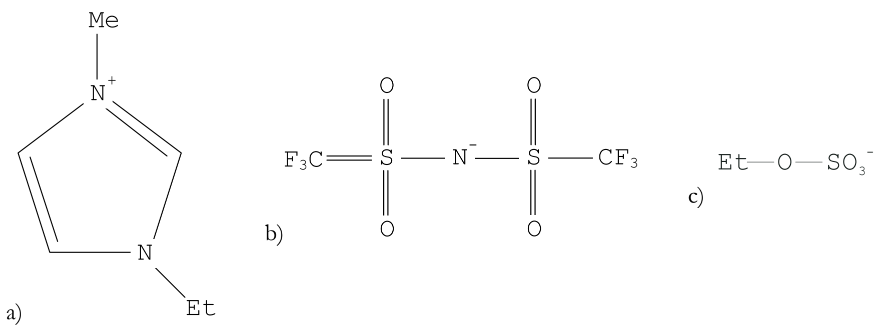

Figure 1: Structure of ions (a) 1-ethyl-3-methylimidazolim (C_2mim^+), (b) bis(trifluoromethylsulfonyl)imide ($TFSI^-$), (c) ethylsulfate (ES^-)

Table 1: Viscosity and conductivity of ionic liquids at 25 °C

Ionic liquid	Conductivity (at 25 °C), S m^{-1}	Viscosity (at 25 °C), cP
C_2mimES	0.382 (Vila et al., 2006)	97.58 (Gomez et al., 2006)
C_2mimTFSI	0.9 (Tokuda et al., 2006)	32 (Crosthwaite et al., 2005)

Table 2: Properties of solvents used in ink formulation

Solvent	Molecular formula	Boiling point in °C (Lide, 2004)	Viscosity
1-methyl-2-pyrrolidinone	C_5H_9NO	202	1.65 cP at 25 °C (Sigma Aldrich)
propylene carbonate	$C_4H_6O_3$	240	56.0 cP at 20 °C (Panjin Yunjia Chemical Co.)
2-ethoxyethanol	$C_4H_{10}O_2$	135	1.98 cP at 20 °C (Fisher Scientific, 2009)
di(propylene glycol) methyl ether mixture of isomers	$CH_3OC_3H_6OC_3H_6OH$	190	2.01 cP (Nth Degree Tech)
dipropylene glycol	$C_6H_{14}O_3$	230.5	48.45 cP at 20.25 °C (Wolfram Alpha, 2012)

2.2 Ionic liquid purification

Purification was required for the two selected ionic liquids because even small amounts of impurities can significantly influence IL properties (Seddon et al., 2000) and therefore the supercapacitors' performance (Conway, 1999). The purification procedure used in this work is described below using purification of C_2mimTFSI as an example. High purity water (18 MΩ·cm) was added to C_2mimTFSI at a 1:1 ratio, combined with high purity activated charcoal (Sigma Aldrich), and stirred for a twenty-four hour adsorption process. This mixture was filtered through a 55 μm pore filter paper in a Buchner funnel and through a 0.1 μm pore polytetrafluoroethylene (PTFE) syringe filter (Watman) to remove charcoal particles. Further purification was performed using an extraction technique. High purity ethyl acetate (Sigma Aldrich, 99.9 %), was added in a 1:1 ratio of ethyl acetate to the IL and water mixture. This mixture was agitated with a stir bar until well mixed then poured into a separatory funnel. This solution was allowed to sit until the split between the liquid layers clarified. The layer with the IL was recovered and the procedure was repeated. In case of water miscible C_2mimES IL, isopropanol (SigmaAldrich, 99.9 %), was used for the adsorption process and high purity water for the extraction. After extraction, ethyl acetate and water were evaporated under low heat at 60 °C and 10 mbar of vacuum for twenty-four hours. Finally, the IL was purged for four hours with high purity Ar to remove the rest of the water. Approximately 7 mL of the purified IL was placed in a three electrode electrochemical cell for purity analysis. The electrochemical cell consisted of a polished glassy carbon electrode as the working electrode, platinum wire as the counter electrode, and silver wire as the pseudoreference electrode. The IL was further purged for one hour before shutting off the purge and applying an Ar blanket to the cell. Cyclic voltammetry was performed on the IL to determine the presence of remaining impurities as well as at what potentials the IL remained stable. Cyclic voltammetry is a technique of sweeping potential (between -2.5-3 V to 2.5-3 V in this particular IL selection) of the cell and recording the resulting current response. The presence of unusual peaks within the electrostability range of the IL would indicate if the IL required a repeat of the purification process. The remaining purified IL was sealed with a PTFE cap and stored in a Lab Conco Dry Box Vacuum Chamber.

2.3 MWCNT preparation

Bucky gels were prepared by mixing CNTs with ionic liquids by two methods. In the first method, MWCNT were ground manually with one of the two ILs in an agate mortar and pestle for ten minutes. Measuring and grinding of the MWCNTs was handled in a negative pressure glove box. In the second method the MW CNT and ILs were manually ground for only thirty seconds. The material was then transferred to Pascall Engineering 60 Hz Mechanical Agate Mortar and Pestle for automated grinding for one hour.

2.4 Electrode pellet formation

MWCNT paste samples were processed into pellets using a pellet press fabricated for this purpose. The pellets were used to characterize the material before printing. Aluminum stock was used to fabricate the pellet press body and punches. The inner diameter of the pellet press was 13 mm. Flat PTFE discs of 13 mm were punched from a sheet of material as separators between the bucky gel and the aluminum punches. Pellets were made by loading the pellet press in a specific order. The bottom punch was loaded followed by a PTFE disc. The measured amount of MWCNT paste was then placed in followed by another PTFE disc and the second punch. The set-up was loaded into a Carver Hot Plate Uniaxial Press Model 3851-0. Pressure was applied to the pellet press between the two plates to a pressure setting of 2 metric tons (147 MPa). The finished pellets were weighed and then their thicknesses measured using an Electronic Thickness Gauge (ETG). The average thickness was 100 microns. Measured pellets were then placed in the Thermo Scientific Napco Vacuum Oven Model 5831 at 60 °C for drying.

2.5 Ink formulation

Inks were formulated using three different percent compositions of MWCNTs and one of the solvents (Table 2). The ink materials were mixed for 30 minutes using an IKA Lab Egg Stirrer at a medium mix setting. Finished inks were set aside for one day what allowed for material to settle. The inks were then inspected visually for separation of the CNTs from the solvent. If separation was minimal (or absent), inks were then tested by coating 25 micron thick film with a drawbar on a transparent polyethylene terephthalate (PET) sheet to simulate a print of the ink. The ink with the best uniformity of drawdown was selected as the basis for all further ink formulations.

2.6 Printing

Screen printing was used to transfer MWCNT paste ink through a stenciled design for supercapacitors. The design was a 13 mm diameter circle to match the size of the pressed pill electrode for the supercapacitor. The electrode prints were made by applying ink to a 110 screen count mesh with a 2 : 2 liquid emulsion with a stenciled image onto carbon foam substrate. This print was cured in an IR tunnel oven. The printing process was repeated 2-3 times to generate a printed electrode with thickness of 25 - 30 μm.

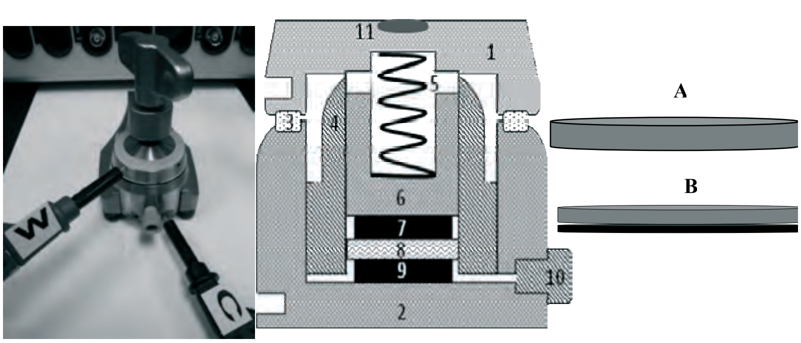

a b c

Figure 2:
(a) electrochemical cell;
b) cross-section of the cell:
(1) stainless steel lid, (2) titanium cell base,
(3) polyethylene ring spacer,
(4) polyether ether ketone sleeve,
(5) gold plated spring,
(6) titanium piston, (7) electrode,
(8) membrane, (9) electrode,
(10) PTFE plug,
(11) place for a tightening screw;
(c) types of electrodes:
(A) pressed MWCNT pellet,
(B) printed MWCNT paste on carbon foam

2.7 Supercapacitor assembly

Supercapacitors were assembled in an EL-Cell GmbH Electrochemical Test Cell ECC-REF (Figure 2a). The cross section of the cell is shown in Figure 2b. Two identical electrodes (7 and 9) were pressed between current collectors (2 and 6) with a membrane (8) in the middle. Pressure applied to the stack was due to a spring (5) tightened by a screw (11) (Figure 2a). The electrodes were pressed pellets or punched printed discs with 13 mm diameter (Figure 2c). The membrane was a porous polypropelene film (20 microns thick, 14 mm in diameter) soaked with either C_2mimTFSI or C_2mimES to match the ionic liquid used in the particular electrode set. The supercapacitor assembly was done in an inert environment inside a polyethylene glove bag from Glas-Col purged with ultra-high purity Ar. The cell was placed in the vacuum oven overnight to remove any trapped gas or moisture.

2.8 Measurement method of supercapacitors

A Metrohm Autolab Potentiostat PGSTAT302N was used to test the assembled supercapacitor cells. Cyclic voltammetry measurements were performed to determine the voltage range the cell operated at before the materials suffered decomposition.

It is a common practice to test and compare electrode material performance before calculating final device performance (Stoller and Ruoff, 2010). This not only avoids the impractical assembly of full size packaged cells but also allows accurate comparisons of the results for different materials and of different research groups. The supercapacitor specific capacitance (capacitance per gram of active materials (CNTs), F g^{-1}) was found by charging the cell to 2.3 V and discharging it at different current densities (amperes per gram of active material (CNTs), A g^{-1}).

Equation [1] was used to calculate the specific capacitance using the resulting discharge curve (Figure 3). In this equation, I is the constant current of discharge, V is voltage, t is time, and dV/dt is the slope of the discharge curve. The point V_{max} was the maximum operating voltage.

The slope was calculated using Equation [2] where V_{max} corresponds to the beginning of the linear portion of the discharge curve after the initial nonlinear IR drop at time t_1 and $V_{1/2max}$ is half of the V_{max} value at time t_2 (Figure 3). The capacitance [1] was divided by the active mass of the CNT electrodes, m, to give the specific capacitance in F g^{-1} using Equation [3] (Stoller and Ruoff, 2010). Active mass in the electrode pellets was the mass of CNTs and in the printed electrodes was the sum of masses of CNTs and carbon foam.

$$C = \frac{I}{\left(\frac{dV}{dt}\right)} \quad [1]$$

$$\frac{dV}{dt} = \left(\frac{V_{\max} - V_{\frac{1}{2}\max}}{t_2 - t_1}\right) \quad [2]$$

$$C_{sp} = 4\left(\frac{c}{m}\right) \quad [3]$$

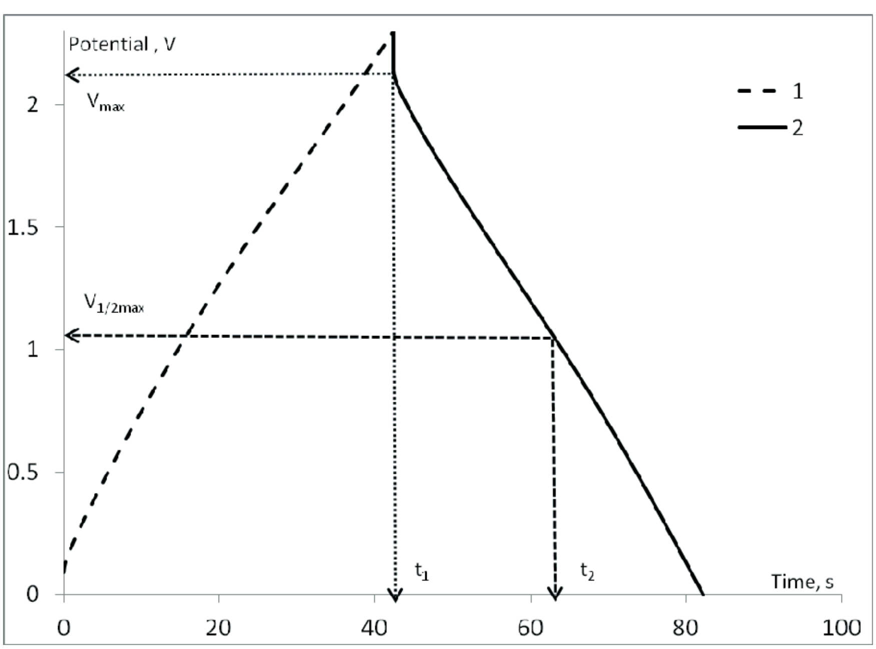

Figure 3: Charge [1] and discharge [2] curve of C_2mimTFSI/MWCNT supercapacitor at 0.5 A g^{-1} and 25 °C

3. Results and discussion

3.1 Improving performance of electrode pellets

The bucky gel pellets were used to estimate composition of electrodes and conditions of their preparation at which the CNTs and ionic liquids performance is favorable for supercapacitors. MWCNT paste electrode pellets were developed from 90 % C_2mimTFSI and 10 % MWCNT. Several compositions have been tried and the pellets made from these mixtures were found to hold their shape the best after pellet pressing. The dependence of specific capacitance on discharge current density of the C_2mimTFSI/MWCNTs supercapacitor is presented in Figure 4 curve (a).

The C_2mimTFSI/MWCNTs was ground for 10 minutes. Pellets were baked overnight at 60 °C and assembled into supercapacitors under Ar atmosphere. The supercapacitors were charged to 2.3 V and discharged at different current densities at 25 °C. The value of 2.3 V was found as a safe maximum potential for investigated supercapacitors from cyclic voltammograms (at this voltage no decomposition of ILs were found).

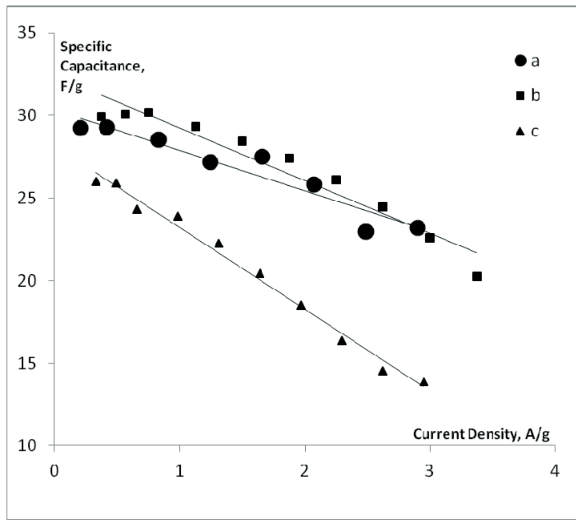

Figure 4: Dependence of specific capacitance on current density for MWCNTs/C2mimTFSI electrodes charged to 2.3 V: (a) ground 10 minutes (b) C2mimTFSI ground 1 hour (c) C2mimTFSI ground 1 hour with Teflon® binder

The specific capacitance was highest with 29.3 F g^{-1} at the low current density of 0.4 A g^{-1}. Specific capacitance decreased to 10.8 F g^{-1} at a current density of 3.7 A g^{-1}. These measurements were used as the baseline for comparing effects of different electrode compositions and electrode preparation conditions on supercapacitor performance. Four parameters were investigated and compared against the baseline: changing the overnight baking temperature, the MWCNT grinding time, adding a PTFE binder for pill integrity, and the IL anion.

Bucky gel pellets were baked overnight in the vacuum oven at 60 °C and 150 °C. The baking was needed for removing water impurities and improved ionic liquid wetting of the CNTs. Pellets dried at 150 °C showed decreased performance as compared to pellets dried at 60 °C. This could happen due to partial decomposition of IL under high temperature and vacuum or due to other reactions activated by these conditions, for example, reactions with functional groups present on MWCNTs. Thus, drying temperature of 60 °C was chosen for further experiments. Grinding the gels for longer periods of time was found to improve the performance of supercapacitors. This was probably due to improved wetting of the carbon nanotubes with IL. The grinding also improved the texture of the gel and in turn improved the integrity and formability of the pellets. Figure 4 curves (a) and (b) compare specific capacitance at different current densities for C_2mimTFSI/MWCNTs supercapacitors with pellets ground for 10 and 60 minutes, correspondingly, and charged to 2.3 V. The specific capacitance is higher for the supercapacitor with MWCNT pastes ground for 1 hour at all discharge current densities. Therefore, the grinding time of 1 hour was used for MWCNT pastes in further investigations. PTFE binder was used to investigate the binder influence on the supercapacitor performance. The binder was not needed for the pellets formation but was a necessary component for printed supercapacitor. It is used for ink adherence to substrates. The binder also further improved the pellets integrity. However, the addition of 1.76 % of PTFE binder was found to reduce capacitor performance (Figure 4 curve (c)). C_2mim TFSI/MWCNTs supercapacitors with PTFE charged to 2.3 V demonstrated specific capacitance in average 10 F g^{-1} lower than similar supercapacitors without the binder. This probably happened due to blockage of some of the available MWCNTs surface area where the double layer can form. The binder also could increase the overall resistance of the supercapacitor.

The influence of ILs on the supercapacitor performance is demonstrated in Figure 5. Two ILs with different properties (Table 1) were investigated in this work. The results for C_2mimES system are shown in Figure 5 curve (b). At higher current densities, charging to 2.3 V and discharging gave higher specific capacitances for C_2mimES than the C_2mimTFSI supercapacitor. The supercapacitor with C_2mimES showed high capacitance of 25.2 F g^{-1} at high current density of 5.9 A g^{-1}. This performance was somewhat surprising as C_2mimES has lower conductivity and nearly three times higher viscosity than C_2mimTFSI. The results can be explained by better ability for dispersion of MWCNTs in C_2mimES ionic liquid.

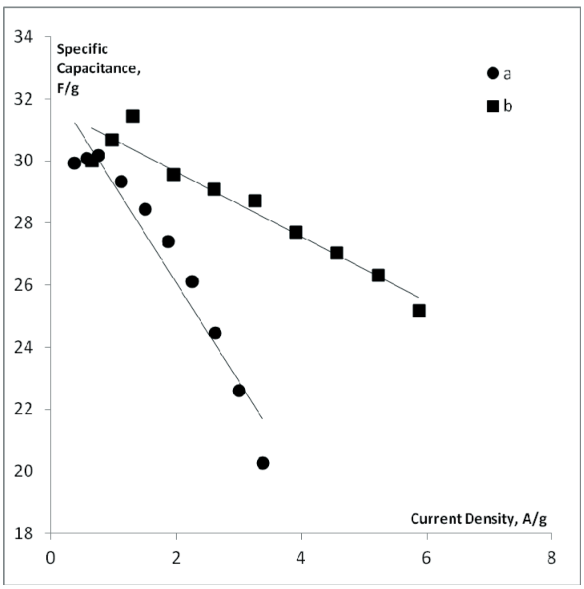

Figure 5: Dependence of specific capacitance on current density for MWCNTs/IL supercapacitors charged to 2.3 V with (a) C2mimTFSI and (b) C2mimES

3.2 Ink formulation

Five solvents with relatively high boiling point and viscosities (Table 2) 1-methyl-2-pyrrolidinone (MP), propylene carbonate (PC), 2-ethoxyethanol (EE), di(propylene glycol) methyl ether mixture of isomers (DGME), and dipropylene glycol (DG) were explored for preparation of inks from MWCNT pastes.

Initially, the solvents were tested for their ability to wet the carbon foam substrate and for their miscibility with both ionic liquids. Each solvent rapidly absorbed into the porous carbon foam substrate proving adequate wettability. All solvents were miscible with both ILs. The next step was to create various concentrations of the solvents with the bucky gel formulation. Three concentrations were prepared: 91 w% solvent to 9 w% bucky gel, 80 w% solvent to 20 w% bucky gel, and 60w% solvent to 40 w% bucky gel.

MP was discovered to function most optimally for dispersing the MWCNT paste evenly with a printable viscosity at a concentration of 60 % solvent and 40 % bucky gel. The ink was visually dispersed in the glass vial after one day, and using a drawbar showed that MP had the smoothest and most consistent deposit of ink on the PET substrate.

Through the pellets formation study it was observed that the use of binder decreases the performance of the supercapacitor. Therefore, only a minimal amount (0.7 % of the entire formulation) of PTFE binder was used in all formulations for a stable electrodes structure. This miniscule amount was also necessary for adhesion of the ink to the carbon foam substrate.

3.3 Printing

Printing of electrodes was carried out on porous carbon foam material (15 microns thick). Optimized conditions found from the pellets performance were used.

Carbon foam was used as a substrate for electrode printing. However, it also contributed to the electrode performance as carbon foam is a conductive and porous material. Figure 6 curve (1) exhibits the performance of the carbon foam when measured in the electrochemical cell without any print enhancement. These results reflect the capacitor performance charged to 2.3 V.

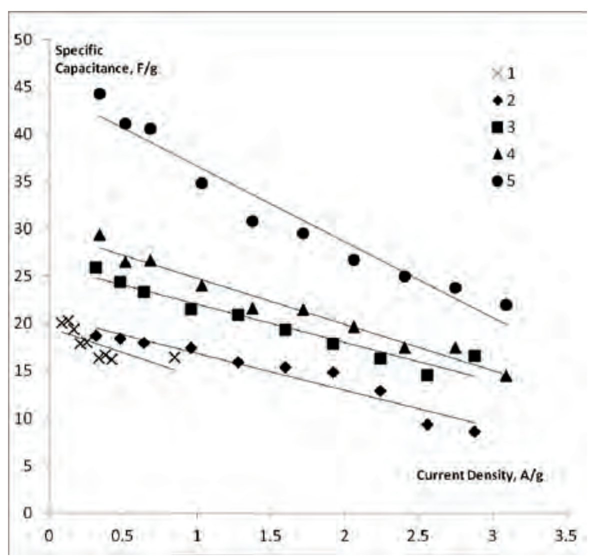

Figure 6: Dependence of specific capacitance on current density (1) carbon foam and C_2mimTFSI at 2.3V, (2) C_2mimTFSI at 2.3V, (3) C_2mimTFSI at 3.0V, (4) C_2mimES at 2.3V, (5) C_2mimES at 3.0V

As is seen in Figure 6 curve (1), 20 F g^{-1} was the highest achieved specific capacitance at 0.1 A g^{-1}. The carbon foam could not be charged/discharged at current densities more than 1 A g^{-1} due to its resistance. The effective current density more than tripled using the carbon foam in conjunction with printed MWCNTs and IL. This allowed for faster charging time of the supercapacitor (Figure 6 curves (2) and (4)). Moreover, we were able to charge the supercapacitor up to 3 V without noticeable decomposition of ionic liquids on cyclic voltamogram (not shown here). Specific capacitance for C_2mimTFSI supercapacitors charged to 3 V was in average 5 F g^{-1} higher than for supercapacitors charged to 2.3 V at all current densities as seen in Figure 6 curves (2) and (3). The specific capacitance had significantly higher values for C_2mimES supercapacitors charged to 3 V (Figure 6 curve (5)). It increased to 44 F g^{-1} at 0.4 A g^{-1} as compared to 29 F g^{-1} at the same current density for the C_2mimES supercapacitor charged to 2.3 V.

The printed supercapacitors showed slightly decreased performance than the supercapacitors made from MWCNTs pellets. This performance difference can be seen when comparing Figure 5 curve (a) and Figure 6 curve (2) for C_2mimTFSI supercapacitors and Figure 5 curve (b) and Figure 6 curve (4) for C_2mimES supercapacitors. However, this decrease is not significant if the inclusion of low surface area carbon foam electrodes, addition of Teflon binder, and the more complicated assembly technique are all taken into consideration.

It is more relevant that the data be displayed in terms of surface area because mass is not the best determining factor of the performance of a thin printed supercarpacitor. This is due to the small amount of materials for thin electrodes where it is difficult to precisely measure the mass. Mass can also be inconsistent due to the porous nature of the carbon foam. Each 13 mm diameter circle of carbon foam can weigh a different amount. Capacitance per cm^2, on the other hand, demonstrates how much charge can be stored per geometric area of the printed energy storage device in a precise manner. The recalculated data per surface area for printed supercapacitors is shown in Figure 7. The data shows that the C_2mimES based supercapacitor charged to 3 V outperformed the C_2mimTFSI based supercapacitor with outstanding 0.97 F cm^{-2} at low current density and 0.48 F cm^{-2} at 0.07 A cm^{-2}.

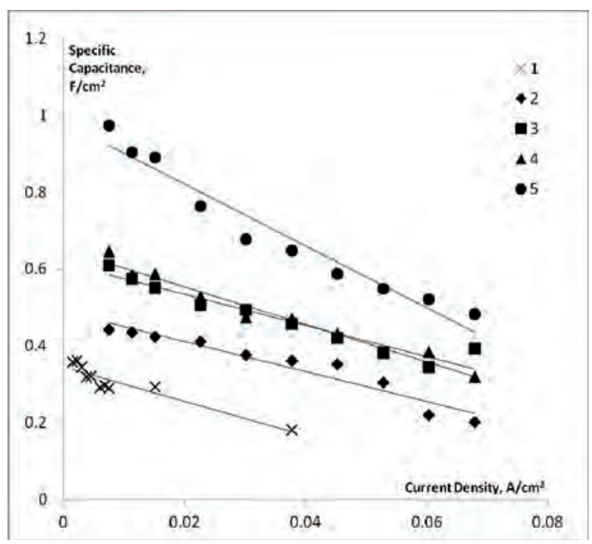

Figure 7: Dependence of specific capacitance on current density calculated per square area of electrodes (1) carbon foam and C_2mimTFSI at 2.3 V, (2) C_2mimTFSI at 2.3V, (3) C_2mimTFSI at 3.0V, (4) C_2mimES at 2.3V, (5) C_2mimES at 3.0V

In order to compare performance of printed MWCNTs electrodes with commercially available supercapacitors we assumed that MWCNTs will constitute one third of the final device mass. The energy and power (E and P_{Max}, correspondingly) were calculated using equations [4] and [5]:

$$E = \frac{CV^2}{2}, \quad [4]$$

$$P_{max} = \frac{V^2}{4R}, \quad [5]$$

where R refers to the equivalent series resistance. The values were divided by tripled mass of MWCNTs to get energy and power densities.

Data calculated for C_2mimES based supercapacitor charged to 3 V is presented on Ragone plot (Figure 8).

According to the latest measurements (Burke and Miller, 2011), the best commercial carbon/carbon devices have an energy density range of 3 - 6 Wh kg^{-1} and power density range of 0.1 - 3 kW kg^{-1}. Hybrid supercapacitors can reach up to 30 Wh kg^{-1} energy density and 4.5 kW kg^{-1} power density.

MWCNTs/ILs printed electrodes developed in this work are classified as carbon/carbon devices and their performance approximation (Figure 8) is comparable with the performance of recent (Burke and Miller, 2011) commercial supercapacitors. Both C_2mimTFSI and C_2mimES MWCNTs printed supercapacitors were charged and discharged 150 times at 0.5 A g^{-1} current density. The results are shown in Figure 9. After an initial decline to 78 % for C2mimES supercapacitor and to 86 % for C_2mimTFSI, the specific capacitance established after approximately 100 cycles.

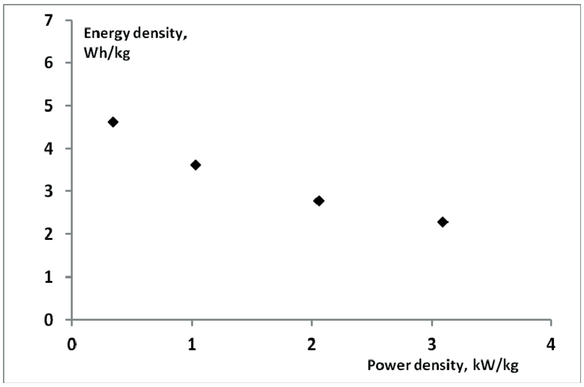

Figure 8:
Ragone plot of MWCNTs/ C_2mimES device performance (33% of device mass is assumed to consist of MWCNTs)

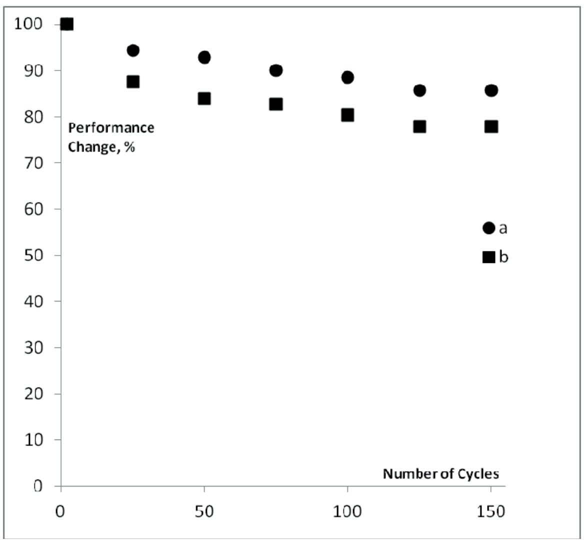

Figure 9:
Percentage change in specific capacitance of printed on carbon foam MWCNTs supercapacitors based on ionic liquids (a) C_2mimTFSI, (b) C_2mimES

4. Conclusions

Supercapacitors based on MWCNTs as a high surface area material and two ionic liquids, 1-ethyl-3-methylimidazolium bis(trifluoromethylsulfonylimide) and 1-ethyl-3-methylimidazolium ethylsulfate, as electrolytes have been investigated. Under optimum conditions of their preparation, both types of supercapacitors charged to 2.3 V showed specific capacitance around 30 F g^{-1} at a current density below 1 A g^{-1}. The C_2mimES supercarpacitor showed 25.2 F g^{-1} at high current density of 5.9 A g^{-1}, whereas the C_2mimTFSI supercapacitor could perform only up to 4 A g^{-1} and its specific capacitance quickly declined.

A technique was developed to print MWCNTs/ILs supercapacitors using specially formulated inks for screen printing and carbon foam as a substrate. The printed supercapacitors performed nearly as well as when compared to the MWCNT/ILs pellet supercapacitors. This is interesting considering the challenges presented by the substrate and binder required for successful printing. The best result was obtained for printed C_2mimES supercapacitor charged to 3 V when specific capacitance reached 0.97 F cm^{-2} at 0.008 A cm^{-2} and 0.48 F cm^{-2} at 0.07 A cm^{-2}.

Cycling the supercapacitors showed that after 100 cycles their performance established at 78 % for the C_2mimES supercapacitor and to 86 % for the C_2mimTFSI supercapacitor.

Performance of these supercapacitors is the same or higher than commercially available supercapacitors and have the potential for further improvement. The printing technique developed for supercapacitors is promising for future manufacturing level scaling and for printing of thin flexible devices.

References

Boyea, J., Camacho, R., Turano, S. and Ready, W., 2007. Carbon Nanotube-Based Supercapacitors: Technologies and Markets. *Nanotechnology Law & Business*, pp. 585-593.

Burke, A. and Miller, M., 2011. Recent test data for new advanced ultracapacitors and projections of future developments. *Proceedings of 21st International Seminar on Double Layer Capacitors and Hybrid Energy Storage Devices*, Florida, US, pp.17-34.

Chen, P., Chen, H., Xu, J. and Zhou, C., 2010. Printed Supercapacitors Based on Single Walled Carbon Nanotubes on Cloth Fabric and Flexible Substrates. *Nano Res*, (DOI 10.1007/s12274-010-0020-x).

Conway, B., 1999. *Electrochemical Supercapacitors: scientific fundamentals and technological applications*. New York: Kluwer Academic/Plenum Publishers, p. 698.

Crosthwaite, J., Muldoon, M., Dixon, J., Anderson, J. and Brennecke, J., 2005. Phase transition and decomposition temperatures, heat capacities and viscosities of pyridinium ionic liquids. *Journal of Chemical Thermodynamics*, 37, pp. 559-568.

Gomez, E., Gonzalez, B., Calvar, N., Tojo, E. and Dominguez, A., 2006. Physical Properties of Pure 1-Ethyl-3-methylimidazolium Ethylsulfate and Its Binary Mixtures with Ethanol and Water at Several Temperatures. *Journal of Chemical and Engineering Data*, 51, pp. 2096-2102.

Hu, L., Wu, H. and Cui, Y., 2010. Printed energy storage devices by integration of electrodes and separators into single sheets of paper. *Applied Physics Letters*, 96(18/183502).

Innovative Research and Products Inc. 2007. *Flexible Thin-Film Batteries: A Global Technology, Industry and Market Analysis*, (ET-104) p. 93.

Ji, X., Hallam, P., Houssein, S., Kadara, R., Lang, L. and Banks, C., 2011. Printable thin film supercapacitors utilizing single crystal cobalt hydroxide nanosheets. *RSC Advances*, 2, pp. 1508-1515.

Katakabe, T., Kaneko, T., Watanabe, M., Fukushima, T. and Aida, T., 2005. Electric Double-Layer Capacitors Using "Bucky Gels" Consisting of an Ionic Liquid and Carbon Nanotubes. *Journal of the Electrochemical Society*, 152(10), pp. A1913-A1916.

Lide, David. ed., 2004. *CRC Handbook of Chemistry and Physics, 85th Edition*. CRC Press.

Ohno, H., 2005. Electrochemical Aspects of Ionic Liquids. 2nd ed. Wiley Journal Polymers for Advanced Technologies, p. 485.

Park, J., 2005. Screen printed carbon nanotube field emitter array for lighting source application. *Journal of Vacuum Science & Technology B: Microelectronics and Nanometer Structures*, 23(2), pp. 749-753.

Seddon, K., Stark, A. and Torres, M., 2000. *Pure and Applied Chemistry*, 72, pp. 2275-2287.

Stoller, M. and Ruoff, R., 2010. Best practice methods for determining an electrode materials performance for supercapacitors. *Energy and Environmental Science*, 3, pp. 1294-1301.

Tokuda, H., Tsuzuki, S., Susan, M., Hayamizu, K. and Watanabe, M., 2006. How Ionic Are Room-Temperature Ionic Liquids? An Indicator of the Physicochemical Properties. *Journal of Physical Chemistry B*, 110(39), pp. 19593-19600.

Vila, J., Gines, P., Pico, J., Franjo, C., Jimenez, E., Varela, L. and Cabeza, O., 2006. Temperature dependence of the electrical conductivity in EMIM-based ionic liquids Evidence of Vogel Tamman Fulcher behavior. *Fluid Phase Equilib.*, 242, pp. 141-146.

Wang, J. and Musameh, M., 2004. Carbon nanotube screen-printed electrochemical sensors. *Analyst*, 129, pp. 1-2.

Internet references

Bourzac, K., 2009. Print-On-Demand Power: Flexible carbon-nanotube supercapacitors could give more power to cell phones and other electronics. *Technology Review*. Available at: < http://www.technologyreview.com/energy/22544/> [Accessed 8 August 2011]

Fisher Scientific, 2009. *Material Safety Data Sheet: Ethylene glycol monomethyl ether*. [pdf] Available at: <http://wku.edu/msds/docs/2855.pdf> [Accessed 15 May 2012].

Panjin Yunjia Chemical Company, Ltd. *Propanediol*. [online] Available at: <http://www.dtjchem.com/template/Propanediol_en.html> [Accessed 15 May 2012].

Sigma Aldrich. *Product Information: 1-methyl-2-pyrrolidinone*. [pdf] Available at: <http://www.sigmaaldrich.com/etc/medialib/docs/Sigma/Product_Information_Sheet/1/m6762pis.par.001.File.tmp/m6762pis.pdf> [Accessed 15 May 2012].

Wolfram Alpha, 2012. *What is the viscosity of 1,3-propylene glycol?*. [online] Available at: <http://www.wolframalpha.com/entities/chemical_viscosities/what_is_the_viscosity_of_1,3-propylene_glycol%3F/vv/mi/rl/> [Accessed 15 May 2012].

JPMTR 012 | 1206
UDC 655:621.38

Research paper
Received: 2012-04-06
Accepted: 2012-07-09

Flat-plate capacitors printed on paper

Maša Horvat [1], *Tjaša Vidmar* [2], *Marijan Maček* [2], *Raša Urbas* [3]
Gorazd Golob [3], *Miha Čekada* [4], *Marta Klanjšek Gunde* [1]

[1] National Institute of Chemistry, Slovenia — E-mails: masa.horvat@ki.si; marta.k.gunde@ki.si
[2] UL, Faculty of Electrical Engineering, Ljubljana, Slovenia — E-mails: tjasa.vidmar@fe.uni-lj.si; marijan.macek@fe.uni-lj.si
[3] UL, Faculty of Natural Sciences and Engineering, Ljubljana, Slovenia — E-mails: rasa.urbas@ntf.uni-lj.si; gorazd.golob@ntf.uni-lj.si
[4] "Jožef Stefan" Institute, Slovenia — E-mail: miha.cekada@ijs.si

Abstract

Multilayered passive electronic elements were screen-printed on the conventional paper and on the paper developed for printed electronics. The solvent-based electrically conductive ink with silver particles was applied for conductive plates and the UV-curable dielectric ink for the interlayer. The conditions for good print and electrical quality were determined other than those recommended by the producer. When dielectric layer was single-printed, the capacitance of flat-plate capacitors and the occurrence of electric defects depend on UV curing energy applied for dielectric layer. The effect was explained by partial dissolving of the bottom conductor with the solvent from the wet top layer. The effect vanishes when the dielectric layer is cured with about three times the recommended UV curing dose. The entire phenomenon disappears completely when the dielectric layer was double printed wet-on-dry, with the recommended UV curing. Capacitors with 10-20% higher capacitance were obtained on smooth surface of paper dedicated for printed electronics.

Keywords: printed electronics, conductive ink, dielectric ink, ultraviolet curing, capacitance

1. Introduction

The suitability of paper to be a substrate for low-cost electronics offers graphic technology to survive full implementation of information technologies (Berggren et al., 2007; Siegel et al., 2010; Leenen et al., 2009). The advantages of printing electrical functionalities on paper were reviewed recently by Tobjörk and Österbacka, naming the promising application area as "paper electronics" (2011). Most encouraging are applications in which a rough and porous paper surface is beneficial over the smooth and impermeable surfaces such as of plastic foils. One such example is the coffee stain effect appearing on ink-jet drops when printed on plastic substrastrate; the effect does not happen on paper without barrier layer (Mercier et al., 2007; Bollström et al., 2009).

While much research has been published about printing of active electronic components, very little has been reported about printing passive components. Nevertheless, capacitors printed on paper which could provide large capacitance and uniform electric field between both conductive plates are a promising application for storing charge and creating a homogeneous electric field (Tobjörk and Österbacka, 2011). Larger capacitance requires conductive plates to be as close as possible, but completely isolated; this requires as thin as possible dielectric layer between them. Such a layer must be completely free of pinholes; any defect leads to electric short-cut which neutralizes the charge stored on conductive plates and breaks the electric field between conductive layers. A material with large dielectric constant must be used (i.e. high-k material) to provide the capacitor with higher capacitance. In addition, a high dielectric strength must be assured to prevent electric breakdown. These requirements could be met by flat-plate capacitors printed on paper (Klanjšek et al., 2011).

This research was dedicated to analyse printing parameters of flat-plate capacitors screen-printed on two different paper substrates, one for conventional printing and the other devoted to paper electronics. It answers two questions: (i) do the flat-plate capacitors printed on the dedicated paper have higher capacitance and (ii) whether flat-plate capacitors can be prepared by single-printed layer instead of double-printed. The research was dedicated also to understand the intrinsic material reasons for the electrical properties of printed flat-plate capacitors. The directions for further research are also described.

2. Materials and methods

Two functional printing inks were used, conductive and dielectric. A silver based ink, designed for printing of RFID antennae onto paper and polyester film was applied as conductor (Electrodag PM-470, Acheson Industries, Netherlands). It consists of finely distributed silver particles in a thermoplastic resin. Its density is around 2 140 kg m^{-3} and the solid content is 58 - 62 %. The Brookfield viscosity is specified to be 11 000 - 4 000 mPa·s (30 °C, 20 r min^{-1}).

The manufacturer recommends at least 15 minutes drying at 120 °C. Sheet resistance (surface resistivity) of 25 µm thick dry layer is defined at 0.008 - 0.015 Ω sq^{-1} which corresponds to specific resistivity (volume resistivity) of 2.0 - 3.75 $\cdot 10^{-5}$ Ω cm. The second ink was a screen printable UV curable flexible dielectric ink designed for polymer thick film application from Acheson Colloiden B.V., Netherlands (Electrodag 452 SS). It is recommended to insulate and protect low voltage circuity on polyester and polycarbonate film. The ink was optimised to have good adhesion also on silver and carbon-based coatings where it is supposed to provide layers without cracking and conductive traces. The ink consists of magnesium silicate pigments in urethane acrylate binder which provides a dielectric constant of 5.09 in dry layers. Its density is 1 250 kg m^{-3} and Brookfield viscosity about 12 000 mPa·s (at 20 °C and 20 r min^{-1}). The ink is translucent green and has no volatile organic compounds. The sheet resistance of a dry 25 µm thick layer is $2\cdot 10^9$ Ω sq^{-1} and the AC dielectric strength is 2 400 V. The ink is recommended to be cured at UV energy of 500-700 mJm^{-2} (Acheson, product data sheets).

Two different paper substrates were used, Pe:smart paper type 2 (Felix Schoeller Service GmBH & Co. KG, Germany), which is dedicated for printed electronics, and Biomatt (Paprinica Vevče, Slovenia), which is suitable for conventional printing. Pe:smart paper is coated on both sides and has additional hydrophilic nanoporous coating on the front surface. It is a very white paper (L^*=95.5, a^*=-1.1, b^*=-2.5), 205 µm thick, with grammage 200 g m^{-2}. The Biomatt is a non-calendered white paper (L^*= 93.1, a^* = 1.1, b^* = -4.6), both-side coated, 140 µm thick, with 150 g m^{-2}.

The applied print forms (Figure 1) contain all shapes necessary to prepare three flat-plate capacitors, C1 (20 x 20 mm^2), C2 (10x10 mm^2) and C3 (5x5 mm^2) and structures to measure electric short-cuts, L1 (2 mm - 2 mm) and L2 (1mm-1mm). Two SEFAR® high-modulus monofilament polyester plain weave meshes were applied; 62/64Y (62 threads/cm, open area 30.1 %, theoretical ink volume 30.4 $cm^3 m^{-2}$) and 120/34Y (120 threads/cm, open area 29.6 %, theoretical ink volume 16.3 $cm^3 m^{-2}$). A squeegee with hardness 75 °Sh was used for printing. Much attention was paid to accurate overprinting of the necessary shapes in the multi-layered structure. Some samples were prepared with single printed dielectric layers and some with double printed. Each layer was dried prior to overprinting.

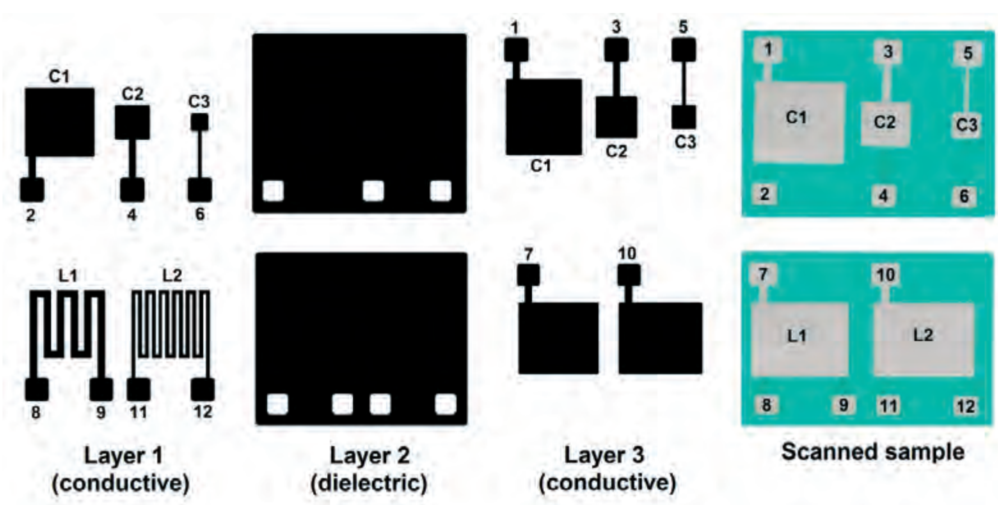

Figure 1: The print forms for the three flat-plate capacitors C1 (20x20 mm^2), C2 (10x10 mm^2) and C3 (5x5 mm^2) (top) and for the testing structures L1 (2 mm - 2 mm) and L2 (1 mm - 1 mm) used to measure the appearance of electrical short cuts. Scanned samples prepared with UV curing of 1400 mJ c^{-2} are shown on the right.

The conductivity of conductive layers depends on several printing parameters (Žveglič et al., 2009; Žveglič et al., 2011). Following our previous research, the highest conductivity is obtained if prints are first air-dried for 5 minutes to achieve proper aligning of conductive particles and then passed through the IR drying tunnel five times at 200 °C; it takes together about 7.5 minutes at 200 °C. Dielectric layers were cured using the UV dryer

Aktiprint L 10-1 (Technigraf Germany) having air-cooled medium pressure mercury lamp with power density 120 W cm^{-1}. The UV curing energy of 450, 900 and 1 400 mJ cm^{-2} were obtained by 100 % power of the dryer using 10, 5, and 3.3 m min^{-1} speed of conveyor belt, respectively. The highest UV energy (2 800 mJ cm^{-2}) was obtained by two successive passes of the sample through the UV dryer at the smallest speed of the conveyor belt (3.3 m min^{-1}). The UV doses were measured by UV integrator (Technigraf Germany) which passed the UV dryer at the above specified conditions.

The topology of surfaces was evaluated by profilometer Talysurf (Rank Taylor Hobson series 2). It scans the surface mechanically with a diamond tip and transforms the data into a height profile of the measured surface.

These data were used to obtain the average surface roughness R_a. The smoothness was evaluated by Bendtsen air permeability tester according to ISO 8791-2:1990. The Cobb water absorbency (ISO 535:1991) was applied to express the amount of water pick-up per unit surface area of the papers used.

Electrical properties of the printed samples were measured by Agilent 4284A precision LCR meter at 1 MHz. Capacity and serial resistance (model Cs-Rs) were measured on square shaped capacitors C1, C2 and C3 (see Figure 1).

From the known surface areas and perimeters of these structures the defect density was also estimated in terms of UV curing energy and paper substrate.

3. Results and discussion

The papers used have different properties (Table 1). The surface roughness (R_a) of the Pe:smart surface is about 8-times lower than that of the Biomatt. However, Bentsen air permeability shows much smaller difference, only a factor of two. The Pe:smart paper has twice as large a water absorptiveness ($Cobb_{60}$) as the Biomatt paper.

Table 1: Surface properties of the applied papers: the average surface roughness (R_a), air permeability (Bentsen) and water absorptiveness ($Cobb_{60}$)

Paper	R_a (μm)	Bentsen (mL min^{-1})	$Cobb_{60}$ (g m^{-2})
Pe:smart	0.11	10	14.9
Biomatt	0.85	5	7.3

The stability of paper substrates against heating and curing of printed layers was analysed by CIELAB colour difference ΔE caused by exposure of papers to a wide range of drying and curing conditions. The ΔE remains well below 1 (precisely, it may reach up to 0.6) at the conditions applied for the present study (Žveglič et al., 2011). Therefore the heating and curing conditions specified in the preceding section can be regarded as acceptable.

The average surface roughness (R_a) of individual layers depends on the applied substrate and mesh density. Three measurements were accomplished on all printed samples (see Figure 1) with the profilometer sampling length set to 4 mm.

All measurements were made on final samples which accomplish all thermal and UV curing processes. The roughnesses of conductive and dielectric layers and of conductive/dielectric and dielectric/conductive double layers printed on paper surfaces are given in Table 2. The layers are denoted by F1 (first conductive layer), F2 (dielectric layer) and F3 (second conductive layer). All dielectric layers were single-printed. While practically no dependence of roughness on the applied UV curing energy was obtained, each result in Table 2 represents the average of 12 measurements, i.e. four samples with three repeats.

Table 2: Average surface roughness (R_a) and standard deviation (σ) of conductive (F1) and dielectric (F2) single layers and of F1/F2 and of F2/F3 double layers printed on Pe:smart and Biomatt papers applying mesh with 62 or 120 threads/cm. All layers have undergone the entire thermal drying and UV curing conditions. The notation F3 means the conductive layer printed over the F2 layer

	Pe:smart				Biomatt			
	62 threads/cm		120 threads/cm		62 threads/cm		120 threads/cm	
	R_a (μm)	σ (μm)	R_a (μm)	σ (μm)	R_a (μm)	σ (μm)	R_a (μm)	σ (μm)
F1	1.39	0.24	1.26	0.10	1.36	0.09	1.15	0.13
F2	1.70	0.37	1.17	0.13	1.16	0.21	0.75	0.20
F1/F2	0.62	0.17	0.60	0.15	0.64	0.13	0.69	0.12
F2/F3	1.72	0.24	1.34	0.26	1.88	0.45	1.12	0.20

In general, the denser mesh (120 threads/cm) gives smoother layers than the coarser one (62 threads/cm). Printing on Pe:smart paper gives layers with larger surface roughness than the substrate (cf. Table 1 and 2), but when the Biomatt paper was applied for printing, smoother samples could be obtained when the dielectric layer is on the top (F2 or F1/F2 from Table 2). Overprinting with dielectric ink gives lower surface roughness in all studied examples; the values are almost independent on mesh density and paper substrate used. The dielectric ink fills the surface irregularities of the F1 layer equally on both papers because the underlying F1 layer makes printing conditions on both papers very similar. Another interesting result is that the conductive ink produces layers with roughness from 1.2 to 1.8 μm with no appreciable dependence on printing basis, i.e. whether it is applied over paper or over dielectric layer. The conductive layer which was freshly printed over the dielectric layer looked well as long as is remained wet; however, several surface wrinkles appeared after its drying. The quality of this conductive layer depends strongly on the UV energy applied for the dielectric layer. The effect is largest at the lowest energy and disappeared above 1 500 mJ cm^{-2} (Figure 2).

It is somewhat less pronounced on Pe:smart paper, but is still clearly observable by bare eye. The visual inspection shows that the effect appears only on places where the conductive layer is printed below the dielectric one (compare Figures 1 and 2).

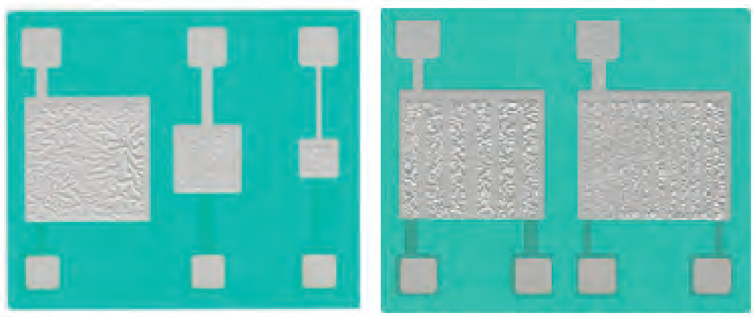

Figure 2: The three printed capacitors (left) and the two testing structure (right) obtained when the dielectric layer was cured by 450 mJ cm^{-2}. The samples on Biomatt paper printed with mesh having 62 threads/cm were scanned. Compare to the Figure 1

The effect was evaluated by average surface roughness of the three-layered prints in dependence on UV energy applied to cure the dielectric layer (Figure 3).

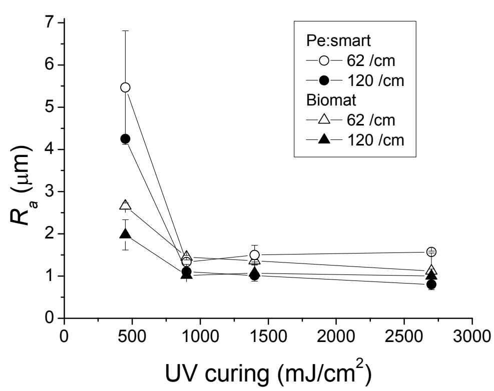

Figure 3: The average surface roughness of three-layered prints in dependence on UV energy applied for dielectric layer. The density of applied meshes is given in the legend. The error bars show the corresponding standard deviation

Because the effect appears in the larger scale, roughness measurements were done on capacitors surface with 8 mm profilometer sampling length. The obtained average R_a is very large at 450 mJ cm^{-2} and drops considerably at 900 mJ cm^{-2}. This effect is larger on Pe:smart paper and if coarser meshes (62 threads/cm) were applied. It vanishes completely at 1 400 mJ cm^{-2}.

The phenomenon is observable very clearly on both testing structures (L1 and L2); they wind and form parallel lines showing the shape of the bottom conductive layer. At low UV curing energy the surface profile of this three-layered structure shows an extremely thick bottom conductive layer which reaches a reliable size when the dielectric layer is cured by at least 900 mJ cm^{-2} (Figure 4).

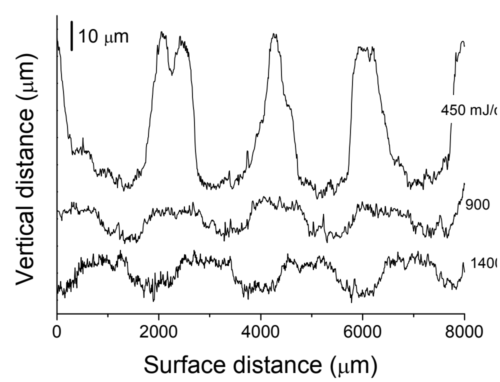

Figure 4: The surface profile of the three-layered test structure L2 printed on Pe:smart paper applying meshes with 120 threads/cm and cured at specified UV curing energy. The bottom conductive layer consists of 1 mm wide parallel lines separated by 1 mm (see L2 on Figure 1)

The effect is larger on Pe:smart and much smaller on Biomatt papers and is stronger for mesh with 62 threads/cm. The wavy surface profile could be used to measure the apparent thickness of the bottom conductive layer (F1). These results are shown in Figure 5. The UV curing above 1 000 mJ cm^{-2} does not influence further on the apparent layer thickness.

The electrical defects, i.e. shorts between bottom and top capacitor electrodes were detected by the help of test structure (between contacts 7-8, 7-9, 10-11 and 10-12, see Figure 1). Shorts are generated mostly (about 95%) in the bulk of the capacitor and rarely (5 %) on the edges. A density of defects 0.13 def/cm^2 was found on structures printed on the Pe:smart paper and 0.35 def/cm^2 for those on the Biomatt paper.

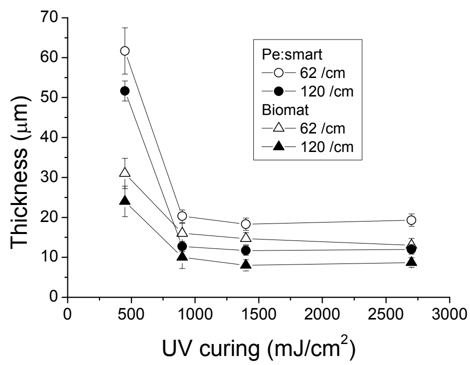

Figure 5: The apparent thickness of the bottom conductive layer as obtained from surface profiles of the three-layered structure (Figure 4) in dependence on UV curing applied for dielectric layer. The density of applied meshes is given in the legend. The error bars show the corresponding standard deviation

The serial capacitance C_s of the three capacitors as a function of UV curing energy applied for the dielectric layer is shown in Figure 6. It increases with UV curing and becomes constant above 1 500 mJ cm^{-2}. It was possible to measure only on few identically prepared samples which were cured below 1 500 mJ cm^{-2} and on all samples with higher UV curing. This phenomenon occurs in the same region where the surface roughness (R_a), the surface profile and the apparent thickness of the bottom conductive layer depend on UV curing (Figures 3-5). The most interesting result is that the capacitances become independent of the applied UV curing energy when the shape of their surface becomes independent on UV curing. Therefore, a curing at least twice heavier than recommended by the producer is needed to reach the electrical functionality of printed capacitors.

The effects presented in Figures 2 - 5 could be explained by swelling of the bottom conductive layer. This may happen if the solvent from the wet top conductive layer protrudes through the dielectric layer (e.g. through its imperfections), dissolves the bottom conductor and increases its thickness. This may cause several irregularities of the corresponding conductor-dielectric inter-layer (e.g. empty spaces between both conductive layer) which diminish the serial capacitance of the printed functionality. Further research is needed to understand the intrinsic material reasons for this phenomenon. The most important issue is how the penetration of the solvent trough the cured dielectric layer is prevented at heavy curing.

The described unusual influence of print quality and electrical functionality on the UV curing energy confirms the need of double-printing (wet-on-dry) of the dielectric layer. In functionalities printed this way no electrical defects were obtained and the corresponding serial capacitance does not depend on UV curing energy (Figure 6). Qualitatively the same results were obtained for both mesh densities applied for printing.

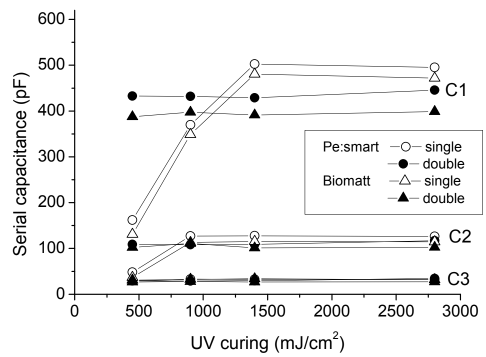

Figure 6: Serial capacitance of the three capacitors, C1, C2 and C3 as a function of UV curing energy applied for single-printed (open signs) and double-printed dielectric layer (full signs). The capacitors were printed on Pe:smart (circles) and Biomatt paper substrates (triangles) applying meshes with 120 threads/cm

In single-dielectric printed structures some places may exist where cracks or analogous defects are formed in the dielectric layer giving rise to conductive traces between both conductive layers which causes electrical defects - it occurs in random places of each individual dielectric layer. In the overprinted layer such locations appear in different places, therefore they cover each other. The double-printed dielectric layer thus diminishes the probability of electrical shorts between both electrodes and protects the solvent from the top conductor to permeate to the bottom one.

It is reasonable to compare capacitances of single-layered and double-layered dielectrics which were cured with at least 1 500 mJ cm^{-2}, to exclude the dependence on UV curing. The capacitance increases with surface area of capacitors; the proportionality constant is a little larger for samples on Pe:smart paper than on the Biomatt. Therefore all printed elements follow the theoretical expectations, with 10-20 % higher capacitance on the Pe:smart paper. In general, up to 15 % higher capacitance was obtained on the single-layered sample when compared to double-printed; this is a consequence of thicker dielectric layer.

4. Conclusions

Flat-plate capacitors were printed on paper surfaces using the solvent-based silver conductive and the UV-curable dielectric inks. Wet-on-dry screen printing technique was applied. The smallest electrical resistivity of the conductor layer was obtained at the highest temperature the substrate can withstand, which is much higher than recommended by the producer. The capacitance of a flat-plate capacitor with single-printed dielectric layer increases with UV curing; these prints have very poor print quality and several electrical shorts between conductor layers. High enough UV curing overcomes these effects when exceeding the recommended curing by a factor of three. The phenomenon is most likely associated with permeating of the solvent from the top conductive layer through the dielectric one during the process of drying. This solvent partially dissolves the bottom conductor which causes several faults in the bottom conductor-dielectric interlayer.

The capacitance becomes independent of UV curing energy if the dielectric layer is double-printed. The second dielectric layer gives two advantages: first, it covers the imperfections of the underlying dielectric layer which electrically isolates both conductive plates, and second, it prevents the solvent from the top conductive plate to cross the dielectric layer during drying. Thus the bottom interlayer is prevented from being deformed and the electrical properties of the flat-plate capacitor become independent of further UV curing.

The smooth hydrophilic nanoporous paper, dedicated to printed electronics, makes it possible to print flat-plate capacitors with 10-20 % higher capacitance than the matte paper dedicated to conventional printing. Better electrical functionality could be due to the larger absorptiveness of the nanoporous paper; this enables printing conductive layers with more compact distribution of silver particles in the final layer, which gives better conductivity. However, the effect is not as large as one could expect on permeability and absorptiveness differences.

One of the possible reasons could be the size of the functional particles in conductive ink used in our study. They are much larger than coating particles and pores on both paper surfaces, therefore they contribute to the formation of conductive paths in the bottom layer. The second reason is that the paper substrates influence only the bottom conductive plate and have no effect on the top conductor. The conductivity of layers determines the amount of charge stored on a conductive plate - however, the capacity of the corresponding conductor is associated with the charging ability of the inferior plate.

Deeper understanding of how the solvent could diffuse through the UV cured dielectric layer (which is supposed to be crosslinked) requires more extensive research. It addresses the structural changes in the dielectric layer that make it completely impermeable even in a single printing. The chemical and physical structure of the over-cured layer will be studied in detail in the future by applying advanced analytical methods (e.g. surface spectroscopic and microscopic analysis).

Acknowledgements

The authors acknowledge the financial support from the state budget by the Slovenian Research Agency (project No. J2-9455). Maša Horvat and Tjaša Vidmar acknowledge the Slovenian Research Agency for young researchers support.

References

Berggren M., Nilsson D., and Robinson N.D., 2007. *Organic Materials for Printed Electronics. Nature Materials, Vol. 6*, pp. 3-5.E

Bollström R., Määttänen A., Tobjörk D., Ihalainen P., Kaihovirta N., Österbacka J., Toivakka M., 2009. *A Mulitilayer Fiber-based Substrate Suitable for Printed Functionality. Organic Electronics, Vol. 10*, pp. 1020-23.

Klanjšek Gunde M., Maček M., Žveglič M:, Muck T., Vidmar T., Plevnjak J., Hauptman N., Urbas R., Golob G., Starešinič M., 2011. *Electrical and Print Quality of Flat-plate Capacitor Screen-printed on Paper. Advances in Printing Science and Technology, Vol. 38*, pp. 231-6.

Leenen M.A.M.. Arnig V., Theim H., Steiger J., Anselmann R., 2009. *Printable Electronics: Flexibility for the Future. Physica Status Solidi A, Vol. 206.*, pp. 588-97.

Mercier C., Peralba M., Dubé M., Bloch J-F., Mangin P. J., 2007. *Effects of Drops Interactions on Ink-jet Print Quality. Advances in Printing Science and Technology, Vol. 34,* pp. 221-30.

Siegel A., Phillips S. T., Dickey M. D., Lu N., Suo Z., Whitesides G. M., 2010. *Foldable Printed Circuit Boards on Paper Substrates. Advanced Functional Materials, Vol. 20*, pp. 28-35.

Tobjörk D., Österbacka R., 2011. *Paper Electronics. Advanced Materials, Vol. 23*, pp. 1935-61.

Žveglič M., Demšar V., Urbas R., Hauptman N., Maček M., Klanjšek Gunde M. 2009. *Electrical Resistivity of Screen Printed Conductive Lines. Advances in printing and media technology. Vol. 36*. pp. 421-7.

Žveglič M., Hauptman N., Maček M. Klanjšek Gunde M., 2011. *Screen-printed Electrically Conductive Functionalities on Paper Substrates. Materials and Technology vol. 45*, pp. 627-32.

JPMTR 013 | 1201
UDC 655:621.38

Research paper
Received: 2012-01-04
Accepted: 2012-06-08

The development of printed electroluminescent lamps on paper

Eifion H. Jewell, Timothy C. Claypole, David T. Gethin

WCPC, Swansea, United Kingdom E-mail: e.jewell@swansea.ac.uk

Abstract

An experimental investigation has been undertaken to examine the suitability of paper as a substrate for screen printed electro luminescent (EL) lamps. EL Lamps based on paper have a number of potential uses in packaging and point of sale applications and offer a lower cost substrate compared to ITO sputter coated PET. Lamps were manufactured on 4 opaque substrates using a top emission architecture with printed PEDOT:PSS being used as the transparent conductor on the upper surface of the lamp. The illumination performance was compared to lamps based on a traditional ITO based bottom emission lamps. Lamp output was around 50 % of the output of the ITO based lamps and could be attributed to a number of factors. The dominant reason is the higher resistance and lower transparency of the PEDOT:PSS material used compared to the ITO. The architecture of the top emission EL lamps also leads to a reduction in lamp output as the phosphor particles provide a topological barrier to the production of a consistent coherent film for the PEDOT:PSS electrode. The properties of the evaluated substrates had no significant influence on the lamp output which demonstrates that EL lamps can be manufactured on a wide variety of paper substrates.

Keywords: screen printing, printed electronics, electroluminescent, paper, PEDOT:PSS, ITO replacement

1. Introduction

Paper has many advantages as a substrate for a wide variety of printed electronics products. It is able to withstand higher temperatures than many polymers, it can be recycled, it is widely used in the printing and packaging industries, it is well understood and it is low cost. Its characteristics and uses for printed electronics are well significant (Tobjörk and Österbacka, 2011). The primary disadvantage of paper for a printed electronics product which possesses electro-optic capabilities is that it is opaque.

Printed Electroluminescent (EL) technology is a mature technology and is used in a variety of applications including emergency lighting, LCD backlighting, promotionnal advertising and mood lighting (Hecker, 2009; Zovko and Nerz, 1999). The maturity of the technology, the low cost of processing and relative insensitivity to the environment (compared to OLED) have made it a commercially viable proposition for illumination. The major disadvantages of the technology which have limited its commercial success are its high voltage (> 100 V), operational life (typically less than 3 000 hrs of illuminetion) and limited brightness (typically 200 cd m^{-2}). In addition, the cost of the ITO substrate provides a commercial barrier to success.

The principal operation is that light is emitted from phosphor material (doped ZnS) when subjected to an AC field. The most common architecture is based on a bottom emission device where the light is emitted from the phosphor material which is printed onto an ITO sputtered transparent substrate (usually glass or PET), Figure 1 (a). In the top emission EL architecture the layers are reversed with a transparent conductive coating being printed on top of the phosphor particles, Figure 1(b). This enables printed EL to be made on opaque substrates.

The characteristics of EL devices are widely reported (Allieri et al., 2002; Ciez et al., 2007) but the literature is dominated by the bottom emission device architecture using ITO sputter coated transparent PET. Blue EL lamps have been produced on paper substrates with a brightness up to 210 cd m^{-2}, (Kim et al., 2010) but this was not a fully printed solution as an additional planarizing and passivation layer was spun coated between the paper and the rear electrode and the top electrode was sputter coated ITO. In order to achieve a completely printed top emission lamp, a liquid transparent conductor must be used.

Recently, some researchers have examined ITO nano particle dispersions (Straue et al., 2011) while others have examined the production of ITO coatings from liquid using the sol-gel route (Kim et al., 1999; Gan et al., 2006). Although these have shown some promise, the development of transparent liquid metal oxide based conductors has not led to commercial materials as material stability, process control required during deposition and cost have been barriers. Subsequently, there has been a greater adoption of printable organic coatings such as PEDOT:PSS (poly-(3,4-ethylenedioxythiophene) doped with poly-(styrene-sulfonate)), (Elschner et al., 2010). Formulations based on PEDOT:PSS have been commercially available and are considered a mature technology. The replacement of ITO by PEDOT has been shown to be beneficial in other electro optic devices such as PDLC (Kim et al., 2010), OPV (Winther-Jensen and Krebs, 2006; Aernouts et al., 2003) and OLED (Jabbour et al., 2001).

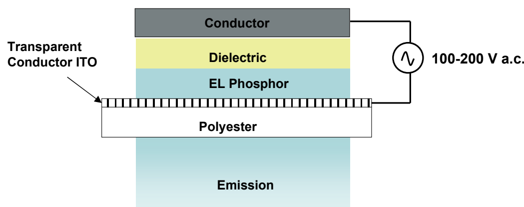

(a)

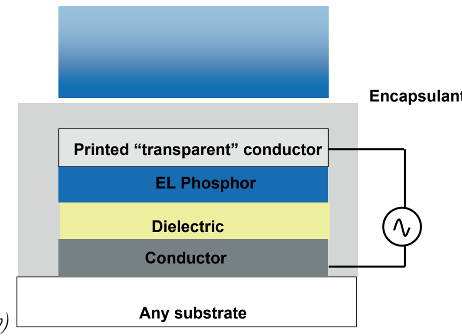

(b)

Figure 1: (a) The conventional bottom emission architecture and (b) The top emission device architecture used in the investiagtion

Electroluminescent lamps based on screen printed PEDOT:PSS have been successfully demonstrated (Weigelt et al., 2012) on transparent polycarbonate substrate. Paper based EL lamps have been demonstrated in the past (Ray et al., 2006) and have also been produced commercially for point of purchase advertising (Quantum paper, 2009) using screen printed PEDOT:PSS as an upper transparent electrode.

The printing of PEDOT:PSS on paper substrates has typically led to lower conductivities (between twice and 100 times) than that which is achievable on plastic substrates (Denneulin et al., 2008). This has been generally explained by the absorption of the PEDOT:PSS into the porous substrate. For the top electrode, as is used in this instance, this should have a minimal effect as the device architecture dictates that the majority of the PEDOT is printed on the phosphor layer.

A clear commercial advantage of top emission EL on paper is reduction in cost of the substrate by several orders of magnitude (ITO sputter coated PET is typically € 20 to 60 per m² dependent on sheet resistance). Against this cost benefit, there is the additional tooling cost of an additional screen for the patterning of the top PEDOT:PSS electrode. There is also the potential loss in lamp output as a result of the lamp architecture and the limited transparency and conductivity of the printed transparent electrode compared to ITO. With this competitive technology in mind, the measured lamp outputs are shown as a percentage of the output of the ITO based lamp as this best reflects the cost reduction pay off for possible reduction in performance. The aim of the investigation was to establish and understand the performance characteristics of printed top emission EL lamps and to establish the effect of substrate on the output.

2. Method

Three paper based substrates were chosen with an additional opaque PET substrate which acted as a control for the experiment. In this way, it was possible to separate any discrepancies which could be attributed to the substrate from those which could be attributed to the build and the use of printed PEDOT:PSS. The paper characteristics represent a range of papers which could be used across the breadth of possible applications, Table 1. Substrate roughness was measured using white light interferometry measuring over an area of 1.2 mm x 0.8 mm.

The phosphor used was a GEM C2061027D13 which was coupled with a GEM dielectric (D2080410D5) and GEM silver (C2090210D12). The samples were cured through an air dryer at 120 °C for 4.5 minutes. The top electrode was printed with a commercial water-based dispersion of PEDOT:PSS from Agfa (Orgacon EL-P3040) which has been formulated as an ITO replacement in bottom emission EL lamps.

Table 1: Substrate characteristics

	PET	Card	Gloss paper	Uncoated
Caliper (µm)	350	200	130	90
Grammage (g m^{-2})	-	220	110	100
Roughness Ra (µm)	0.14	0.83	0.53	2.75

All the printing steps were done on a semiautomatic screen printer (DEK 248) using polyester screens with a mesh number of 61 filaments cm^{-1}, a mesh-opening of 64 µm and a mesh angle 45 °. The printing speed was 70 mm s^{-1} and the snap-off 2.5 mm, i.e. the distance between the mesh and the substrate. The test layout included square test lamps with a side length of 30 mm which were used as a reference test lamps. Larger lamps of up to 10 000 mm² were also produced in order to examine the effect of lamp area on output. In total, 5 lamps were printed on each substrate and the mean results are shown. The substrates were fed into the machine in a random sequence in order to limit any bias in the results due to short term variation such as ink drying in the screen.

In order to examine the relative performance of the PEDOT:PSS lamps, control ITO-PET lamps were constructed using the same batch of material and screen. The ITO possessed a sheet resistance of 80 Ω sq^{-1}. The optimum PEDOT:PSS layer thickness is a compromise between the increased conductivity of thicker layers and reduced light transmission of the thicker film. Thus, in order to estimate the optimum thickness additional lamps were produced with multiple layers of the upper PEDOT:PSS electrodes. Layers of PEDOT:PSS were also printed to transparent PET material such that their transparency and electrical performance could be measured. Transmission measurements were made on a Viptronics transmission densitometer while sheet resistance characterization was carried out using a Keithley 2400 source-measure unit.

The PEDOT:PSS electrodes were coated with silver ink where they were in contact with the substrate in order to ensure a consistent contact between the inverter connections and the electrodes and to limit any reduction in performance of the lamp due to absorption of the PEDOT:PSS electrodes into the paper.

Lamps were manufactured without a top encapsulant such that the light output could be measured without hindrance of the encapsulant. The EL devices were driven by a sinusoidal voltage produced by a power supply for EL lamps LM30 from Light & Motion. The excitation frequency was kept at 400 Hz. The luminance was measured using a Gretag-Macbeth Spectrolino spectrophotometer measuring in emission mode with a measurement spot size of 4 mm.

3. Results

The luminance of the optimum top emission PEDOT:PSS lamps is around 50 % of the conventionally built lamp based on a ITO transparent electrode, Figure 2.

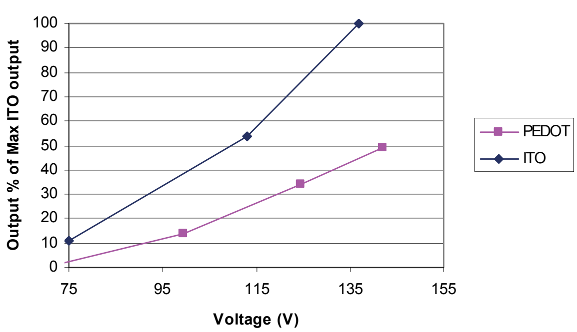

Figure 2:
The comparative performance of a PEDOT:PSS printed top emission lamp and the ITO references

Increasing the excitation voltage increases the output of the lamp, but the increased output of the ITO lamp bottom emission lamp relative to the top emission PEDOT lamp remains consistent over the voltage excitation range.

This difference in luminance is visually evident in Figure 3 which shows both lamps operating driven by identical inverters at the same frequency and voltage.

The effect of the substrate on the output of the lamp is small with a reduction in luminance of around 15 % for the uncoated paper compared to the PET, Figure 4.

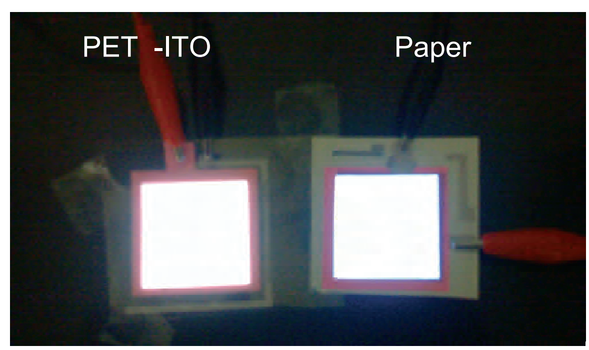

Figure 3: A visual comparison of the emission from the paper based lamps and the ITO/PET. ITO/PET lamp output is 50 cd m^{-2}, paper is approximately 24 cd m^{-2}

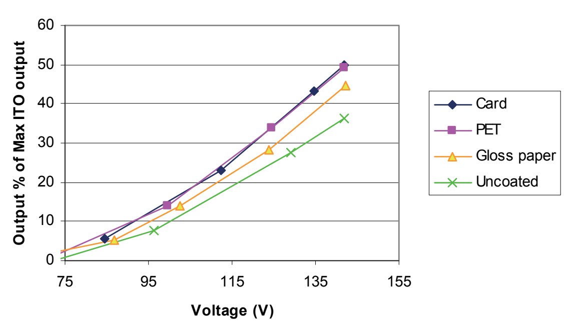

Figure 4: The applied voltage / emission characteristics of the printed EL lamps with 1 layer of PEDOT

The coated card and the PET show near identical characteristics. The lighter grammage gloss paper shows a small reduction (approximately 5 %) in output compared to the coated card. This was attributed to the slight deformation of the substrate which was visible and is thought to be a result of liquid absorption from the thick screen printing ink film. With this thinner substrate the quantity of silver and dielectric ink is above 50 % of the substrate thickness, Table 2. The film thickness of the phosphor layer cannot readily be quoted due to the clustering of the large particles of the zinc sulphide within the coating of binder (Figure 5). While there may be some substrate effects on lighter and uncoated substrate, top emission EL technology is applicable to a wide variety of paper substrates. The additional layers of printed PEDOT:PSS resulted in a reduction in the lamp output, Figure 6.

Table 2: Mean measured film thickness in the finished devices

	PET	Card	Gloss paper	Uncoated
Silver (µm)	10.1	9.7	9.8	8.8
Dielectric (three layers µm)	40.1	39.2	38.5	38.4

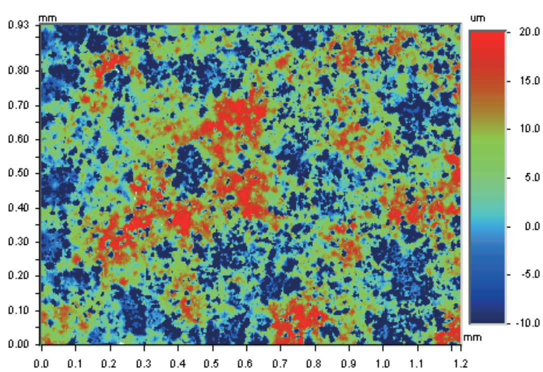

Figure 5: Typical film topology for the phosphor layer highlighting clustered large particles within the ink film

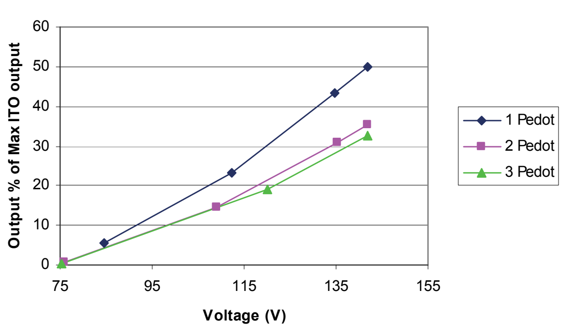

Figure 6: The effect of increasing the number of printed PEDOT:PSS layers on light output on the card substrate

This can be related to the reduction in resistance of the PEDOT:PSS being counteracted by its reduced transparency as the film thickness is increased, Figure 7.

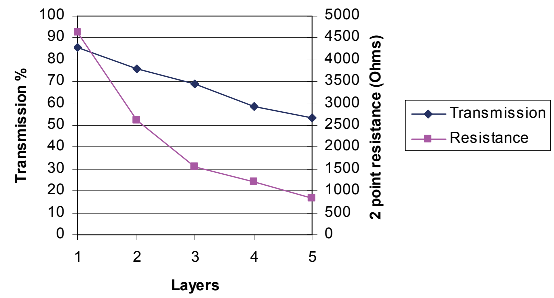

Figure 7 : The effect of the number of increasing PEDOT:PSS layers on the transmission and sheet resistance

The load imposed on the EL inverter is defined by the combined impedance of the lamp which is made from contributions from the top electrode resistance, the lamp capacitance and the bottom electrode resistance. Any increase in the resistive elements will reduce the output of the lamps (Zovko and Nerz, 1999; Weigelt et al., 2012). Increasing the area of the lamps resulted in a reduction in the lamp output, Figure 8.

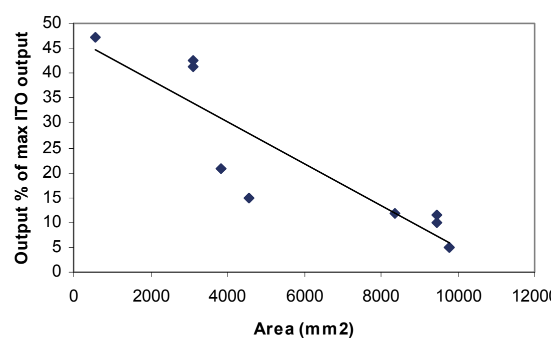

Figure 8: The effect of lamp size on the relative luminance of the top emission lamps on the card substrate

The driver was capable of maintaining the light output of the lamps of the bottom emission ITO lamps as the area was increased. This effectively shows the limitation of the driver which has been optimised for ITO based lamps where the resistive element of the overall load is lower. In order to maintain luminance output for PEDOT:PSS based lamps, the EL inverter characteristics would need to be optimised to take this into account.

4. Discussion

The simplest explanation for the reduced output of the PEDOT:PSS lamps is the relative electro optical properties. The PEDOT:PSS used possesses a transparency of 91 % (AGFA, 2009) at a sheet resistance of around 1 000 Ω sq^{-1} compared to a transparency of over 90 % at sheet resistance of 80 Ω sq^{-1} for ITO coated PET. The performance of the PEDOT is likely to rapidly improve as new formulations develop, resulting in greater transparency and better conductivity. Therefore, the difference in light output between ITO and PEDOT:PSS based lamps is likely to be reduced. The current generation of the screen printable PEDOT:PSS material (EL-P 3145) has a sheet resistance of around 350 Ω sq^{-1} at the 90 % transparency (AGFA, 2011). However, improvements in sheet resistance/transparency will not eradicate all the issues related to the output of top emission EL lamps as there are a number of other possible contributing factors for the reduced output of the top emission printed lamps on paper.

A cross section through the lamp shows that there are phosphor particles whose upper surface lie beyond the PEDOT:PSS layer, Figure 9. These light emitting particles lie partially outside and on the edge of the electric field produced between the silver and PEDOT:PSS electrodes. As these particles are not subject to the same electric-field strength, the light emission from these particles may be significantly diminished leading to lower overall light emission. Further layers of PEDOT:PSS would ensure the inclusion of these particles in the field, but would tend to reduce visible emission due to reduced transparency of the PEDOT:PSS layer.

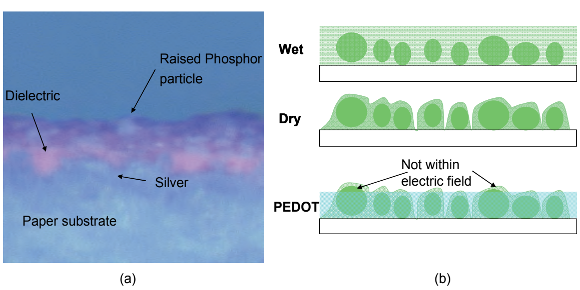

Figure 9: (a) Cross section of the lamps and (b) Schematic of the PEDOT:PSS layer on the phosphor light emitting particles

This underlying topology due to the particles which are proud of the surface also increases the effective sheet resistance of the PEDOT:PSS compared to the sheet resistance of the PEDOT:PSS printed on the bare substrates, Figure 10. This is a physical effect due to the layering of a continuous film on large discrete particles and would likely remain, even with higher transparency and higher conductivity PEDOT:PSS formulations. There may be scope for reducing its effect through surface energy modification which promotes evenness of coating over the microtopography.

The mechanism whereby the topology of the previously printed layers results in changes in following layer morphology also results in a lower capacitance (1.8 nF) for the top emission EL lamps compared to the bottom emission lamps (2.6 nF). In the bottom emission architecture, the first layer of dielectric largely fills in the voids between the phosphor particles while the second and third layers provide the field transmitting insulation required between the two electrodes. In a top emission lamp, as the dielectric is being printed to the relatively smooth silver layer, the cumulative film thickness is increased, resulting in a lower capacitance.

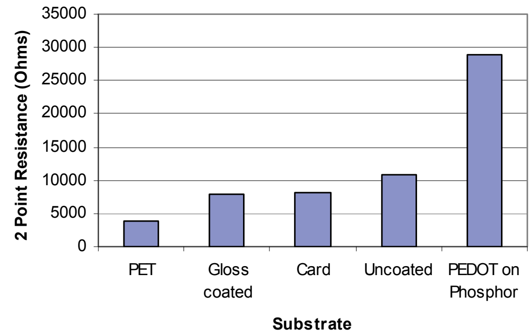

Figure 10: Measured resistance for PEDOT :PSS printed on all substrates and on the phosphor particles

With the present PEDOT:PSS materials, the reduction in brightness with increasing lamp size, would suggest that silver bus bars are required in order to maintain brightness in many practical applications. This would add an additional cost as it requires a further printing operation and associated tooling and would also impose some visual design constraints on printed images as the conductive silver bus bars would need to be included for large lamps. Even with bus bars, there would be a reduction in illumination from larger areas.

The production of the lamps and their performance is relatively independent of the paper coating. This can be attributed to the first layer of silver ink effectively planarizing the substrate for subsequent layers. The minimal paper substrate effects observed are likely to be a result of the absorption of the PEDOT into the paper substrate on the contact which reduces its conductivity Figure 9. This is in line with the findings of Denneulin et al. (2008) and Trnovec et al. (2009).

Although screen printing has been used for the fabrication of printed lamps, the use of these lamps in markets such as packaging could be substantially increased if the lamps could be fabricated using offset lithography or flexography. The particle size of the phosphor and the requirement for over 10 micrometers of dielectric ink does not instantly lend itself to offset lithography, however flexography shows some promise.

Conductive silver and dielectric ink formulations are available commercially and work on developing PEDOT:PSS formulations printable by flexography is at an advanced stage. The main challenge is the formulation of the phosphor ink. Initial formulation trials for flexographic inks have been unsuccessful as the relative density of the phosphor particles causes rapid sedimentation in the low viscosity carrier. Work is ongoing on developing a more stable formulation and optimising the ink transfer process for flexographic EL fabrication.

5. Conclusions

An investigation into the performance of paper based top emission EL lamps has been carried out. The top emission lamps which have an output with around 50 % of their ITO coated PET equivalent.

The deficiencies in the lamp output can in part be related to the relative transparency and conductive performance of the PEDOT:PSS, but the physical layering of the printed PEDOT:PSS also plays a significant part in reducing the light output. The effect of the substrate is minimal with more absorbent substrates reducing light output by around 15 %. Increasing the number of printed PEDOT:PSS layers resulted in a reduction in lamp output as a result of reduced transparency.

References

Aernouts, T., Vanlaeke, P., Geens, W., Poortmans, J., Heremans, P., Borghs, S., Mertens, R., Andriessen, R. and Leenders, L., 2004. Printable anodes for flexible organic solar cell modules. *Thin Solid Films*, Vol. 451-452 , pp. 22-25.

Allieri, B., Peruzzi, S., Antonini, L., Speghini, A., Bettinelli, M., Consolinia, D., Dotti, G. and Depero, L. E., 2002. Spectroscopic characterisation of alternate current electroluminescent devices based on ZnS-Cu. *Journal of Alloys and Compounds*, 341, pp. 79-81.

Ciez, M., Nowak, S., Zaraska, W. and Porada, Z., 2007. Large-dimensional light-emitting elements with printed electroluminophore, *Opto-Electronics Review*, 15(3), pp. 159-162.

Denneulin, A., Blayo, A., Bras, J. and Neuman, C., 2008. PEDOT:PSS coating on specialty papers: Process optimization and effects of surface properties on electrical performances. *Progress in Organic Coatings*, 63(1), pp. 87-91.

Elschner, A., Kirchmeyer, S., Lovenich, W., Merker, U. and Reuter, K., 2010. *PEDOT: Principles and Applications of an Intrinsically Conductive Polymer.* CRC. ISBN-10: 142006911X

Gan, Y., Liu, J., and Zeng, S., 2006. Transparent conductive indium tin oxide film fabricated by dip-coating technique from colloid precursor. *Surface & Coatings Technology*, 201, pp. 25-29.

Hecker, K. ed., 2009. *OEA Roadmap - 3rd Edition 2009*, VDMA.

Jabbour, G. E., Radspinner, R. and Peyghambarian, N., 2001. Screen printing for the fabrication of organic light-emitting devices, *IEEE Journal of Selected Topics in Quantum Electronics*, 7(5), pp. 769-773.

Kim, J.-Y., Park, S.-H., Jeong, T., Bae M.J., Song, S., Lee, J., Han, I.-T., Jung, D. and Yu, S.G., 2010. Paper as a Substrate for Inorganic Powder Electroluminescence Devices. *IEEE Trans. Electron. Devices*, 57, pp. 1470–1474 .

Kim, J.-Y., Woo, H.-Y., Baek, J.-W., Kim, T.-W., Song, E.-A., Park, S.-C. and Ihm, D.-W., 2008. Polymer-dispersed liquid crystal devices using highly conducting polymers as electrodes. *Applied Physics Letters*, 92, 183301.

Kim, S.-S., Choi, S.-Y., Park, C.-G. and Jin, H.-W., 1999. Transparent conductive ITO thin films through the sol-gel process using metal salts, *Thin Solid Films*, 347, pp. 155-160.

Martins, R., Ferreira, I. and Fortunato, E, 2011. Electronics with and on paper. *Physica Status Solidi (RRL) - Rapid Research Letters*, 5(9), pp. 332-335.

Straue, N., Rauscher, M., Dressler, M. and Roosen, A., 2011. Tape Casting of ITO Green Tapes for Flexible Electroluminescent Lamps. *J. Am. Ceram. Soc.*, 1-6. DOI: 10.1111/j.1551-2916.2011.04836.

Ray, W.J., Claypole, T. C. and Jewell, E. H., 2006. Printing as an Industrial Process: Manufacturing Emissive Displays, *Proceedings of TAGA 2006*.

Tobjörk, D. and Österbacka R., 2011. Paper Electronics. *Adv. Mater.*, 23, pp. 1935-1961.

Trnovec, B., Stanel, M., Hahn, U., Hübler, A. C., Kempa, H., Sangl, R. and Forster, M., 2009. Coated Paper for Printed Electronics, *Prof. Papermaking*, 6, 48-51.

Weigelt, K., Jewell, E. H., Phillips, C. O., Claypole T. C., and Huebler A. C., 2012. Bidirectional flexible electroluminescent mouldable lamps fabricated by screen printing. Accepted for publication in *Journal of Print and Media Technology Research.*

Winther-Jensen, B. and Krebs, F.C., 2006. High-conductivity large-area semi-transparent electrodes for polymer photovoltaics by silk screen printing and vapour-phase deposition. *Solar Energy Materials and Solar Cells*, 90, pp. 123-132.

Zovko, C. and Nerz T., 1999. White polymer thick film electroluminescent lamps and their applications for backlighting liquid crystal displays in portable electronic devices. *Displays*, 20, pp. 155-159.

Internet references

AGFA, 2009. *ORGACON™ Transparent, Conductive Screen printing Ink: EL-P 3040*, product information sheet, published by AGFA-Gevaert, version number 20.03.2009 [Online, http://conductive-polymer.com/joomla/files/Orgacon%20EL-P%203040_tcm221-42934.pdf, downloaded March 2009].

AGFA, 2011. *ORGACON^{TM} Screen printing Inks information sheet.* [Online, http://www.agfa.com/sp/en/binaries/Orgacon%20Screen-Printing%20inks%20v110329_tcm221-86918.pdf, downloaded April 2011].

Quantum paper, 2009. <www.quantumpaper.com>. [Accessed February 2009].

Topicalities

Edited by Raša Urbas

Contents

News & more

New liquid image development system

New innovative printing technology incorporates electrophotographic knowledge with a new liquid image development system based on high viscosity toner. Trillium technology utilizes the best of both and closes the gap between speed/cost and quality. As it is toner based and a waterless non-volatile organic compound technology, also enabling printing on untreated substrates. It is fully compatible with the existing paper recycling technologies and has the potential to become fully sustainable from a toner composition perspective.

Trillium is a colloidal suspension (or sol) of toner in a carrier liquid (a pharmaceutical grade white oil), which allows toner particles down to 2 microns in size or up to 4 times smaller than in its dry form. Such small toner particles enable higher resolution and result in less toner consumption. This exceptional implementation of high viscosity toner allows the use of smallest gaps in the transfer zones to deliver a combination of high image quality and high speed. Another key strength of Trillium technology lies in its ability to print mid- to high image coverage at high quality, which makes it particularly suitable for direct marketing and commercial printing applications. Furthermore, the new technology offers a lot more head room for both speed and width improvements in the future.

The new printing process consists of six steps: charging, expose & erase, develop & clean, intermediate transfer, substrate transfer and fixation of the toner. The particles are not charged during manufacturing; instead they are charged just before printing. Trillium incorporates both a transfer and fuse process - unlike the transfuse step of other technologies. This allows for a modular-machine approach and speed increases.

Trillium is absolutely compatible with existing deinking and recycling installations and has already been tested. In addition, it uses the same type of polyester resin system as it is used in Xeikon's dry toners incorporating an environmental friendly catalyst which includes no organic tin compounds.

The carrier liquid is also recycled in the printing process without evaporation, so the toner is 100 % VOC free. Furthermore, since the current toner in an oil colloidal suspension (or sol) can be replaced by bio resins and vegetable oil, the new toner also has the potential to become fully sustainable.

The unique combination offers far lower running costs at significantly improved speeds, while maintaining the high quality levels and eco-sustainability of Xeikon's current presses. For printers, this means no compromising between image quality and productivity/cost. The technology will be first implemented in a range of products dedicated to the document and commercial printing markets.

New test images of ISO 12640 family

The ISO 12640-family defines test images and elements for different purposes and hence color encodings. Parts 1 to 4 are published. The CD ballot of ISO 12640-5 was approved and the DIS ballot is in preparation.

New transmission Densitometer

The new transmission densitometer measures ISO visual diffuse optical density to 6.00D. This wide measuring range allows evaluation of many types of film, laminates, and substrates. The TBX1500™ version also calculates positive and negative dot areas while the TBX2000™ measures percent opacity and transmission. The data can be uploaded to spreadsheets via the USB port. To meet special requirements an optional filter carrier may be supplied allowing supplementary filters to be used to isolate a portion of the spectrum that may be of interest.

Versatile UV/VIS spectrophotometer

The new UV/VIS spectrophotometer with integrated monochromator (in range between 190 and 1 100 nm) is a powerful equipment for universal use in all areas of water and waste water analysis. This includes municipal and Industrial waste water, drinking water, process water, surface water, ground water as well as cooling and boiler feed water. The NANOCOLOR® UV/VIS is also the ideal test unit for quality control in various fields of industry.

Agilent Cary 620 FTIR

The Agilent Cary 620 FTIR spectrochemical microscope delivers unmatched imaging for biomedical and materials research. The microscope performs at a higher level of sensitivity than the Cary 610 FTIR device providing true Focal Plane Array (FPA) imaging, enabling the collection of hundreds to thousands of spectra simultaneously. This provides unlimited possibilities for a diverse range of applications including polymers/materials, pharmaceuticals, biotechnology, chemicals and forensics.

A range of accessories are available that extend the function of the microscope and high performance, flexible operating software delivers intuitive and comprehensive imaging control and data manipulation.

A digital photography tool

The new program solution Photoshop® Lightroom® 4 public beta was built on the vision of the very first Lightroom beta. It provides a comprehensive set of digital photo graphy tools, from simple one-click adjustments and features to cutting edge advanced controls.

Photoshop® Lightroom® 4 enables organizing, enhancing, and showcasing of the images from one fast and nimble application. The program solution is available from both Macintosh and Windows® platforms.

Increased plate coating capacity to meet demand for waterless offset plates

Wishing to meet higher global demand for its pioneering waterless plates Toray plans a new printing plate factory in the Czech Republic. Field testing of the products from the new plant is expected to begin in late 2013, while it will be fully operational in early 2014.

Encompassing both coating and converting capabilities, the new production facility will cover the markets across Europe, the Middle East and North America.

High viscosity liquid toner technology

Newly released white paper on the role of high viscosity liquid toner promises significant productivity gains and opens new markets. The white paper explains in simple terms the technology of electrophotography and outlines the difference between dry and liquid toners. While both toner technologies strive to create the smallest particles possible in order to optimize quality, liquid toner has greater latitude to control the particles. As such, liquid toners use less material which reduces raw materials costs, allow faster linear throughput speeds and use less heat (hence energy cost) to fuse to the substrate.

According to I.T. Strategies the new liquid toner technology will be even more productive than dry toner technology, while maintaining the same high printing quality.

While initial throughput is projected to be 60 m/min (196 ft/min), in theory upper limits of 300 m/min (1 000 ft/min) are possible. This ability to produce higher volumes digitally at lower cost will deliver significant productivity gains to printers and extend the breakeven point for digital printing. At the same time, it provides the opportunity for Xeikon to extend its customer base to those printing high value, high area coverage type documents.

New inkjet dye sublimation printer

This new printer was designed specifically for the sublimation transfer market with high speed and quality capability of printing up to 32.0 m²/h at 540 x 720 dpi. Sublimation transfer printing is widely utilized for sportswear applications due to the elasticity and quick-drying capability of polyester material and in the growing market of soft signage applications, such as flags, retail in-store banners, and tapestries.

The machine can achieve a printing speed of 17.7 m²/h in 6-color mode at the same resolution, thus responding to the needs for high quality prints, with minimal amount of grainy appearance and smooth gradations. These features make the "TS34-1800A" printer suitable for both large-sized zed soft signs as well as apparel applicatications, which require quick response and fine image quality respectively. Improved productivity functions of Mimaki "TS34-1800A" printer which enable advanced print automatization are:

- UISS function (Uninterrupted Ink Supply System) that enables setting two ink cartridges per color in 4-colour mode. When an ink cartridge is used up, the system switches automatically to the second cartridge of the same color, preventing the printing process from stopping due to running out of ink.
- MBIS (Mimaki Bulk Ink System) which provides a large volume continuous ink supply with 2-litre ink aluminum bags. As a result, ink costs and environmental footprints are substantially reduced.
- Automatic drying fan that increases the ink drying speed remarkably, enabling continuous media take-up even during high speed printing. Consequently, printing efficiency improves dramatically.

Print management software

Pageflex iWay™ print management software brings together web-based ordering, pre-press, production and delivery, and fully automates these processes for digital and hybrid print service providers. It enables streamlineing of the production process and offers new services to the customers. With it multiple web stores with customized buying experiences to meet the needs of a variety of customers and users can be created.

Pageflex iWay™ 6.0 now supports more language versions and currencies while Pageflex 8.0 includes all the other Pageflex tools which have been translated into ten languages, including Dutch, French, German, Italian, Spanish, Portuguese, Polish, Russian and Chinese.

In addition to editing iWay web portals, users of iWay can now also produce the templates for documents with advanced management.

Pageflex also presented solutions for ordering prints via mobile devices. Beside that new opportunities for multichannel communications media support, including video and multichannel marketing were also introduced.

Sheetfed printing solution

One of new products displayed at drupa 2012 was a new sheetfed printing solution DIGILINE. The industrial digital printing device codes, serialises, personalises and prints products, made from different materials and formats, with variable data and information.

The flexible, versatile, user-friendly and scalable system is ideally suited to customer and security requirements in sheetfed and flat product printing. It is designed for required solutions to code and serialise product as excise labels, lottery and event tickets, or travel tickets as well as flat packaging.

The modular, fully integrated, standardised system solution impresses with best printing results in terms of quality and production speed. The complete solution consists of a transport system for sheets and flat products, digital inkjet printers (OMEGA or DELTA), formulated curing modules, controllers with ink supplies as well as a camera-based verification system with fully automated waste gate of possible printing errors that are automatically detected and eliminated during the on-going production process.

A system controller with ink supply is integrated for the seamless control of the production and information flow without restricting which modules can be integrated. The camera-based verification system VERICAM™ includes a mechanical waste gate that detects and immediately eliminates possible printing errors during the production process to guarantee a zero-error rate and 100 %, consistent quality control.

Toray is investing more than 50 million USD to respond to the growing demand for waterless plates. They are convinced that their commitment will send a right signal to the newspaper industry and encourage further investment in the best available technology for newspaper and semi commercial production.

The move will improve technical support to customers as well as reduce costs through simplified process flow and logistics.

Flexo plates for greener and healthier printing

Jet Technologies has offered a new generation of digital water wash flexo plates AWP DEF. This newly developed photopolymer plate technology satisfies the most severe criteria in terms of high quality printing and does more to match current technologies. Color transport, developing time and persistence of developed plate are the properties which are as least as good as asserted classic digital flexo plates with usual developping manners.

Solutions for dry offset printing

One among many offered drupa 2012 solutions are the solutions for dry offset printing. Novelties enable printers to improve flexibility and performance of dry offset printing. The main advantage of the new solution is better quality of prints on any paper or paperboard.

Wide range of quality printed materials enables easier adjustments to the market needs. Short time of printing preparation and direct finishing, possible by the use of UV dyes for dry offset printing, ensure higher production capacity and fast order realization.

Bio printing substrate

BioMedia Display Film is a flexible printing substrate that uses the renowned coating technology to create print surfaces that minimize the environmental impact without compromising image quality.

As a no-compromise alternative to vinyl and PVC, BioMedia Display Film has a universal microporous coating, which means that high-quality image results are produced across a wide range of commercial printing equipment including Aqueous, Eco-solvent, Solvent and Latex printers.

This equates to less stock holding and inventory expenditure as well as the flexibility to decide which printer platform is most suitable for the end application or indeed production capacity. The range also includes a UV display film which gives further flexibility to the print provider.

By stocking one product range for use across all of their printers, print service providers not only reduce the environmental impact of their printing activity but can do so without any loss in image quality or media performance.

BioMedia Display Film, available in standard roll sizes and in 300, 400 or 550 micron variants, is suitable for most indoor applications as a direct replacement for coated vinyl or polyester media and is fully compatible with BioMedia Rigid Boards and BioMedia Laminates for a fully integrated biodegradable display system.

New recycled paper

Anatalis has developed new recycled paper Image Recycled High White which possesses the whiteness of CIE standard in values of 147 with the opacity of 95.

It is available in bright white and high white variety, ISO 80 and ISO 70. Both versions of Image Recycled Bright White are a high performance, multipurpose paper made from 100 % recovered paper, guaranteed for full color laser and inkjet printing.

Distinguished by excellent whiteness and smoothness it offers color printing extra lift and contrast. The paper is FSC certified and available in 80, 90 and and 100 gsm and sizes A4 and A3.

Image Recycled High White Blue Angel is a 100% recycled office paper guaranteed for single color inkjet and laser printing, it is suitable for high volume printing and copying, for in-house reports, presentations and low resolution imagery.

The increased demand for just-in-time production, serialization, late-stage customisation and the overprinting of pre-printed products within the printing processes is due primarily to the necessary cost reductions in security printing. This is why optimised printing processes, short response times and minimised downtimes in production are in demand.

Hybrid sheetfed press combining offset and digital technologies in a single system

First fully-integrated hybrid sheetfed press combining offset and digital technologies in a single system enables customers to print high-quality sheetfed jobs that include variable or versioned information in a single step.

The new hybrid press provides a single step of offset printing, inkjet printing, and an optional inline varnish station. The varnish option is valuable to direct mail printers because it enables a true print and ship capability, which leads to faster time to mail, invoicing and payment. Direct mailers will also benefit from new abilities to run B2 size sheets, which today cannot be post-printed with laser systems.

The RYOBI 750 series prints up to 10 000 sheets per hour. Customers can select one of the following inkjet printing options on the Ryobi 750 series press: two heads with one drier; four heads with driers; and four heads with driers and an inline UV varnish station.

Inkjet printing inline with offset printing delivers a number of significant benefits, including faster job turnaround time, lower costs and higher productivity for imprinting applications when compared to standard sheetfed laser printing. The typical production process involves printing direct mail shells on an offset press, letting the shells dry, and imprinting them on a laser printer. Hybrid printing eliminates drying time and enables imprintting on the sheets as they pass through the offset press.

A new press in the XL series

The new version of the Speedmaster XL 105-P with 18 000 sph offers a significant speed over its predecessor and presents the next step in the evolution of the XL range of presses. Beside mentioned the machine offers unique features, from the automatically adjusted transfers cylinders, venture guide plate system, dynamic sheet brakes and suction disc delivery. Modified storage drum and improved reversing drum with new pincer gripper system increase the retaining force and ensure precise registration. New CleanStar, at the delivery end, supports more efficient powder extraction and minimizes powder levels around the press.

As demonstrated at an open house at Heidelberg's Melbourne Print Media Academy, the XL 105 also boasts simultaneous plate change, which allows press operators to get the next job ready in the time it would normally take to change one plate on a printing unit. It also showed off Prinect Inpress Control for inline color control on the fly. This spectrophotometric inline measuring system is integrated into the press and is capable of measuring process colors, spot colors and register in the print control strip. If any corrections are required, these are forwarded directly to the Prinect Press Centre where they can be adjusted without affecting productivity.

Silicone coating technology

The new production line features most recent technical advances in the field of equipment for silicone coating for release liners, especially in regard to the coating units, the drying system and the remoisturizing system, together with the unparalleled web handling know-how. The ROTOSIL is a machine for siliconizing and adhesive coating on paper and other web materials. It is suitable for label manufacturing and it could be processed on materials like paper, film and laminates.

The production line enables printing in web width from 1 700 mm up to 2 400 mm at the maximum speed of 1 000 m/min. By using different coating methods silicone can be applied. The adhesive coating system can use water-based adhesives or hot melt adhesives.

Different drying systems are available depending on machine performance and materials to be processed. The production line is controlled by the Cosmoline PRO, a fully integrated operator-machine interface system. This includes the control and storage of all machine parameters in recipes and also as the management of the treaters, heating unit, alarms and data loggers. Different winder types are available depending on the machine performance required. The efficient technical solutions that optimize the use and recovery of electrical power enable an important reduction in the level of energy consumption.

Solution for booklet label applications

The latest solution which has been designed for sector-specific applications offers maximum flexibility for applications in chemical engineering, security printing, packaging, as well as pharmaceutical, cosmetics and industrial applications. This integrated end-to-end system is suitable for coding, serializing and verifying roll materials, sheets and 3D products.

The modular design of DIGILINE includes components for variable inkjet printing on a variety of different materials, verifying the print results and product tracking throughout the entire logistics chain. An OMEGA DoD inkjet printer with environmentally-friendly SMARTCURE UV LED curing system as well as the VERICAM camera-based verification unit are combined with the DIGILINE. The key feature is the ability to print and code from the first label. In the event of production-related pauses, the BLS machine software from Atlantic Zeiser ensures the transport runs automatically to the point of the last correctly printed label.

The innovative developments in the DIGILINE meet a common requirement for specialist and booklet label producers, as well as for self-adhesive identification solutions with added value for the chemical, medical and pharmaceutical industry. The result is zero-error production, high print quality and variability for frequently changing print data, all meeting the most stringent safety standards. The degree of variability and flexibility of DoD inkjet solution permits the efficient coding and serializing of minimal batch sizes. The protective transport ensures optimum adhesion of the

Multi-purpose vinyl substrate

New multipurpose inkjet 2006 Apolar, which has been for the first time presented at drupa 2012, is a white polymeric calendered self-adhesive vinyl with a special adhesive, providing outstanding adhesion to low-energy surfaces such as polyethylene and polyurethane. With its grey barrier coat it is perfect for overposting applications requiring higher opacity and can be used on a variety of (super) wide format inkjet printers using solvent inks.

AVERY DENNISON

Avery MPI 2006 Apolar is highly recommended for a wide range of applications on flat and slightly curved substrates. Due to its special adhesive it is suitable for difficult surfaces such as low surface energy substrates (eg. HDPE or PP).

All digital packaging solution

Now high quality short run offset printing is combined with digital cutting and creasing in one solution - Presstek 75DI which represents an end-to-end solution for converters.

High quality, B2 sheet size and ability to print on substrates up to 31 points (0.8 mm) in thickness distinguish this solution. The Presstek 75DI goes from digital file to sellable sheet in six minutes and prints at 16 000 impressions per hour. It is the most economical press on the market today for color jobs with run lengths between 500 and 20 000 impressions, which encompasses a growing percentage of print jobs in the folding carton market.

The Presstek 75DI is available in 4- to 10-color configurations.

Included Highcon Euclid converting machine uses precision laser optics and polymer technologies to transform cutting and creasing from an analog to a digital workflow, dramatically streamlining the finishing process.

The International Circle actions for the future

This year, the International Circle of Educational Institutes for Graphic Arts Technology and Management (IC) offered its members two interlinked events. Beside the annual conference, the IC organised a one-day symposium on drupa. Current concepts of graphic and related education were presented by eight invited speakers, concluded by a lively discussion of the lectures given. More than 40 participants from 13 countries all over the world attended. As indicated with the title of the conference "Better anticipation of future skills - towards a stronger partnership between education and industry", the central topic was the future requirements of graduates to make their ways for another forty or fifty years of their professional life. The IC also used this opportunity to strengthen its relations to other organizations active in the educational field, including, e.g., intergraf and EGIN and it also took part in the iarigai "Open Doors Event".

The 44th annual IC conference, held from 19 to 22 June in Budapest, Hungary, was hosted by the Faculty of Light Industry and Environmental Protection Engineering of Óbuda University which celebrates its 40th anniversary in 2012. Participants from 12 countries presented scientific and educational papers. A new feature to the conference was a round-table discussion on the future of education for the printing trade and the role of the IC in it.

Professors Gillian Mothersill and Ian Baitz, of the Ryerson University, invited the audience and all members of the International Circle to the 45th IC annual conference, which will be held in Toronto, Canada, from 2 to 6 June 2013.

Technology for girls summer camp

Many young girls are not only interested in reading books and magazines, but also how the printing is carried out. Twelve of them, aged between 12 and 14 years, were invited by KBA to spend a part of their summer holidays in the company operations in Würzburg. The group showed great interest in construction of printing machines and assisted in number of operations. After a week of work and learning, the young team presented and explained their hand-made models of printing machines.

booklet labels in the printing process. Track & Trace integrates easily into a new or existing production line enabling the inclusion of all standard product tracking codes on booklet labels or packaging. The codes include GS1, all types of numeric codes, and 1-D and 2-D barcodes (Datamatrix), which are used to check the legitimacy of the packaging and product online.

Track & Trace also includes an optical checking system. In a quick single step cameras automatically read and verify the selected layout and check the digits. And the solution affords users maximum flexibility when it comes to late-stage customization. If the check code does not match the reference data, the module rejects the packaging. The assigned Track & Trace code can then be added to the packaging in a subsequent print run.

Creasing & perforating system

One of the new paper finishing systems Foldmaster Touchline CP375 offers more flexibility and automation comparing to any other product in paper finishing. Touchline stands for efficient and automated processes in creasing, perforating (across the sheet and longwise), slitting and folding: all in one pass. Touchline models can handle paper stocks from 80 to 400 gsm in sizes from 105 x 148 mm to 375 x 1 050 mm (with table extension).

Due to the interchangeable tools, the new Touchline CP375 can be diverted from a creasing into a perforating machine or vice versa. In conjunction with the online creasing and folding machine TCF375, the CP375 will be able to produce even more complex jobs online: perforating, slitting, creasing and folding all in one single operation.

Developing business through innovation

On the forthcoming Packaging Innovations Show in London in October 2012, Kodak is planning a great comeback to the market by launching the new flexo plate.

This innovative product, primarily intended for packaging printing sector, is based on the Thermal Imaging Layer. Laminating the Thermal Imaging Layer to the FLEXCEL NX Plate eliminates all oxygen between the layer and the plate, allowing stable, full-amplitude, flat top dots to form. The results are consistent, predictable printing, even of subtle gradations and challenging shadows and highlights. The new plate is offering significant advantages:

- Highlight and shadow dots as small as 10 microns
- Imaging at up to 9.5 square meters per hour
- Full-amplitude, flat top dots that reduce dot gain and remain constant with over-impression
- Plates enable excellent ink transfer, smooth solids, uniform lay down, robust on-press performance, and excellent ozone resistance.

Key issues will be discussed in an open forum, where the expert team will share the knowledge and deepen product understanding.

Bookshelf

WEB2PRINT

The Electronic Document Scholarship Foundation (EDSF) has released a new book written by Jennifer Matt entitled Web2Print. The author is a well known, world leading expert in web2print strategies and large scale implementations and integrations. She is also president of Web2Print Experts, Inc. an international strategic consulting and software development company which specializes in large scale web-to-print solutions, implementation, software customizations and integrations.

The comprehensive how-to book suggests a common language for discussing the various components of web-to-print, so printers can first define their online strategy and then choose the enabling web technology that best supports this strategy.

The book was prepared in collaboration with HP, first printed on drupa 2012 using HP Indigo digital presses and was distributed for free among visitors of the event. The book is now available online in Adobe PDF formatted version for iPad and print. For those who would like to have a hardcopy the book is available for purchase online.

WEB2PRINT
Author: Jennifer Matt
Publisher: The Electronic Document Scholarship Foundation (2012)
137 pages Adobe PDF
Paperback available online

Frontiers in Antennas

Next Generation Design & Engineering

Edited by one of the world's foremost authorities on smart antennas and featuring contributions from global experts, this book discusses the latest advances in antenna design and engineering. This pioneering guide deals primarily with novel antenna designs and frontier numerical methods.

The book covers a variety of different topics among which are Ultra-wideband antenna arrays using fractal, polyfractal, and aperiodic geometries; Smart antennas using evolutionary signal processing methods; The latest developments in Vivaldi antenna arrays; Effective media models applied to artificial magnetic conductors and high impedance surfaces; Novel developments in metamaterial antennas; Biological antenna design methods using genetic algorithms; Contact and parasitic methods applied to reconfigurable antennas; Antennas in medicine: ingestible capsule antennas using conformal meandered methods; Leaky-wave antennas; Plasma antennas which can electronically appear and disappear; and Numerical methods in antenna modeling using time, frequency, and conformal domain decomposition methods. Each chapter provides in-depth details on a unique and modern antenna technology.

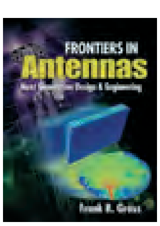

Frontiers in Antennas
Author: Frank B. Gross
Publisher: McGraw-Hill Professional (2011)
ISBN 978-0071637930
544 pages
193 mm x 242 mm
Hardcover

Digital Label Printing

A "How to" guide for the label converter

Michael Fairleys

Tarsus Publishing Ltd.
ISBN 978-0954751845
84 pages
Paperback

This new book brings together the combined knowledge and expertise of some of the world's leading experts to provide a comprehensive guide to understanding how digital label printing technologies work, as well as the enhanced requirements that digital printing brings to color management, origination and pre-press, the new demands made on label substrates, available finishing solutions, and how converters should look at the management and marketing of the digital label printing operation.

The book is illustrated with around 80 diagrams, charts, tables and illustrations. It aims to provide a convenient reference source for label converters that are both looking to invest in digital printing, or have already been operating digital presses for some time.

Portable Consumer Electronics:

Packaging, Materials, and Reliability

Sridhar Canumalla & Puligandla Viswanadham

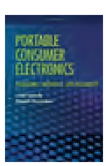

PennWell Corp. (2010)
ISBN 978-1593701253
454 pages
155 mm x 234 mm
Hardcover

Portable consumer electronic devices have experienced exponential growth in recent years. Although the reliability implications and performance criteria of these products are significantly different from electronic hardware of the past, no single volume has covered the materials, design, and reliability aspects of these products until the publication of this new book.

The book provides a comprehensive account of the key aspects of packaging for portable consumer electronic devices, including first- and second-level packaging; printed wiring board technology; assembly technology; reliability statistics and engineering; and failure analysis.

Colour design: Theories and applications

Review by Ondrej Panak, University of Pardubice

The use of colour in designer's tasks requires relatively broad knowledge of different colour aspects to overcome misunderstandings in workflow processes or even disappointment of the final results. The book, edited by Janet Best, introduces the most important issues that have to be considered while understanding, specifying, communicating and using colour in a wide range of its applications.

The book has an article-based format of four parts, containing 23 chapters, each written by academic or industrial specialists in the topics introduced. Each chapter consists of its own abstract, introduction and subchapters, some sections are supported by author's recommendations of further information and each chapter ends with list of references. The text is extensively supported by full coloured images and graphs.

Since colour is specified as a visual property of light, Part I covers perception and psychological aspects of colour. Part II focuses on objective description of colour and how colour is communicated and approved. Part III views colour from historical, design and colouration perspectives. Part IV contains four chapters focused on colour in practical applications.

The content of the book is well structured. Most chapters are written that even inexperienced readers will get the important basic information. However, some of the chapters might be more difficult to read for non-academic readers. For some readers the repetition of materials in several chapters may be purposeless. On the other hand, the article-based formatting supports the possibility to purchase selected chapter only.

The book covers multidisciplinary approach to colour with extensive references for further reading and it might reach its goal "to be an invaluable reference tool for all those researching or working with colour and design in any capacity".

Colour Design
Edited by: Janet Best
Publisher: Woodhead Publishing (2012)
ISBN 978-1845699727
672 pages
156 mm x 234 mm
Hardcover

Paper Folding Templates for Print Design

Formats, Techniques and Design Considerations for Innovative Paper Folding

Trish Witkowski the industry's authority on folding has introduced her new work, which presents a comprehensive visual resource for designers or producers of folded materials for print and direct mail.

Based upon 15 years of studying and collecting folded materials from all around the world, the author presents the basic and advanced paper folding techniques, trends and low budget tricks. Numerous folded formats and some new folding ideas are innovatively presented together with additional categories such as dimensional, proprietary and branded solutions.

Paper Folding Templates for Print Design
Author: Trish Witkowski
Publisher: HOW Books (2012)
ISBN 978-1440314124
192 pages, paperback
168 mm x 218 mm

Events

FACHPACK - Packaging, Technology, Processing and Logistics

Nuremberg, Germany
25 to 27 September 2012

FachPack, one of the most noted packaging exhibitions in Europe will present a comprehensive program in the areas of packaging, technology and logistic. This exhibition, to be held at the Nuremberg Exhibition Centre, will combine packaging process chain under the roof of one event.

Around a third of the exhibition will be dedicated to packaging materials and supplies and packaging ancillaries. The second third will focus on packaging machinery, labeling and marking equipment, peripheral packaging machinery and processing. Exhibitors will also present innovations in the area of packaging design, packaging printing and processing. Offers such as conveyor, storage and order picking systems, as well as packaging logistics services complete the program.

By introducing the new "PackBox forum", devoted to the triad of inspiration, innovation and information, organizers hope to provide the knowledge on topics from the entire product spectrum of FichPack. Short presentations and panel discussions will take place in three knowledge blocks on each of the three days of the exhibition - free and without registration. Beside mentioned program special shows on Easy-to-Open Packaging, Packaging Design, Packaging in Medical Technology and Pharmacy, The Long Way to the Shelf and Marketplace for Innovative Logistic Solutions are planned.

With around 1 400 exhibitors and expected 35 000 visitors, from 70 different countries, FachPack will again impress with its creative working atmosphere in which information and contact care are just as important as answering the specific technological questions.

EcoPrint Europe 2012

Berlin, Germany
26 to 27 September 2012

EcoPrint Europe 2012 is a new event for the creative and print community with a focus on sustainable print business.

Exhibition is designed to provide answers, insight and innovation through high quality seminars presented by the world's leading sustainable brands and experts. Marketers for leading consumer brands will be provided with the insight direct from their peers, agencies or print service providers will be given the information needed to equip their business with the right thinking, and the latest products and processes to meet this sustainable demand.

In order for the world's leading brands to meet the targets laid out by their public commitments to sustainability, brands and retailers are changing the way they produce their product and this is impacting upon their print supply chain. And print production is a significant part of any brands communication channels.

Graph Expo - Print Integrated

Chicago, Illinois, USA
7 to 10 October 2012

Graph Expo 2012 is one of the premier international trade events for the graphic communications industry in United States. The show will feature leading manufacturers and suppliers exhibiting newly released products, technologies and services in press offset, digital printing, commercial printers, and package & specialty printers.

Apart from the exhibition, the event will also include more than 50 free educational seminars and workshops on more than twenty subject categories, created by industry experts, to provide the attendees with market forecasts and practical information on key technologies, essential business strategies, and the action-oriented solutions to boost the sales and profits.

Graph Expo 2012 will be a not-to-be-missed event for those seeking the latest information in prepress, printing, finishing, converting, mailing, wide format and digital technologies.

PolygraphInter

Moscow, Russia
9 to 12 October 2012

PolygraphInter is the main national printing exhibition in Russia, awarded with the sign of International Union of Exhibitors and Fairs of the CIS and Baltic states.

The show gathers qualified buyers of prepress equipment, digital image capture equipment, digital and traditional presses, wide format inkjet printers, bindery and finishing equipment, converting equipment and appropriate supplies, media and substrates, chemicals and supplies, services to the trade and many more.

ICE Asia

Shanghai, China
10 to 12 October 2012

ICE Asia is China´s only independent exhibition for the paper, film, foil and non-wovens converting industry. The exhibition offers an ideal platform for suppliers and buyers, retailers, consultants and developers to make new contacts and to discover solutions and assess market trends.

The Joint conference on 3D Imaging and Modelling and 3D Data Processing, Visualization and Transmission

Zurich, Switzerland
13 to 15 October 2012

The interest in creating and acquiring 3D material is increasing. New platform - 3DimPVT provides a platform for disseminating research results covering broad variety of 3D field. Topics in 3D research in computer vision and graphics, signal processing, optic sensors, visualization, representation and transmission, geometric modelling and application as well as many more will be covered.

This 3DimPVT will be collocated with 3D-TV conference. The events will provide a unique forum for disseminating and discussing ideas and results that cover a broad scope of topics related to 3D research in computer vision and graphics.

VIEW CONFERENCE

The creative power of technology
Turin, Italy
16 to 19 October 2012

In October 2012 the premiere international event - 13th International Computer Graphic Conference VIEW CONFERENCE, entitled The creative power of technology, will take place.

Conference is focused on computer graphics, interactive technologies, animation & vfx, design and videogames.

The event will continue to propose the most up-to-date discussions by world-class experts through lectures, meeting, exhibits, screening and demo presentation which will reveal the new digital frontier sweeping from cinema to architecture, automotive design to advertisment, from medicine to videogames.

EcoPrint's speaker program is designed to connect different parties with leaders in sustainability such as Michael Braungart and a group of top brands such as Coke, Nike, Toyota, P&G, Aveda, DM Drogerie Markt and IKEA and leading outdoor advertising agencies such as JC Decaux & Clear Channel as well as high level insight from the world's leading business research organization, McKinsey & Co.

EcoPrint's exhibitors will be showcasing the latest sustainable technological innovation providing visitors with leading technology and education on sustainable print and this further informs and inspires the leading print professionals who attend EcoPrint, to add value to their campaign, solution, service and ultimately business.

The World Association of Newspapers and News Publishers (WAN-IFRA) is announcing several important events during the autumn and winter of 2012.

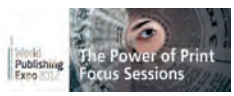

The Power of Print 2012

Frankfurt, Germany
23 to 28 September 2012

The Power of Print represents a focused series of short conferences at the World Publishing Expo 2012. The main purpose is to bring topics of interest and add a user experience´s view, creativity and ingenuity to new and applied technology. Specialists and industry experts will report about their experiences conducting projects and give examples of best practice in the area of newspaper production. Topics will cover Innovation in Printing, Selling Print Capacity and retrofit - upgrading press. Each session will last two and a half hours, allowing plenty of time to visit World Publishing Expo.

WAN-IFRA India 2012

Pune, India
26 to 27 September 2012

For the first time WAN-IFRA India Conference will take place in the second best city in India - Puna. The 20th annual conference of WAN-IFRA South Asia will consist of three parallel tracks: Newsroom Summit, Printing Summit, and Cross-media Advertising Summit. The program will discuss the business and technology challenges and provide a direction into the future of news publishing industry in the region. The conference draws much significance in the backdrop of the digital media revolution facing the South Asian news publishing industry in one hand and the challenge on managing the growth of print media business on the other hand. The conference will be preceded by 3 pre-conference workshops on topics of Green Publishing, Online video production and Multimedia advertising sales.

World Publishing Expo 2012

Frankfurt, Germany
29 to 31 October 2012

Technologies and markets are changing, but one thing remains certain: Newspaper printing is a growing market in many regions of the world. Even in western market there are not only declining circulations to be found but also numerous encouraging examples of successful and exciting print products. Case studies and the innovative technology enabling them will be presented at the World Publishing Expo.

PPP AFRICA - Plastics, Printing, Packaging

Nairobi, Kenya
6 to 8 October 2012

The 16th PPPEXPO Kenya International Trade Exhibition on plastics, printing and packaging is set to present over 10 000 products, equipment and machinery from over 30 countries. Trade visitors from all over the East & Central African countries are being invited directly and in collaboration with several regional trade bodies in Kenya, Tanzania, Ethiopia, Uganda, Somalia, Mozambique and Congo.

Though Kenya by itself is one of the biggest markets in Africa, major emphasis is being laid upon attracting traders and importers from neighboring countries. The experience and comments of exhibitors at previous events indicate substantial gains from a number of unexpected foreign visitors. A significant rise in such statistics would ensure additional business especially for the foreign participants who form almost 80 - 85 % of the exhibition.

SGIA Expo

Las Vegas, USA
16 to 19 October 2012

The SGIA Expo is a community event hosted by the Specialty Graphic Imaging Association. The association has a long history of support for screen printing applications, primarily for the production of large format graphics and decals. Their members have done a great job of holding on to their customer base as technology quickly evolved and that is what makes the association and the SGIA Expo so successful.

SGIA attracts exhibitors from all over the world. SGIA Expo plays a big part in presenting new solutions of the full range of wide format digital imaging and its applications. Exhibitors from all over the world present and share their knowledge as well as solutions from the most advanced wide format digital imaging solutions to basic entry-level solutions.

The SGIA Expo is the only place to see the industry´s most innovative imaging developments - offering the complete range of technologies, educational programs, ideas and networking opportunities.

This year the organizers have joined photo imaging and fine art professionals in new Photo Imaging Pavilion and they have for the first time also added a new Color Management Zone, which will ensure increased exposure and more idea and networking opportunities. Many of zones will feature short educational presentations designed to help attendees clarify questions for exhibitors and fine-tune their decision-making process.

Along with the annual Expo, SGIA will in Las Vegas Convention Centre organize the Printed Electronics and Membrane Switch Symposium, where particpants will gain knowledge on the latest technology developments, advanced production methods as well as innovative printed electronics and membrane switch manufacturing processes.

Nordic Wood Biorefinery Conference

Helsinki, Finland
23 to 25 October 2012

VTT and Inventia are organizing an international event, 4th Nordic Biorefinery Conference which will be held in Helsinki this October.

The event presents the leading meeting forum for wood biorefinery professsionals. Conference program will consist of keynote lectures, invited and submitted papers, as well as poster presentations.

Topics of the program will cover Industrial wood biorefining projects (including pulp mill modifications), Emerging new wood biorefineries and biorefinery products, Policy issues relevant to biorefining, Socio-economic aspects of wood biorefining, Key research programs and projects as well as Market aspects.

The conference will give a comprehendsive overview of the recent progress in wood biorefining research and commercialization.

Vietnam Print & Label Graphic Technology fair

Saigon, Vietnam
24 to 27 October 2012

Vietnam Print & Label Graphic Technology is an international exhibition for printing, packaging and labeling technologies. This four day event, hosted by Chan Chao International Co. limited, will focus on new emerging trends in the industry. This 12th exhibition in a roll will provide a great variety of information in different graphic fields for different profiles of visitors.

Attendees will be able to find novelties in print works & digital production, labeling, publishing and bindery as well as in graphic design.

Label Expo India

New Delhi, India
29 October to 1 November 2012

LabelExpo India 2012 is the largest event for label, product decoration, web printing and converting industry in South Asia. The sixth edition of the show will offer more products, more launches and more live demonstrations than any other industry event in the region. At this year´s fair more than 200 local and international press and material manufacturers will be exhibiting. The fair is mostly aimed at label and packaging printers/converters, brand owners and label designers. The trade will showcase the latest advances in label materials, films, sleeves and wrap technologies. According to the organizers around, 27 working presses will be presented at the show all giving live demonstrations. In addition Label Expo India will again host to the LMAI Avery Dennison Label Awards.

PAP-FOR RUSSIA

St. Petersburg, Russia
30 October to 2 November 2012

This Eastern Europe pulp and paper event for unveiling paper industry, organized by Reed Exhibitions, is one of the highly prioritized shows which will offer viable platform for entrusted manufacturers and suppliers of paper making equipment, chemicals, measurement equipment and products of varied industries.

This year´s event will host 350 exhibitors who will showcase bags, pulp, bond paper, paperboard, corrugated containers, folding boxes, paper coating and glazing, paper machines, printing presses end many more.

Along with the exhibition conference, seminar and round tables will be held offering help in exploring the sector more effectively.

The aim of the event is to present the latest novelties and technologies from regional and international markets to trade audience as well as to offer the most acute topics for discussion and to advice on the better decisions.

PACK EXPO International 2012

Chicago, USA
28 to 31 October 2012

With an expanded focus on processing and integrated processing-packaging system Pack Expo International 2012 presents an event with the most innovative technologies and solutions. The event will deliver solutions from more than 1 800 suppliers in designated industry pavilions. Beside mentioned it will also offer the latest insights and discussions on topics relevant to the industry.

Partnering with leading industry associations, companies and field experts the show will also offer educational opportunities. Conference organized at Pack Expo will include in-depth discussions on topics of Food safety and Product security, Sustainability and Packaging materials, Pharmaceutical and medical devices, Beverage, Manufacturing solutions, Track and trace as well as Transportation and logistics. Top companies (Bayer, Nestle, Pfizer and many more) representatives will give speeches at the conference.

Pack Expo will also offer Pack Expo Lecture series, Food Safety Summit and Amazing Packaging Race in which participating exhibitors will contribute a donation of 500 USD towards the Educational & Training Foundation. Their financial support will help provide scholarship and other educational assistance to students at PMMI´s Partner Schools in the United States and Canada.

Paper Recycling Conference

London, United Kingdom
6 to 7 November 2012

Constant changes in fiber market which have been critical to both the supply and the consumption side of industry have presented a basis in preparing this eighth edition of European Paper Recycling Conference.

Sessions in conference program will ensure addressing of the hottest issues as well as they will examine recent developments impacting the paper industry, opportunities in new geographic markets (not only in Europe but also in China, India and the Middle East), the impact of pending rules and restrictions to trade and case studies of technologies and techniques proven to boost fiber recovery.

Furthermore, in response to the recent trend of traders and collectors diversifying into plastics, a new session has been introduced for 2012 that will examine plastic recycling opportunities.

Paper Recycling Conference Europe assembles recovered paper merchants, brokers, consumers, mill representatives and equipment and service suppliers involved in paper recycling. Unlike many other paper industry events, this one is designed to bring the supply and consuming sides of the industry together to create an active dialogue and generate trading opportunities.

With an expected attendance of more than 300 participants, this Paper Recycling Conference Europe 2012 provides an ideal platform for networking and business development.

Packprint Summit 2012

Dubai, United Arab Emirates
6 to 7 November 2012

Packprint Summit 2012 is the first event of its kind in the Middle East that focuses purely on package printing. Comprising of a two-day conference and table-top exhibition, the event offers attendees an educational platform to learn about current package printing trends and technologies and network with the world´s leading suppliers and industry experts.

The event is aimed at package printers and the entire spectrum of printing professionals. Including the most knowledgeable and experienced printing and packaging speakers and plenty of networking opportunities, Packprint Summit Middle East 2012 presents a place where entire package printing industry can meet and do business under one roof.

Specialty Papers 2012

Chicago, Illinois, USA
7 to 8 November 2012

Smithers Pira, in partnership with TAPPI, is announcing the 4^{th} annual Specialty Papers Conference which will take place in Chicago, Illinois, USA from 7 to 8 November 2012. This year´s program will focus on markets and trends in specialties and pulp, packaging & printing advances, perspectives from paper makers and new developments in coating, fibers and equipment.

The conference program will cover a wealth of new topics; interesting discussions on advanced synthetic fibers for paper making and nanocellulose fiber for barrier coating will be of the main. Organizers are also very pleased that the conference program will include the presentations from members of the Functional Paper Society from Japan.

SIGGRAPH ASIA 2012

Singapore
28 November to 1 December 2012

SIGGRAPH Asia has been for years serving as the platform for the advancement of graphic, animation, art and technology. This year's 5^{th} ACM SIGGRAPH Conference and Exhibition on Computer Graphics and Interactive Techniques in Asia will take place in Singapore.

The SIGGRAPH Asia conference attracts the most respected technical and creative people from all over the world. The conference features a myriad of stellar and innovative contributions from artists, designers, animators, researchers, and developers both from industry and academia. The event is sponsored by The Association for Computing Machinery, an educational and scientific society uniting the world´s computing educators, researchers, and professionals to inspire dialogue, share resources and address the field´s challenges.

UV Printing User Forum

Munich, Germany
7 to 8 November 2012

This year's two-day Fogra user forum will try to look at new developments in the UV printing market, it will offer some answers if electron-beam curing will replace UV printing, and give the current status of using UV LED´s as a radiation source. Beside mentioned the forum will also cover the topic of consumables for UV printing.

Conclusions made on the forum will be upgraded with one-to-one exchange of experience.

Color and Imaging Conference

Los Angeles, CA, USA
12 to 16 November 2012

CIC presents the venue for sharing cutting-edge research in the areas of color perception, color theory, color photography, mobile imaging, display systems, printing, and color workflow. Participants who come from varied backgrounds and research areas in industry and academia enable encountering of new ideas and exchanging of different vies with peers and industry-respected experts.

With this year's new topics on color in entertainment and multimedia the organizers hope to bring together experts from the color, motion picture/digital cinema, and gaming communities to engage in dynamic discussion on color issues related to these industries.

In addition to technical sessions and short courses designed for the beginner, practitioner and veteran, the organizers are planning an evening lecture on an entertaining topic related to color imaging, and several stimulating keynotes by leading world-class experts.

This year also marks the 20^{th} anniversary of the CIC and a special evening event will be held to celebrate 20 years of high quality research presented at CIC.

Print world 2012

Toronto, Canada
17 to 19 November 2012

Print World is the only show in North America with an exclusive focus on shorter-run printing. Now the third-largest trade show in North America, Print World will welcome more than 200 exhibitors (300 companies) to 125 000 sq. ft. of space at Toronto's premiere show facility, the Direct Energy Centre on the Exhibition Place grounds. More than 8 000 industry representatives attended the last show and are expected again at Print World 2012.

This year, Print World will expand the scope of the show with four areas of focus in addition to commercial printing: POSTAL WORLD, dedicated to direct mail and transactional printers, mailing houses and their suppliers; PUBLISHING WORLD, featuring the latest technologies for book and magazine publishers and printers; LABEL AND PACKAGING WORLD catering to label and package printers; and SIGN WORLD for sign and large-format printers and suppliers. Several attractions and a successful conference schedule will also form part of the show. The conference will include high-profile keynote speakers, and several seminars that deliver high-quality actionable advice from leading industry experts on a wide variety of management and technology topics.

EL 2012

Hong Kong
10 to 14 December 2012

EL 2012 is a biannually conference and a workshop mainly focused on electroluminescence. The meeting includes plenary and invited talks, contributed presentations and posters.

This year's conference will cover a wide variety of topics including LEDs and OLEDs, phosphors for displays, backlight and lighting, LCD technology, 3D displays, microdisplays, projection displays, display optics, electronics and materials, and more. Divided into five different topic sessions Organic light emitting diodes (OLEDs), Inorganic electroluminescent displays (ELDs), Emissive Materials for Displays and Lightings, LED Materials and Devices, and Industry and Emerging Related Materials and Techniques it will not only offer attracting good science and technology but also an excellent opportunity for exchanging the knowledge and sharing new ideas.

This year, the conference will introduce a new program - Technical Briefs. The other programs include Art Gallery, Computer Animation Festival, Courses, Emerging Technologies, Posters, Symposium on Apps, and Technical Papers.

The trade exhibition, to be held from 29 November - 1 December 2012, will offer participants from hardware and software vendors to studios and educational institutions a platform to market their innovative products and services to computer graphics and interactive techniques professionals and enthusiasts from Asia and beyond.

Both events are expected to attract more than 7 000 professionals, coming from 52 countries, which will attend the conference and exhibition. There you will be allowed to see, meet, and interact with the international computer graphics and interactive techniques community.

Printed Electronics USA 2012
co-located with
Photovoltaics USA 2012

Santa Clara, California, USA
5 to 6 December 2012

Printed Electronics USA 2012 and co-located Photovoltaics USA 2012 are two attractive events on printed, organic and flexible electronics. Events, organized by the IDTechEx, are designed to bring venture capitalists and other investors together and with that helping to accelerate adoption of the technology. The conference covers end user needs, technical progress and new products using flexible and printed electronics. It is of vital interest to industries as diverse as chemicals, consumer goods, healthcare, military, electronics, advertising and publishing. This event, the world's largest on the topic and growing rapidly every year, offers information and networking hub on the topic.

Printed and potentially printed electronics is of vital interest to different industries. It is allowing electronics to be used in places it has never been before and offers new exciting form factors and enhancements to existing electronics. This event showcases all the technology has to offer.

The international exhibition and trade show covers all the applications, technologies and opportunities. It offers the full picture of end-use application requirements, manufacturing processes and materials for displays, photovoltaics, energy storage, sensors, logic, memory and lighting that are printed, flexible or based on the new organic or inorganic electronic materials. An original feature of the event will be the Manufacturing street on the tradeshow, that will bring together organizations that are substrate suppliers, printers, post print handlers, testers and integrators, who will make devices in front of your eyes on production ready equipment. The manufacturing chain will be aligned in a step by step process showcasing how to make printed electronics devices, considering each step in turn.

This co-located conference will be shedding light on the latest trends from major innovators in the solar cell sector. All the latest developments in thin film, organic, printed photovoltaics as well as emerging technologies growing alongside the more established ones, such as luminescent concentrators and infrared harvesting.

JPMTR

Call for papers

Authors are invited to prepare and submit complete, previously unpublished and original works, which are not under review in any other journals and/or conferences.

The journal will consider for publishing papers on fundamental and applied aspects of at least, but not limited to, the following topics:

- Printing technology and related processes

  Conventional and special printing; Packaging, Printed functionality (incl. polymer electronics, sensors, and biomaterials); Printed decorations; Printing materials; Process control

- Premedia technology and processes

  Color reproduction and color management; Image and reproduction quality; Image carriers (physical and virtual); Workflow and management

- Emerging media and future trends

  Media industry developments; Developing media communications value systems; Cross-media publishing

- Social impact

  Media in a sustainable society; Consumer perception and media use

Submissions for the journal are accepted at any time. If meeting the general criteria and ethic standards of the scientific publication, they will be rapidly forwarded to peer-review by experts of high scientific competence, carefully evaluated, selected and edited. Once accepted and edited, the papers will be printed and published as soon as possible.

There is no entry and/or publishing fee for authors.

Authors are asked to strictly follow the guidelines for preparation of a paper (see abbreviated version on inside back cover). Complete guidelines can be downloaded from

http://www.iarigai.org/publications/

Papers not complying with the guidelines will be returned to authors for revision.

Submissions and queries should be directed to

journal@iarigai.org or office@iarigai.org

Subscriptions 2013

Journal of Print and Media Technology Research is published in print version and distributed by subscription only, solely or in package with the annual edition of the Advances in Printing and Media Technology. Following subscription models are available:

Journal of Print and Media Technology Research*

A peer-reviewed quarterly
ISSN 2223-8905

A **Regular** annual subscription (4 issues p. a.) — **300 EUR**

B **Members** of iarigai - one copy (4 issues) free of charge
Additional copies for members - discount 20% — **240 EUR**

Advances in Printing and Media Technology - Vol. 40**

(hard bound book with selected and edited full conference papers)
ISSN 2225-6707, ISBN 978-3-9812704-5-7

C **Regular** rate per copy — **155 EUR**

D **Members** of iarigai - one copy free of charge
Additional copy for members - discount 20% — **124 EUR**

Two-in-one package (JPMTR and Advances - Vol. 40)**

(valid only if ordered together)

E **Annual** subscription to the journal + **current volume** of the Advances in Print & Media Technology Research (full regular price 455 EUR) — **359 EUR**

F **Additional** package for members (extra discount 26 EUR) — **333 EUR**

Select one of the offered subscription models (A - F) and place your order online at:

http://www.iarigai.org/publications

(open: Order/Subscribe here)

or send an e-mail order to: office@iarigai.org

* Single copies of JPMTR can be purchased only if available and upon a separate request
** Vol. 40 of the Advances In printing and Media Technology will be published in November 2013

Guidelines for authors

Authors are encouraged to submit complete, original and previously unpublished scientific or technical research works, which are not under review in any other journals and/or conferences. Significantly expanded and updated versions of conference presentations may also be considered for publication. In addition, the journal will publish reviews as well as opinions and reflections in a special section.

Submissions for the journal are accepted at any time. Papers will be considered for publishing if meeting the general criteria and ethic standards of the scientific publication. When preparing a manuscript for JPMRT, please strictly comply with the journal guidelines, as well as with the ethic aspects. The Editorial Board retains the right to reject without comment or explanation manuscripts that are not prepared in accordance with these guidelines and/or if the appropriate level required for scientific publishing cannot be attained.

A - General

The text should be cohesive, logically organized, and thus easy to follow by someone with common knowledge in the field . Do not include information that is not relevant to your research question(s) stated in the introduction.

Only contributions submitted in English will be considered for publication. If English is not your native language, please arrange for the text to be reviewed by a technical editor with skills in English and scientific communication. Maintain a consistent style with regard to spelling (either UK or US English, but never both), punctuation, nomenclature, symbols etc. Make sure that you are using proper English scientific terms.

Do not copy substantial parts of your previous publications and do not submit the same manuscript to more than one journal at a time. Clearly distinguish your original results and ideas from those of other authors and from your earlier publications - provide citations whenever relevant. For more details on ethics in scientific publication, please consult:

http:// www.elsevier.com/ethicguidelines.

If it is necessary to use an illustration, diagram, table, etc. from an earlier publication, it is the author's responsibility to ensure that permission to reproduce such an illustration, diagram etc. is obtained from the copyright holder. If a figure is copied, adapted or redrawn, the original source must be acknowledged.

Submitting the contribution to JPMTR, the author(s) confirm that it has not been published previously, that it is not under consideration for publication elsewhere and - once accepted and published - it will not be published under the same title and in the same form, in English or in any other language. The published paper may, however, be republished as part of an academic thesis to be defended by the author. The publisher retains the right to publish the printed paper online in the electronic form and to distribute and market the Journal (including the respective paper) without any limitations.

B - Structure of the manuscript

Title: Should be concise and unambiguous, and must reflect the contents of the article. Information given in the title does not need to be repeated in the abstract (as they are always published jointly).

List of authors: i.e. all persons who contributed substantially to study planning, experimental work, data collection or interpretation of results and wrote or critically revised the manuscript and approved its final version. Enter full names (first and last), followed by the present address, as well as the e-mail addresses.

Separately enter complete details of the corresponding author - full mailing address, telephone and fax numbers, and e-mail. Editors will communicate only with the corresponding author.

The title of the paper and the list of authors should be entered on a separate cover page (numbered as 0). Neither the title nor the names of authors can be mentioned on the first or any other following page.

Abstract: Should not exceed 500 words. Briefly explain why you conducted the research (background), what question(s) you answer (objectives), how you performed the research (methods), what you found (results: major data attained, relationships), and your interpretation and main consequences of your findings (discussion, conclusions). The abstract must reflect the content of the article, including all the keywords, as for most readers it will be the major source of information about your research. Make sure that all the information given in the abstract also appears in the main body of the article.

Keywords: Include three to seven relevant scientific terms that are not mentioned in the title. Keep the keywords specific. Avoid more general and/or descriptive terms, unless your research has strong interdisciplinary significance.

Abstract and keywords should be entered on a separate page, numbered as page 1. Do not continue with the main body of the text, regardless of the possible empty space left on this page.

Introduction and background: Explain why it was necessary to carry out the research and the specific research question(s) you will answer. Start from more general issues and gradually focus on your research question(s). Describe relevant earlier research in the area and how your work is related to this.

Methods: Describe in detail how the research was carried out (e. g. study area, data collection, criteria, origin of analyzed material, sample size, number of measurements, equipment, data analysis, statistical methods and software used). All factors that could have affected the results need to be considered. Make sure that you comply with the ethical standards, with respect to the environmental protection, other authors and their published works, etc.

Results: Present the new results of your research (previously published data should not be included). All tables and figures must be mentioned in the main body of the article, in the order in which they appear. Do not fabricate or distort any data, and do not exclude any important data; similarly, do not manipulate images to make a false impression on readers.

Discussion: Answer your research questions (stated at the end of the introduction) and compare your new results with the published data, as objectively as possible. Discuss their limitations and highlight your main findings. At the end of Discussion or in a separate section, emphasize your major conclusions, specifically pointing out scientific contribution and the practical significance of your study.

Conclusions: The main conclusions emerging from the study should be briefly presented or listed, with the reference to the aims of the research and/or questions mentioned in the Introduction and elaborated in the Discussion.

Introduction, Methods, Results, Discussion and Conclusions - as the scientific content of the paper - represent the main body of the text. Start numbering of these sections with page 2 and continue without interruption until the end of Conclusions. Number the sections titles consecutively as 1, 2, 3 ..., while subsections should be hierarchically numbered as 2.1, 2.3, 3.4 etc. Use Arabic numerals only.

Note*: Some papers might require different structure of the scientific content. In such cases, however, it is necessary to clearly name and mark the appropriate sections.*

Acknowledgments: Place any acknowledgments at the end of your manuscript, after conclusions and before the list of literature references.

References: The list of sources referred to in the text should be collected in alphabetical order on a separate page at the end of the paper. Make sure that you have provided sources for all important information extracted from other publications. References should be given only to documents which any reader can reasonably be expected to be able to find in the open literature or on the web. The number of cited works should not be excessive - do not give many similar examples. Responsibility for the accuracy of bibliographic citations lies entirely with the authors.

Please use only the Harvard Referencing System. For more information consult, e. g., the referencing guide at:

http:// libweb.anglia.ac.uk/referencing/harvard.htm.

List of symbols and/or abbreviations: If non-common symbols or abbreviations are used in the text, you can add a list with explanations. In the running text, each abbreviation should be explained the first time it occurs.

Appendix: If an additional material is required for better understanding of the text, it can be presented in the form of one or more appendices. They should be identified as A, B, ... etc., instead of Arabic numerals.

Above sections are supplementary, though integral parts of the Scientific content of the paper. Each of them should be entered on a separate page. Continue page numbering after Conclusions.

C - Technical requirements for text processing

For technical requirement related to your submission, i.e. page layout, formatting of the text, as well of graphic objects (images, charts, tables etc.) please see detailed instructions at http:// www.iarigai.org/publications/journal.

D - Submission of the paper and further procedure

Before sending your paper, check once again that it corresponds to the requirements explicated above, with special regard to the ethic issues, structure of the paper as well as formatting. Once completed, send your paper as an attachment to: **journal@iarigai.org**. You will be acknowledged on the receipt within 48 hours, along with the code under your submission will be processed. The editors will check the manuscript and inform you whether it has to be updated regarding the structure and formatting. The corrected manuscript is expected within 15 days.

Your paper will be forwarded for anonymous evaluation by two experts of international reputation in your specific field. Their comments and remarks will be in due time disclosed to the author(s), with the request for changes, explanations or corrections (if any) as demanded by the referees.

After the updated version is approved by the reviewers, the Editorial Board will consider the paper for publishing. However, the Board retains the right to ask for a third independent opinion, or to definitely reject the contribution.

Printing and publishing of papers once accepted by the Editorial Board will be carried out at the earliest possible convenience.

3-2012

Journal of
Print and Media Technology
Research
A peer-reviewed quarterly

The journal is publishing contributions in the following fields of research:

- Printing technology and related processes
- Premedia technology and processes
- Emerging media and future trends
- Social impacts

For details see the Mission statement inside

Submissions and inquiries
journal@iarigai.org and office@iarigai.org

More information at
www.iarigai.org/publications/journal

Publisher
The International Association of Research
Organizations for the Information, Media
and Graphic Arts Industries
Washingtonplatz 1
D-64278 Darmstadt
Germany

Prited in Croatia by Narodne Novine d.d.